PART 1 — TRANSMITTING POWER SOURCES

Section

Section	Page
Radio Frequency Sources	2
Radio Frequency Tube Sources	10
Radio Frequency Solid State Sources	28
Optical Frequency Source Characteristics	46
Laser Mode Coupling and Frequency Stabilization	78
Laser Oscillators and Amplifiers	100

INTRODUCTION – TYPES OF TRANSMITTING SOURCES

An understanding of the types, characteristics and operating parameters of known rf and optical transmitting power sources is required to design space tracking and communications systems.

In this section, radio frequency (rf) sources and optical frequency sources are described in terms of operating fundamentals and performance characteristics. The discussion is limited to factors useful in predicting the principal electrical and mechanical characteristics of space tracking and communications systems.

The division of the spectrum between rf and optical frequency source types was arbitrarily chosen at approximately 300 microns.

Radio Frequency Sources include both oscillators and amplifiers, for either may be used as the basic transmitter device. The rf discussion is limited to continuous wave devices as cw sources generally are significantly more efficient than non-continuous power sources. A natural classification of rf sources results as a function of frequency because of the fundamental mechanisms involved in the generation of rf energy. For this discussion, the frequency radio range is divided as follows:

VHF/UHF	100 MHz to 1000 MHz
Microwave	1 GHz to 30 GHz
Millimeter	30 GHz to 300 GHz
Submillimeter	300 GHz to 1000 GHz

The Optical Frequency Sources include ultraviolet, visible and infrared laser sources (to 300 microns). The discussion sets forth the general relationships between applicable operating characteristics (optical gain, saturation, noise) and applicable physical and atomic parameters (length, transition probabilities, line width, etc.).

Following the general introduction, a more detailed theory of selected gas laser sources is presented, including considerations unique to each particular laser. While selection of the lasers described was made on the basis of practicality, the individual discussions are generally representative of a class of lasers. For example, the theory of the blue and green transitions in singly-ionized argon will generally apply to all singly-ionized laser transitions.

In addition, an attempt is made to indicate the confidence with which the theories are held.

Transmitting Power Source Discussion Covers Both Theory and Performance of RF and Optical Frequency Sources

Radio Frequency Sources	Optical Frequency Sources
• Theory of Radio Frequency Sources • VHF/UHF Sources • Microwave Sources Klystrons Traveling-wave tubes Cross-field Devices • Millimeter Sources • Submillimeter Sources • Performance of Vacuum Tube Sources • UHF Sources • Microwave Sources • Millimeter Sources • Solid State Microwave Sources • Weighting Factors	General Theory of Laser Sources Argon Ion Laser CO_2 Laser Laser Mode-Coupling Laser Stabilization Laser Oscillators Laser Amplifiers Evaluation of Gas Laser Sources

SUMMARY OF RADIO FREQUENCY TRANSMITTING SOURCES

Frequency bands are indicated for radio frequency power sources.

Radio frequency sources are described in terms of operating theory and performance characteristics.

Radio frequency sources include both oscillators and amplifiers, for either may be used as the basic transmitter device. The rf sources are limited to continuous wave devices as cw sources generally are significantly more efficient than non-continuous power sources. A natural classification of rf sources results as a function of frequency because of the fundamental mechanisms involved in the generation of rf energy. The frequency range is divided as follows:

UHF	100 MHz to 1000 MHz
Microwave	1 GHz to 30 GHz
Millimeter	30 GHz to 300 GHz
Submillimeter	300 GHz to 1000 GHz

The figure indicates, in summary form, available power levels available from rf sources.

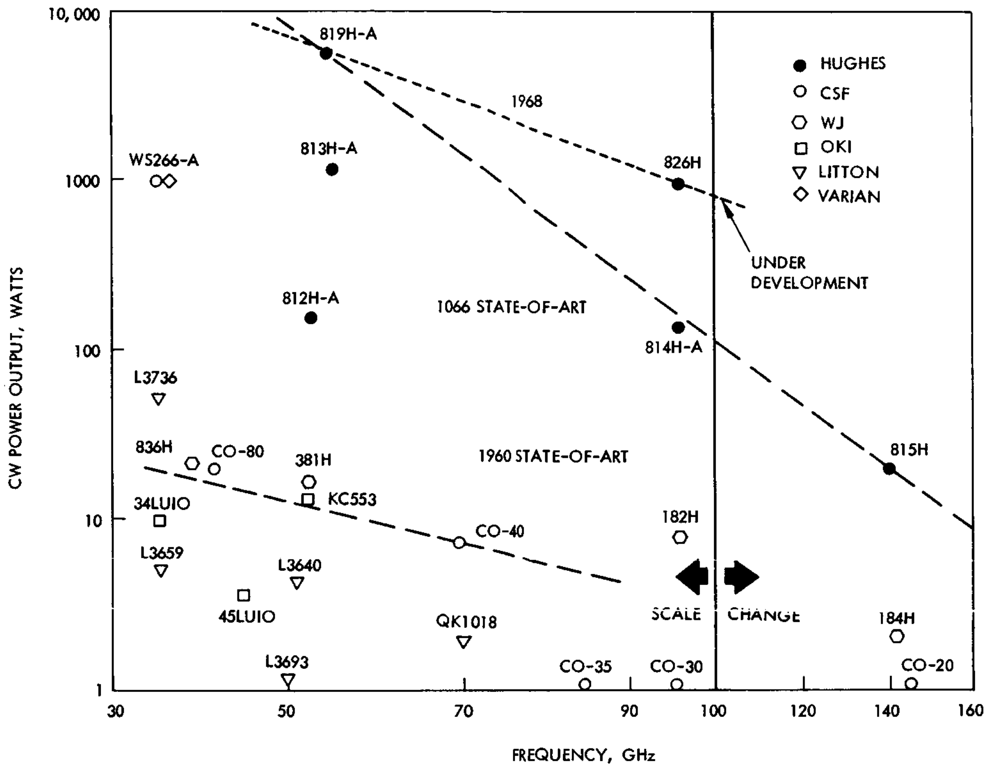

Power Characteristics of Available High Power CW Sources

Most significant is 35 percent efficiency achieved in the 813H and marked increase in available power which has occurred since 1960. The letter -A stands for amplifier and the letter -O signifies oscillator.

SUMMARY OF GAS LASERS AS TRANSMITTING SOURCES

A CO_2 transmitter for a spaceborne communication link and an Argon laser for an up link beacon appear to be the best choice for laser space communication.

The Table summarizes the characteristics of six wavelengths produced by gas lasers. Hundreds of other wavelengths are available, but these six have been selected as representative of each type (ion, molecular, and neutral gas). The reported output power, length and input power are given for the lasers selected.

Notes

1. This is a Hughes airborne quartz laser with a 46 cm bore length ~1 meter overall package length. It requires a magnetic field of ~1000 gauss, which implies a heavy structure and possibly more power.

2. This laser was reported by Raytheon in Electronic News; it is a quartz tube. The power out is 18 watts, provided the beam in the cavity was chopped to prevent damage to the mirrors.

3. This was produced under carefully controlled conditions at Bell Labs.

4. This is a commercially available Spectra-Physics model 125. 50 mw is guaranteed, but selected tubes produce 100 mw.

5. This is the Spectra-Physics model 125. It may be possible to double the power in a tube this size, but drastic improvements are quite unlikely at this wavelength.

6. This is an Hughes Research Laboratories (HRL) Laboratory-type tube. The output may be doubled, but more power than this is doubtful in a tube this size.

7. This is a TRG Laboratory-type tube and represents approximately two years of effort in developing a high power Xe laser. It is probably close to the ultimate for a tube this size.

8. This is an HRL Laboratory-type tube using flowing CO_2-N_2, mirrors were not optimized; more output power can be expected from this same tube (~20 watts). Seven watts were obtained with the tube sealed.

9. This is the Bell Telephone Laboratories work (C. K. N. Patel, Appl. Phys. Lett., 1 July 1965). A flowing gas system was used with a mixture of CO_2, N_2, O_2, H_2O.

10. This is a BTL result with a tube 4 inches in diameter and 12 feet long. Helium was used. It is hard to estimate how much power will eventually be obtained from a tube of this size. (C. K. N. Patel).

11. This is a small, non flow tube, with external mirrors; suitable for spacecraft. This work is due to T. J. Bridges and is rather preliminary. An account of similar tubes appears in the 1 November 1965 Appl. Phys. Letters.

In comparing the various lasers listed in the table, the suitability of the output signal for the communications task at hand must be kept in mind. All of the lasers listed can be made to operate in the lowest order spatial mode (TEM_{00}) alone with more or less difficulty. The task is easier at the shorter wavelengths where the laser output is visible and the characteristic beam size is small (proportional to the square root of the product of wavelength and a cavity parameter related to mirror radius). Mode selection at infrared wavelengths may be done with an image-converter or by using a heterodyne detector. Production of a single-frequency output is still quite difficult because of the longitudinal mode structure of the long Fabry-Perot cavities used. Only the 10.6μ CO_2 and 3.5μ Xenon lines are narrow enough to produce reasonable output by keeping the Fabry-Perot resonator short enough so that only one longitudinal mode oscillates. This is done to the narrow doppler-broadened line widths of these two transitions (50 MHz for 10.6μ CO_2 and 120 MHz for 3.5μ Xe). Even these two transitions will require further mode selection techniques if longer, higher power tubes are considered. Because of the broad doppler line widths of the Ar and He-Ne lasers, single-frequency operation through the use of a sufficiently short Fabry-Perot resonator entails a drastic loss in output power. Techniques involving 3 mirror resonators allow the use of longer tubes at the expense of added complexity both mechanical and electronic (servo-controlled mirror positioning), but still sacrifice output power because the entire line is not used. The most promising technique developed to date is that of intracavity mode locking[1] with a subsequent coherent recombination[2] or selective output coupling[3]. This technique has been demonstrated in the laboratory, but practical power levels at a single frequency are yet to be obtained. In any case the additional complexity will contribute to the weight, length and inefficiency of the laser, although perhaps not to a significant extent.

It appears that, at present, the best laser for optical space communications at present would be a small, efficient, light weight 10.6μ CO_2 laser in the spacecraft with coherent detection (superheterodyne) on the ground, employing a cooled Hg:Ge detector. The up-link would be best handled by a high-power multimode argon laser on the ground, employing pulse amplitude or pulse polarization modulation, and a simple ruggedized photomultiplier video receiver in the spacecraft. These conclusions are, of course, subject to revision as the state of the laser (and detector) art progresses.

---

[1] Harris, S. E., and McDuff, O. P., Appl. Phys. Letts., 5, pp. 205-206, November 15, 1964.

[2] Massey, G. A., Ashman, M. K., and Taig, R., Appl. Phys. Letts., 6, p. 10, 1965.

[3] Hanes, S. E., and McMurtry, B. J., (to be published).

SUMMARY OF GAS LASERS AS TRANSMITTING SOURCES

Gas Laser Performance

Gas	Wavelength, microns	Manu-facturer	Output Power, watts	Length, meters	Input Power, watts	Efficiency	Note
Ar II	0.5	HRL	4.0	0.46	4,000	1×10^{-3}	1
Ar II	0.5	RAY	8.0	1.6	20,000	4×10^{-4}	2
He-Ne	0.63	BTL	1.0	5	500	2×10^{-3}	3
He-Ne	0.63	S-P	0.1	1.7	~200	5×10^{-4}	4
He-Ne	1.15	S-P	0.03	1.7	~200	1.5×10^{-4}	5
He-Ne	3.39	HRL	0.01	1.7	80	1.8×10^{-4}	6
He-Xe	3.51	TRG	0.08	2.0	~200	4×10^{-4}	7
CO_2	10.6	HRL	10	2.0	150	6.7×10^{-2}	8
	10.6	BRL	12	2.0	—	3×10^{-2}	9
	10.6	BTL	130	4.0	~1,000	$\sim 1.3 \times 10^{-1}$	10
	10.6	BTL	0.1	0.5	30	3.3×10^{-3}	11

TRANSMITTING POWER SOURCES

Radio Frequency Tube Sources

	Page
Fundamentals of UHF Sources	10
Fundamentals of Microwave Sources	12
Hughes 394H TWT Performance	16
Fundamentals of Millimeter and Submillimeter Sources	18
Weighting Factors	20
Performance of Vacuum Tube Sources	22

FUNDAMENTALS OF UHF SOURCES

Negative grid tubes dominate the rf power sources in the VHF/UHF region (100 MHz to 1000 MHz).

Conventional tubes such as triodes and tetrodes are used in external resonant circuits for Class A or B operation. At the higher frequencies, these resonant circuits take the form of coaxial lines. Electron transit time effects limit the extension of these techniques to higher frequencies, and, at these higher frequencies, power limitations occur due to the thermal capability of the collector and the envelope seals.

The Table gives relative advantages and disadvantages for this type of source.

Relative Advantages and Disadvantages of Negative Grid Tube Characteristics Summary

Advantages	Disadvantages
1. Good phase stability and tracking characteristics, because of short transit time. Typical sensitivity to change in voltages is: Screen – 1 degree per 1 percent E_{sg} at 1 GHz Plate – 0.5 degree per 1 percent E_p. Phase variations due to drive level and filament voltage changes are negligible. Because the gridded tube has short electrical length, its phase tracking characteristics are determined primarily by the associated circuitry. Mass-produced double-tuned circuits show typical phase track deviations of 5 degrees over the usable bandwidth. A suitable secondary coupling can be chosen to give linear phase-frequency characteristics.	1. Limited gain-bandwidth product. 1000 to 2500 MHz for class A operation and 500 to 1000 MHz for class B are typical. These values hold for operations to about 500 MHz; above this frequency, the product drops off rapidly. 2. Operating frequency is limited to less than 1000 MHz. Above this, transit time is long enough to create current wave-form distortion in the plate current. The result is decreased gain-bandwidth product and lower efficiency. 3. Higher-power tubes are disproportionately expensive. This is attributed to the fact that higher-power tubes have not been manufactured in such large quantities as the smaller ones.
2. High Efficiency. At 500 MHz, typical plate efficiencies approach 70 percent for class C operation. Overall efficiencies of 50 percent, including filaments, are common. 3. Economy. Most coaxial tubes have a simple structure and are easily mass-produced. It is usually possible to select a tube already in mass production. This affords additional economy. 4. Inherent Filtering Action. For a double-tuned reentrant cavity, in which a tetrode normally operates, the roll-off is at a rate of 12 db per bandwidth octave. For a 2 percent bandwidth device at 500 MHz, typical second harmonic suppression is more than 80 db for class B operation.	4. Reliability and life expectancy. The cathode of gridded tubes must deliver a greater current density than that required by other devices. In addition, maximum r-f current must be instantaneously available for the cathode, thus requiring that the cathode operate at a comparatively high temperature. As a result, normal cathode life expectancy is generally 2000 to 5000 hours, though some tubes are rated at 5000 to 15,000 hours. However, arcing and other failure mechanisms reduce the MTBF of most types to about 3000 hours.
5. Much more experience exists in design of vacuum tubes than in other types. 6. No focusing magnets or field are required, therefore weight and volume are reduced.	5. The tetrode is a filamentary device requiring a variety of electrode voltages. Distribution of these voltages within a complex system can be troublesome. 6. Arcing problems are generally greater than in other devices due to close spacing of elements.
7. Tetrodes can operate from a dc supply on the plate. Because the control or screen grid can act as a switching element, efficiency is greater and noise is lower. 8. Tetrodes are constant-current generators and tolerate mismatches better than devices depending upon traveling- or standing-wave operation. 9. They are relatively insensitive to temperature up to the rating of the envelope seals.	7. High output capacitance limits bandwidth.

FUNDAMENTALS OF MICROWAVE SOURCES

At microwave frequencies, where electron transit time effects are significant (1 GHz to 30 GHz), some form of velocity modulation tube is employed to overcome these limitations.

Basically, the velocity modulation technique provides a means for a bunch of electrons containing the input dc power to remain is approximate time or space synchronism with a component of the ac wave so that power can be transferred continuously. Transit time effects are no longer of consequence because an electron continues to see the same phase of the ac field in spite of the axial motion of the bunch of electrons. The electrons give up either kinetic energy in the case of a klystron or traveling-wave tube, or both kinetic and potential energy in a cross-field tube. The interaction region normally takes the form of a slow-wave circuit in the vicinity of the electron bunches such that the electrons see the rf fields associated with the wave propagating structure. The various types of these tubes are classified in Table A and described below.

Klystrons

The klystron amplifier is a well developed, reliable, and in many cases a long-life device. If conservatively designed, it should be capable of meeting space requirements. The requirement for a high voltage and a high power modulation technique reduces the overall efficiency of a transmitter chain using a klystron as the final power amplifier. Table B summarizes the significant advantages and disadvantages of klystrons.

TWT's

The traveling wave tube is inherently a high average power amplifier so there exists no problem in achieving the parameters necessary in a space system. Furthermore, the TWT can be made with large gains without sacrificing any of its outstanding electrical characteristics and without increasing prohibitively the overall package size and weight. Periodic focusing of TWT's has resulted in a very lightweight, compact structure ideally suited to spaceborne applications, especially in the frequency range from 2 - 14 GHz. Herein lies one of the significant advantages of the TWT compared to its counterpart in the klystron field. At present, klystrons are often focused with heavy, bulky permanent magnets of the horseshoe variety. These large magnets create an extensive leakage field which affects all of the surrounding electronics, and furthermore, there is no easy method of shielding these fields without degrading the klystron performance.

By appropriately designing the electron gun optics so that the emission density at the cathode surface is quite low, TWT's can be made to yield an arbitrarily long life. This has been established, for example, with the Hughes Aircraft TWT's used is communications satellites and other space programs without a single failure attributable to the tube design. An expected life greater than 40,000 hours has been established beyond all reasonable doubts for these tubes.

Table C summarizes the significant advantages and disadvantages of traveling wave tubes.

Table A. The Types of Microwave Velocity Modulation Tubes are Classified in Terms of Oscillators and Amplifiers

			Interaction Circuit					
			Backward Wave		Forward Wave		Standing Wave, cavity	
			Oscillator	Amplifier	Oscillator	Amplifier	Oscillator	Amplifier
Electric-Magnetic Fields	Crossed Field (M-type)	Injected Beam	M-BWO M-Carcinotron	M-BWA Bitermitron	TPOM	CFA TPOM Bimatron		
		Continuous Cathode	Stabilotron	Amplitron CFA	VTM	FWA-CFA Dematron	Magnetron	Circlotron
	Linear (Single or Parallel) Field (O-type)	Injected Beam	O-BWO O-Carcinotron	O-BWO		TWT TPO	Klystron Reflex Klystron Monofier Monotron	Klystron

Table B. Klystron Amplifier Characteristics

Advantages	Disadvantages
1. Single envelope is practical for gains up to 30 db, depending on output power levels.	1. Longer electrical length per db of gain as compared to cross-field devices.
2. Much development experience exists both at high power (megawatts) and lower drive levels (tens of kws).	2. Gains are about half those obtained with TWTs.
3. Bandwidths to 10 percent have been achieved in high-power units; 5 percent or less is more realistic at low power.	3. Klystrons require a filamentary cathode and gun for operation, thus more electrode voltages are needed.
4. Klystrons can be made to operate with dc beam supplies by employing switching or modulating anodes.	4. Higher beam voltages required for a given output power than in crossed-field devices.
5. Klystrons still offer higher power than any other tube type.	5. Bandwidth limitations are severe at low power (tens kws); 2 to 5 percent is typical.
6. Focusing is normally performed by solenoids.	6. Good voltage regulation may be required for acceptable phase stability.
7. More design and development experience exists on this type of beam device than on any other.	7. Efficiencies of 25 to 35 percent are typical.
8. Higher perveances have been achieved than in TWTs. This permits lower beam voltages for equivalent output power.	8. Structure offers moderate filtering; may require separate high power filters at an additional cost to the system.
9. System reliability is enhanced in cases where 30 db gain is sufficient, since a single amplifier stage is adequate.	9. Reliability not reasoned to be as good as cold cathode devices operated without gun.
10. Cooling techniques are known and optional; air and liquid are common.	
11. Since the klystron is a unidirectional device, operation into a mismatched load is possible without isolation, depending on system limits of power and phase shift.	
12. More recently developed electrostatically focused klystrons offer reduced size and weight.	
13. Shorter electrical length per unit gain than the TWT, thus suffering less voltage-phase sensitivity.	

FUNDAMENTALS OF MICROWAVE SOURCES

Crossed-Field Devices

This general category of tubes includes the conventional magnetron oscillator, the amplitron amplifier, and the many linear beam-type magnetron amplifiers. These devices are, in general, more efficient, ligher and smaller for a given output power than any other tube device. The basic problem with these tubes is their relatively short life. Recent advances, such as the coaxial magnetron oscillator, show promise of increasing the life; however, extensive data on these increases is not yet available. Table D summarizes the significant advantages and disadvantages of crossed-field devices.

Table C. Traveling Wave Tube Characteristics

Advantages	Disadvantages
1. Single envelope is practical for gains to about 60 db.	1. Long electrical length per db of gain in comparison to other tubes.
2. Much development experience exists both at high power levels (megawatts) and lower drive levels.	2. Phase sensitivity of rf output is very dependent on beam voltage, because the device operates on the principle of synchronism between electron velocity and rf velocity on the slow-wave structure.
3. Bandwidths beyond 10 percent are common in today's TWT's.	3. TWT's require a filamentary cathode and gun for operation – more electrode voltages are thus needed.
4. Can operate with dc beam supplies by employing switching or modulating anodes. Grid control is possible at power levels below 10 kw.	4. Low perveance of TWT's requires higher beam voltages for a given power output compared to other devices. High perveances involve hollow beams, whose increased current density may cause focusing difficulties and cathode loading problems.
5. Long length, small-diameter form factor is suitable for phased arrays limited to tube diameters of less than $\lambda/2$.	5. High gains usually require solenoid focusing (or a recently proposed magnetic matrix focusing technique). Solenoids for high power tubes are large, require substantial power, and create packaging and distribution problems.
6. Several types of slow-wave structures can be cascaded in a single envelope to optimize the rf coupling design.	6. Acceptable phase stability calls for good beam voltage regulation.
7. Focusing can be accomplished by electromagnets, permanent magnets, or electrostatically, depending on system requirements resulting in low external magnetic fields.	7. Efficiency is $\approx$ 25 percent without depressed collectors. Depressed collectors raise efficiency by $\approx$ 10 percent.
8. Reliability is enhanced by single-stage operation.	8. Electrical structure offers very little filtering. Separate high-power filters may be needed.
9. Depressed-collector techniques ease regulation requirements on high-current beam supply.	
10. Cooling techniques are known and operational; air and liquid are common.	
11. Severed or attenuated slow-wave structures enable operation without circulators into a mismatched load, depending on the limits of phase tolerance.	
12. No doubt exists about development and mass production of TWT's.	
13. Light weight compared to alternate tube implementations.	
14. Several lower power tubes can be operated in parallel to achieve higher power, higher reliability, and higher heat dissipation over larger areas.	

Table D. Crossed-Field Tube Characteristics

Advantages	Disadvantages
1. Gains to 45 db possible with injected beam variety; 10 percent bandwidth typical.	1. Limited gain of 10 to 15 db for distributed emission and types.
2. Good phase stability; fairly independent of anode voltages, since velocity synchronism is not an operating requisite.	2. Has very limited dynamic range of output power for a particular anode voltage and varying input power.
3. Distributed emission type has shortest electrical length per unit gain of all tubes.	3. Crossed-field tubes are bidirectional. Any reflections into the output will return directly to the driver or input circuit. A circulator or isolator is thus necessary.
4. Can operate with a cold cathode; electron gun or filaments are avoided.	4. Injected beam types require very good regulation of sole voltage for good phase stability. Typical values are 20 degrees for a 1 percent change in sole voltage.
5. Reasoned to have long life compared to filamentary devices.	5. In distributed emission types it is difficult to initiate emission.
6. Small in size and relatively light in weight.	6. Perveance of injected beam types is comparable to that of TWT's, thus requiring higher beam voltages for a given output power.
7. Distributed-emission type provides the lowest anode voltage for a given power output. This simplifies the power distribution system.	7. Relatively short life.
8. Air or liquid cooling is acceptable.	
9. Highest microwave tube efficiencies: Injected beam – 35 to 50 percent Distributed emission – 45 to 65 percent	
10. Operated at saturation to give a constant output independent of input power variation; makes a good limiter.	
11. Can be used in a duplexed system with receiver and duplexer on the low input side.	
12. Structure is ideally suited for mass production under tight mechanical tolerance control.	

HUGHES 394H TWT PERFORMANCE

A space qualified traveling wave tube is described in some detail as representative of spacecraft power amplifiers.

Highly reliable traveling wave tube manufacturing techniques were developed at Hughes Aircraft Company during the 1960 to 1965 period. As a result several space qualified TWT have been provided for various United States spacecraft. These spacecraft include the Syncom series of spacecraft, Surveyor, Mariner, Lunar Orbiter, the ATS spacecraft, Apollo, and Intelsat I, II, IV. This series of tubes has an output power range of 2 to 20 watts.

Typical of these tubes in many respects is the 394H, the tube used in the Apollo spacecraft. One feature that is not typical of most of these tubes is the ability to change the power output. The 394H has two power outputs, 5 watts and 20 watts. This was incorporated in order to consume less d. c. power when a high power output was not needed.

The figure illustrates the 394H and the table gives typical specifications.

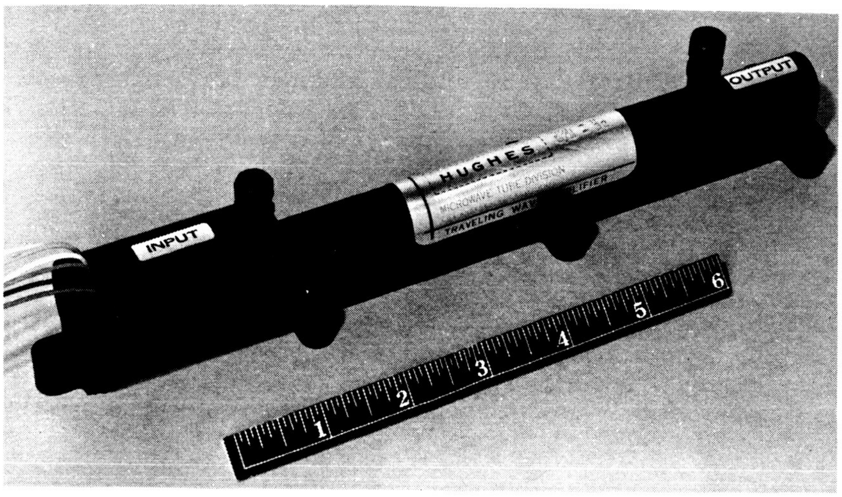

Hughes 394H Traveling Wave Tube

Specifications for 394H TWT

	5 Watt Mode	20 Watt Mode
Frequency	1.8-2.6 GHz	1.8-2.6 GHz
Power Output	5 W	20 W
Duty	CW	CW
Gain	20 dB	26 dB
Efficiency*	25%	33%
Beam Voltage (Cathode) E_b 2	-1175 V	-1425 V
Beam Current I_b	26 mA	60 mA
Helix Current I_w	0-6 mA	0-10 mA
Anode 1 Voltage E_a	-350 V	0 V
Anode 1 Current I_a	0.1 mA	0.1 mA
Anode 2 Voltage E_a	+100 V	+100 V
Anode 2 Current I_a	0.1 mA	0.1 mA
Collector Voltage E_c	-550 V	-450 V
Collector Current I_c	20-26 mA	50-60 mA
Heater Voltage	5.2 V	5.2 V
Heater Current	.3 A	.3 A
Expected Life	90,000 hrs.	25,000 hrs.
Cooling	Conduction	Conduction
Focusing	PPM	PPM
Weight	20 oz.	20 oz.
Length	9.5 in.	9.5 in.

*Midband efficiency including heater power.

FUNDAMENTALS OF MILLIMETER AND SUBMILLIMETER SOURCES

Linear beam and traveling-wave tubes are the types best suited for use as millimeter sources (30 GHz to 300 GHz). Submillimeter sources are still in the research and development stages and use harmonic generation to obtain the desired frequencies.

Millimeter Sources

Most of the successful attempts to develop sources in the millimeter wave region of the spectrum have involved extensions and extrapolations of the microwave device techniques. However, since the slow-wave circuit must have dimensions comparable to a wavelength, the problems of electron control and circuit thermal dissipations become formidable. The linear beam, or O-type distributed interaction device overcomes these difficulties better than the klystron or crossed-field tube for rather fundamental reasons.

In the traveling-wave tube the electron stream need not touch the rf circuit, and the beam collection function is accomplished by a separate and easily cooled electrode. A distributed interaction device, such as a traveling-wave tube, has an additional advantage over a single output gap tube, such as a klystron, for when all the power must be transferred to the output circuit via a single gap, high Q circuits are involved with the problems of multipactor effects and voltage breakdown.

Surprisingly, the efficiency of the overall device in millimeter wavelengths does not suffer appreciably when compared to microwave tubes. Because the millimeter interaction efficiency is necessarily low, the beam has a more uniform distribution of velocities. Accordingly, the collector electrode can be operated closer to cathode potential without danger of returning slow electrons into the circuit region. This operation results in a recovery of the overall conversion efficiency.

Submillimeter Sources

The conventional techniques of rf device design become impractical at frequencies over 300 GHz. Barring a technological breakthrough, one of the better means of producing power at these frequencies involves harmonic generation. Because large powers are available in the millimeter wave region, comparatively low harmonics are needed with reasonable conversion losses. The problem resolves itself to the development of a non-linear device that can accept large input powers. One of the likely candidates for this application is high pressure gas discharge plasmas. Notable success has been achieved in this area and there appears to be considerable promise for further development.

WEIGHTING FACTORS

Rule of thumb relationships are given to relate frequency, power and weight. Bounds on power output as a function of frequency is also given.

Because of the complexity of the tube design problem, it is difficult to reduce the available tradeoffs to simple scaling laws for all parameters. The general rule is to indicate the difficulty in achieving a particular performance level relating any two designs according to the factor of power times the square of the frequency. While this guide represents a gross oversimplification, it is still probably the best first approximation to a general scaling factor.

Some of the scaling laws pertaining to particular tube parameters can be given crude approximations. Since power, weight, voltage, bandwidth and frequency are the most important considerations for system application, the following guide is intended to relate these parameters.

For Constant:	then:	
Frequency	Power	Proportional to $(\text{Voltage})^{1/2}$
Power	Frequency	Proportional to Voltage
Frequency	Weight	Proportional to (% Bandwidth)

Figure A indicates the frequency power relationship based on an rf heating limitation, while Figure B indicates the fabrication tolerances required to achieve satisfactory TWT performance.

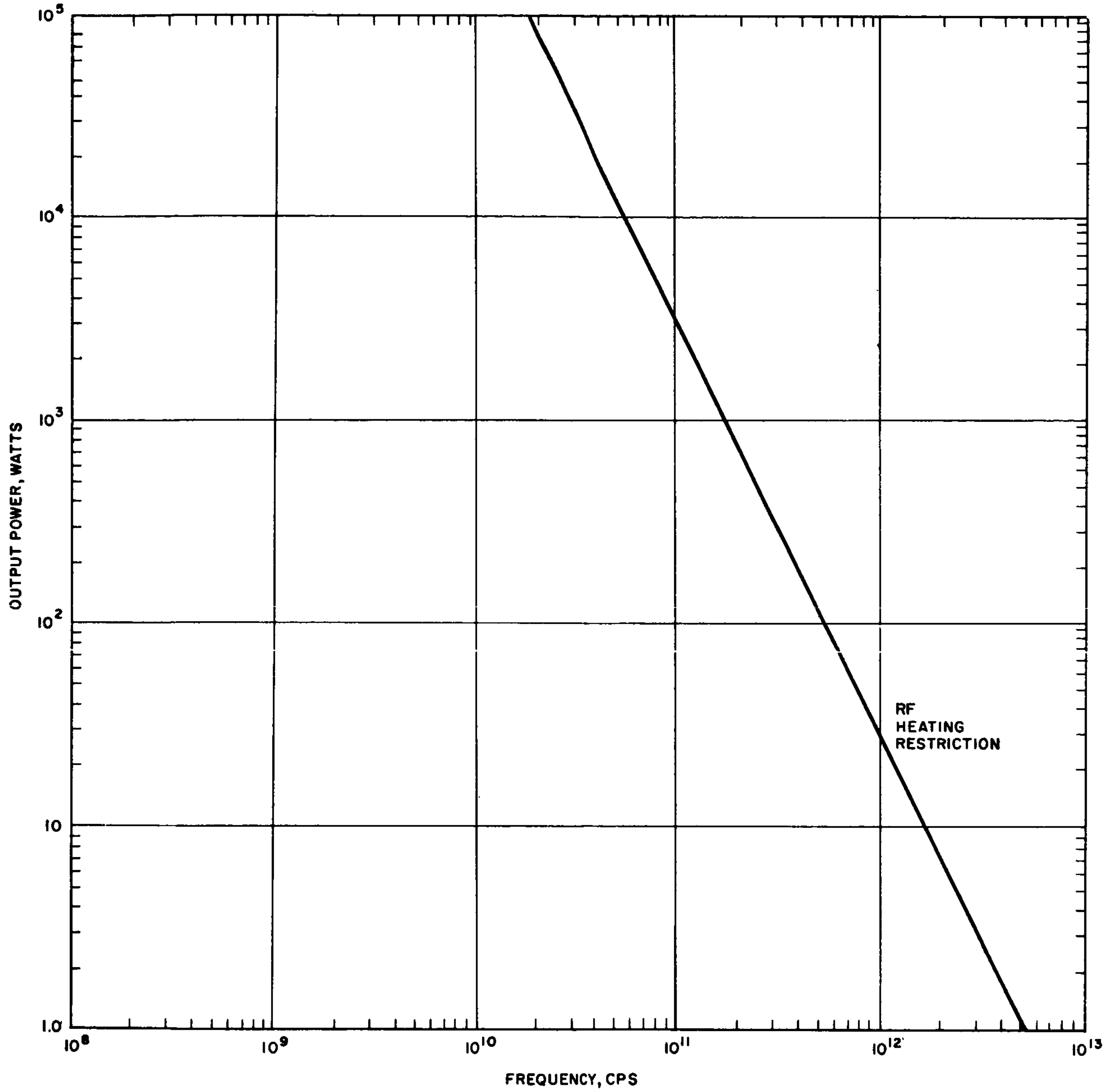

Figure A. Power Limitations for a Single TWT, as a Function of Frequency

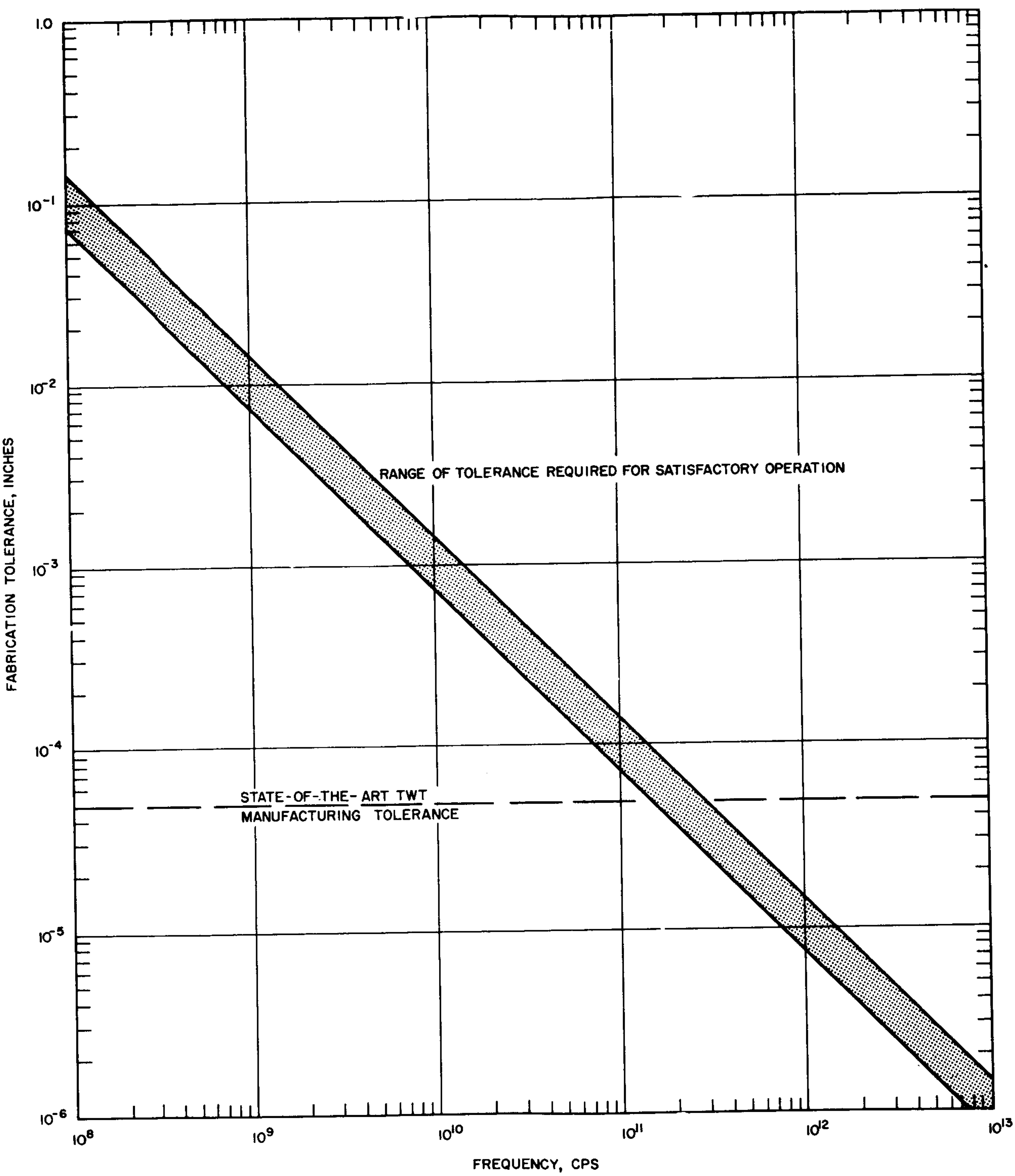

Figure B. Required Manufacturing Tolerances in TWT's as a Function of Frequency

PERFORMANCE OF VACUUM TUBE SOURCES

UHF, microwave, and millimeter wave sources provide a wide selection of unique performance parameters.

UHF Sources

The present state-of-the-art in UHF power grid tubes varies from a 100-MHz tube that supplies 100 kilowatts and weighs 100 pounds, to a 1000-MHz tube that supplies 100 watts and weighs 5 pounds.

Microwave Sources

Microwave sources fall into two general classifications. First are the relatively low power tubes that are very light and provide long and reliable life operation. Several such tubes have been used in current spacecraft with excellent results. In general, they provide from 2 to 20 watts in the range of 1 to 10 GHz and weigh about one pound. However, these tubes cannot compete on a power/weight basis with the brute force power tubes that have been built without primary concern for total system weight. The latter tubes demonstrate power in excess of 100 kw, although the weight of the tube and magnet system can easily exceed 1000 pounds. Indeed, development is in progress on a tube to produce one megawatt of cw power at X-band. While the weight and voltage penalty for these tubes is high, they are without competition for transmitting maximum power levels.

Millimeter Wave Sources

Available power levels for millimeter waves between 30 and 100 GHz have increased by three orders of magnitude since 1960, and the efficiency of millimeter sources has increased to be competitive with microwave sources. One kilowatt cw sources are now available at 35 and 55 GHz with efficiencies up to 35 percent. These levels are being achieved in devices using reasonable voltages and having operating lives of many thousands of hours. Methods are being developed to permit economical manufacture. New techniques are being exploited to realize lightweight sources suitable for airborne and space use.

It is convenient to separate the cw millimeter sources into low and high power categories. Since there seems to be a relative abundance of sources delivering tens of milliwatts, but very few delivering over 1 watt of cw power, a division at the 1 watt level has been chosen to separate "low" power from "high" power millimeter sources.

All of the commercially available low power prime sources are either backward-wave oscillators or klystrons. The power available from the prominent tube lines supplied by various manufacturers is shown in Figures A and B for the millimeter portion of the spectrum. Extensive lines of low power backward-wave oscillators are marketed by four companies. The most complete line is the Bendix TWO series, which covers the entire range from 40 to 140 GHz. Most of these tubes can be procured with either solenoids or permanent magnets. They use Karp structures and can be electronically tuned over 15 percent ranges. Maximum operating voltages are 3500 volts or less.

Sperry has developed a similar line of tubes covering the range up to about 90 GHz. Designations are SBM 421 and SBE 402. These tubes are packaged in permanent magnets and weigh only 7 pounds. Both tubes use the Karp structure and maximum operating voltage is 3200 volts.

Siemens-Halske markets the RWO 40, 60, and 80 covering the frequencies from 26.5 to 90 GHz. Power output varies from 60 to 5 mw. The RWO 60 weighs about 17 pounds. These tubes require several variable voltages for various focusing electrodes. They use a form of interdigital slow-wave structure and convergent electron guns.

CSF of France dominates the very high frequency range beyond that shown in Figure A. The COE-20 will deliver 500 mw over a 10 GHz range at about 140 GHz, and will deliver about 1 watt over a few gigahertz. This is the first tube discussed which uses the Millman structure and is more typical of the high power designs. The COE 10 delivers 10 to 20 mw over a 10 percent range of 300 GHz. The COS-09 delivers 30 to 50 mw in the 350 GHz range. The COS-07 delivers 5 to 10 mw in the 400 GHz range, while the COS-06 delivers 5 mw in the vicinity of 485 GHz. This company (CSF) has demonstrated an oscillator which delivers 1 mw at 708 GHz, the highest frequency oscillator ever generated by this means. All of these tubes use the same general structure together with highly convergent electron guns. For the most part, operating voltage is kept to 7000 volts or less.

Many companies market extensive low power klystron lines operating up to 170 GHz. Most extensive coverage is achieved by Varian, which lists tubes capable of delivering 100 mw or more to 140 GHz, and 50 mw to 170 GHz. Maximum voltage is 2500 volts. The tubes are extremely light in weight and are air cooled. Oki Electric of Japan lists a series of reflex klystrons covering the range from 30 to 100 GHz. Available performance data indicate power levels of over 100 mw in the 30 GHz range to about 60 mw in the 75 GHz range. Amperex (Philips) lists the DX 184, 151, 242, and 237 which operate at 8 mm, 3.2 mm, and 2.5 mm, respectively. They deliver several tens of milliwatts up to 100 mw. Raytheon markets an extensive line with frequency coverage to about 120 GHz in its QKK series. Power levels vary from 100 mw at the lower frequencies to 20 mw at the higher frequencies. Litton Industries also markets several relatively high powered reflex klystrons in the 35, 50, and 70 GHz ranges.

The high power CW tubes shown in Figure C delivers 1 watt or more. All of the tubes which meet this requirement, except CMO8X, are linear beam, O-type devices. The type number of each is shown, followed by the letters O or A to designate it as an oscillator or amplifier. The oscillators shown in Figure C are of either the floating drift tube klystron type or the Millman backward-wave oscillator type, or are closely related to these types of tube.

Hughes markets backward-wave oscillators delivering 15, 8 and 2 watts at 5.5, 3.2, and 2 mm, respectively. These tubes are air cooled and operate at efficiencies up to 15 percent. All use depressed collectors to achieve this relatively high efficiency and low power dissipation in the tube.

PERFORMANCE OF VACUUM TUBE SOURCES

Litton markets the Elliott line of floating drift tube klystrons which operate in the 35 and 50 GHz ranges. The highest power available is 50 watts at 35 GHz from the L3736. All of the tubes are liquid cooled and mounted in permanent magnet packages weighing about 10 pounds.

Oki lists the 35F10 and 50F10 laddertrons which deliver 10 and 2 watts, respectively. Their principle of operation is similar to the floating drift tube klystron except that a distributed interaction is provided in the cavity. CSF lists another Millman type of oscillator which delivers 8 watts over an extensive range at 70 GHz. Watkins-Johnson advertises the W-J 266 amplifier which includes an internal feedback mechanism to make it oscillate.

Hughes lists the 812H, 813H, and 814H traveling-wave amplifiers which deliver 150 and 1200 watts at 5.5 mm, and 150 watts at 3.2 mm. These tubes use coupled-cavity slow-wave structures and highly convergent electron guns. The 812H and 814H are air cooled while the 813H requires liquid cooling. All of the tubes use depressed collectors (operating at about 30 percent of beam potential) to maximize efficiency. The 812H and 813H operate at 30 to 35 percent efficiency, while efficiency of the 814H is 20 percent. Small signal gain of the 813H is 26 db, with saturated gain over 20 db.

Two new tubes have been developed which have significantly advanced the state of the art of high power Millimeter Wave Source generation. The Hughes 819H has demonstrated over 5 kw of average power output at 55 GHz with a large signal gain of more than 20 db. Collector depression results in efficiencies of about 30 percent. The Hughes 826H tube has shown output power of almost 600 watts at 94 GHz. This tube has been operated in excess of 10 percent duty cycle with such very long pulse widths that the design is believed to be fully capable of cw operation. With reference to Figure C, these results obviously describe a new boundary to the state-of-the-art. In six years, the available output power has been increased by approximately two orders of magnitude. The W-J 226 also uses the coupled cavity circuit and delivers 1 kw at 35 GHz. Gain is 13 db and operating efficiency is about 10 percent. This tube is also liquid cooled, but does not incorporate a depressed collector.

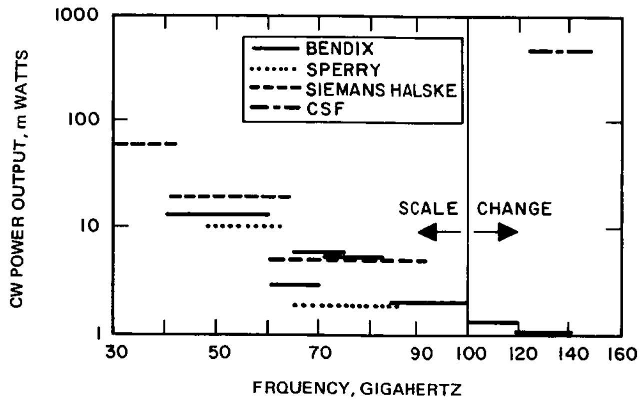

Figure A. Power Characteristics of Available Low-Power Backward-Wave Oscillators

Sperry and Bendix use Karp structure, and CSF used the vane line. In general, these tubes use low operating voltages and are suited for local oscillator and laboratory source use.

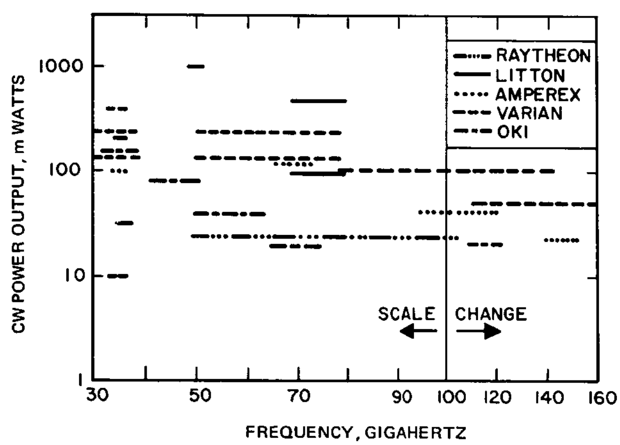

Figure B. Power Characteristics of Available Low Power Klystrons

All tubes are reflex klystrons and are light in weight since they use no magnetic focusing fields. They are particularly suited as pump, local oscillator, and laboratory signal sources.

PERFORMANCE OF VACUUM TUBE SOURCES

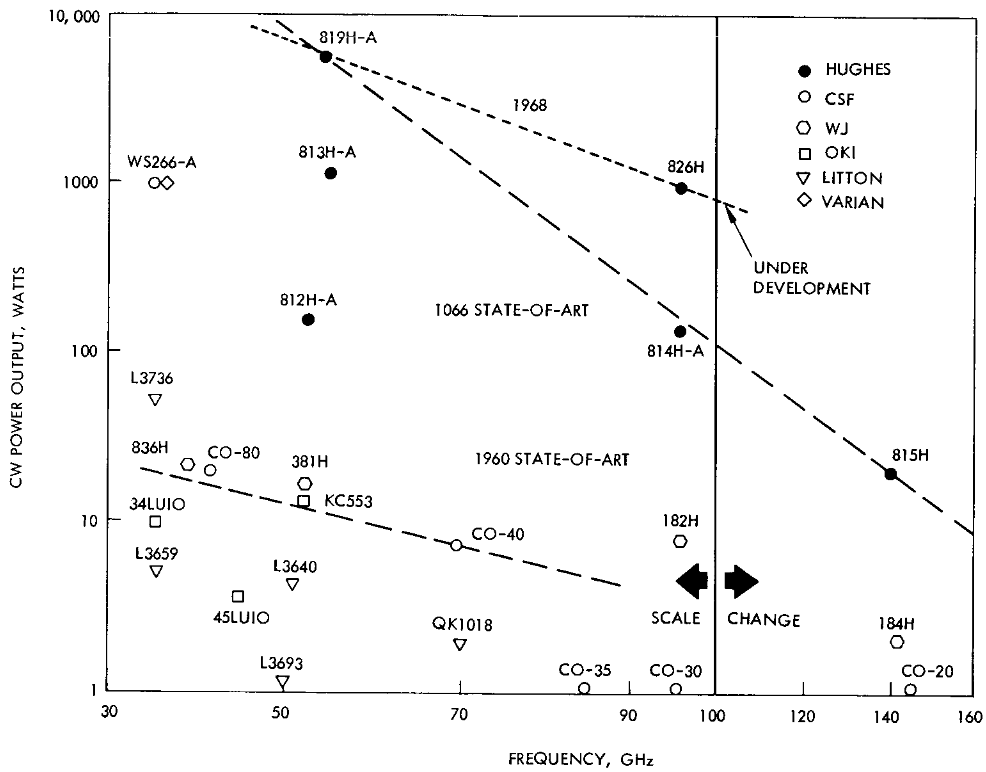

Figure C. Power Characteristics of Available High Power CW Sources

Most significant is 35 percent efficiency achieved in the 813H and marked increase in available power which has occurred since 1960. The letter -A stands for amplifier and the letter -O signifies oscillator.

TRANSMITTING POWER SOURCES

Radio Frequency Solid State Sources

Page

Introduction to Solid State Sources 28

Theory of Operation for Impatt Oscillators 30

Theory of Operation for Gunn Oscillators 32

LSA (Limited Space Charge Accumulation) Power Sources 36

State of the Art for LSA, Impatt, and Gunn Microwave Sources 38

Radio Frequency Burden Relationships 42

INTRODUCTION TO SOLID STATE SOURCES

IMPATT and Gunn solid state microwave sources hold promise of producing, for their extremely small size, relatively high power levels at high efficiencies. Transistor power output is given as a function of frequency.

Most active microwave solid state devices can be used either as oscillators or amplifiers, depending on the associated external circuitry and choice of operating point on the device characteristic. This discussion is limited to the oscillator mode of operation, since, to date, significant data is available only for this mode. The various microwave solid state oscillator sources are classified as follows:

- Parametric oscillators
- Tunnel diode oscillators
- Transistor oscillators
- Transistor oscillator - varactor multiplier combination
- Impact avalanche transit time (IMPATT) oscillators
- Gunn effect oscillators

Parametric oscillators are not of prime interest since they require auxiliary high frequency pump oscillators. Tunnel diode oscillators operate at high frequencies, but appear to be power limited. Thus, these two types are excluded from further consideration in this discussion. The power generation capabilities of transistor oscillators and associated varactor multipliers are summarized briefly. The bulk of the discussion is devoted to the IMPATT (IMPact Avalanche Transit Time) and Gunn oscillators, which appear at this time to offer potential for high power levels at high efficiency.

Transistor Oscillators

Extensive efforts have been underway for many years to improve the power-frequency characteristics of transistor oscillators. Recent progress has been achieved through use of paralleled transistors, monolithic integrated circuit techniques, and incorporation of improved varactor multipliers. The current state of the art as summarized by Matthei[1] is shown in the figure. The stimulus for study of the IMPATT and Gunn oscillators is provided by the fact that the power frequency performance of the figure is already exceeded in many instances with rudimentary versions of these more recent devices.

[1] Matthei, W. G., "Recent Developments in Solid State Microwave Devices," Microwave Journal, 9, No. 3, p. 39, March 1966.

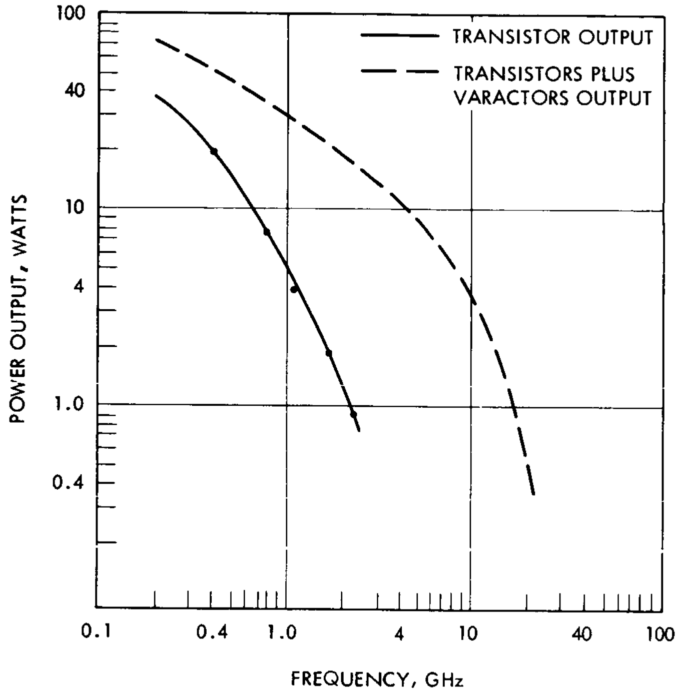

State of the Art of the Power Output of
Primary Transistor Oscillators and
Transistor Varactor-Multipliers
Versus Output Frequency

THEORY OF OPERATION FOR IMPATT OSCILLATORS

Physical constants of IMPATT oscillators are used to describe the operation of IMPATT oscillators and the frequency of oscillation.

In general, IMPATT oscillators involve the use of a semiconductor biased in the reverse direction and mounted in a microwave cavity. Bias is applied so that the operating point occurs in the avalanche breakdown region of the diode characteristic. Negative resistance and oscillations have been obtained in simple reverse biased p-n junctions as well as in the more complex n^+pip^+ configuration as first proposed by Read.

Gilden and Hines[1] have depicted the typical p-n junction in reverse bias for avalanche conditions as shown in Figure A. The active zone is composed of the thin avalanche region followed by the depletion zone through which carries drift at the saturation velocity, V_D. The realization of a negative resistance is associated with a 90-degree phase lag between current and applied ac voltage which occurs in the avalanche process, followed by a further 90-degree lag during the transit time of the carriers through the depletion zone.

Hines has shown that the equivalent impedance of the diode can be expressed as

$$Z = R_s + \frac{\ell_D^2}{V_D \epsilon A} \frac{1}{1 - \frac{\omega^2}{\omega_a^2}} + \frac{1}{j\omega C} \frac{1}{1 - \frac{\omega_a^2}{\omega^2}} \qquad (1)$$

under the condition that the transit time through the depletion layer (expressed in radians)

$$\theta = \frac{\omega \ell_D}{V_D} = \omega \tau_D$$

is less than $\pi/4$. R_s is the bulk resistance of the region outside the depletion zone, ℓ_D is the length of the depletion zone, A is the junction area, and C is the capacitance of the depletion and avalanche zones, i.e.,

$$C = \frac{\epsilon A}{\ell_a + \ell_D}$$

---

[1] Gilden, M. and Hines, M. E., "Electronic Tuning Effects in Read Microwave Avalanche Diodes," IEEE Trans on Electron Devices, ED-13, No. 1, p. 169, January 1966.

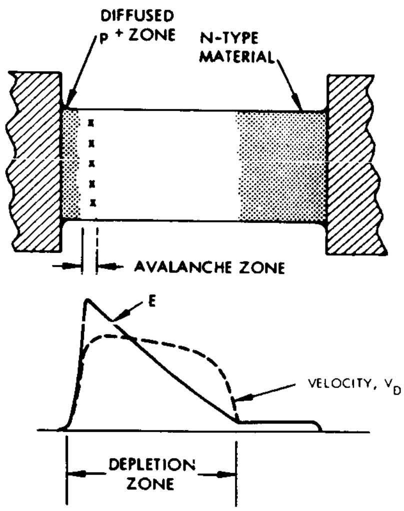

Figure A. Typical P-N Junction in Reverse Bias (Conditions at Avalanche)

THEORY OF OPERATION FOR IMPATT OSCILLATORS

The parameter ω_a is the avalanche frequency and is given by

$$\omega_a^2 = \frac{2\alpha' V_D I_o}{\epsilon A}$$

where α is the ionization coefficient and the prime denotes the derivative with respect to electric field, and I_o is the bias current. It is important to note that ω_a is a function only of the materials, junction geometry, and bias current. The equivalent circuit suggested by equation (1) is shown in Figure B, where the variable resistance R_D represents the second term and the impedance of the tuned circuit the third term. Note that for $\omega < \omega_a$, R_D is positive and the tuned circuit presents an inductive reactance. For $\omega > \omega_a$, R_D becomes negative and the reactance becomes capacitive. This dependence is sketched in Figure C. The oscillator is formed by supplying an inductance L in parallel through microwave circuitry; the negative of this inductive reactance is plotted in Figure C. The oscillator will operate at frequency ω_r where the diode capacitive reactance is equal to the inductive reactance; ω_o is the resonant frequency of the system at zero bias current. Tuning of the oscillator is accomplished either by varying I_o (and thus ω_a) or by varying L through mechanical adjustment of the microwave cacity. The operating frequency of the IMPATT oscillator will be given approximately by

$$f \approx \frac{V_D}{2\ell_D}$$

Since V_D is approximately twice as high for gallium arsenide as compared with silicon, the former will be more desirable for higher frequency operation. On the other hand, silicon technology is more advanced, and the higher defect density and higher thermal resistivity of gallium arsenide may limit its power capability.

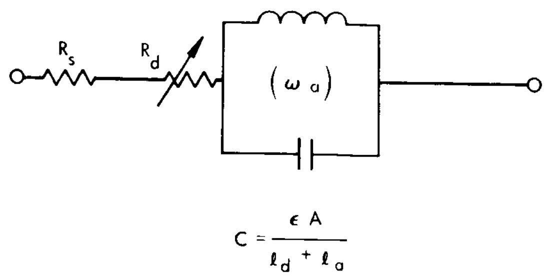

Figure B. Equivalent Circuit for Avalanche Diode at Small Transit Angle

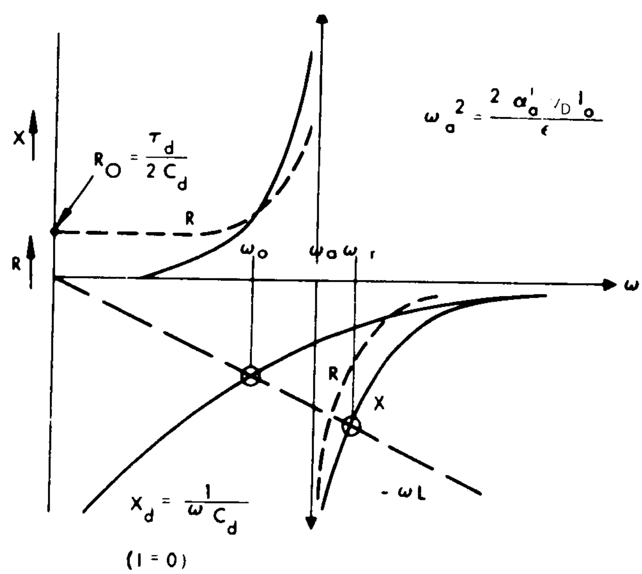

Figure C. Frequency Dependence of the Real and Imaginary Parts of the Diode Impedance

THEORY OF OPERATION FOR GUNN OSCILLATORS

The theory of the Gunn oscillator is described and the oscillation frequency is related to the operating constants.

Unlike the IMPATT oscillator, the Gunn effect oscillators do not require the formation of a junction. The effect takes place in a sample of the bulk material which is supplied with ohmic contacts on each side. Typical length of the samples is 25 to 200μ. Gallium arsenide is the most common material; however, the effect has been observed in cadmium telluride and indium arsenide. Typical doping densities for gallium arsenide are 10^{13} to $10^{14}/cm^3$.

Two modes of operation associated with the general Gunn effect concept have been observed. The first, as originally observed by Gunn,[1] takes place in the parameter range

$$\rho L > 2 \times 10^{12} \text{ cm}^2$$

where ρ is the doping density and L the length of the sample. A second mode of operation as observed by Thim,[2] et al., occurs in the range

$$2 \times 10^{12} > \rho L > 10^{10} \text{ to } 10^{11} \text{ cm}^2$$

The Gunn effect is essentially a current instability which occurs when an electric field of 3 to 5 kv/cm is applied across the bulk semiconductor. Associated with this field is saturation of the drift velocity of the carriers, thus removing the response out of the ohmic range. Increasing the field slightly beyond the onset of current saturation results in an instability which is manifested by large periodic spikes in the current.

This effect is explained for gallium arsenide by a decrease in average mobility of the carriers as field is increased beyond the threshold. In the energy band structure of gallium arsenide, in addition to the low lying principal conduction band, there are six satellite bands lying approximately 0.36 eV above the principal band. The mobility of electrons in the principal band is much higher than for that of the satellite bands. When the electric field reaches the threshold value, many electrons acquire sufficient energy to transfer to the satellite conduction bands where their mobility is low. Thus, on the average, a decrease in mobility occurs, and consequently a reduction in current, or, equivalent, a negative resistance characteristic evolves.

---

[1] Gunn, J. B., "Instabilities of Current in III-V Semiconductors," IBM Journal Res. Develop., 18, No. 2, pp. 141-159, April 1964.

[2] Thim, H. W., et al., Microwave Amplification in a dc Biased Bulk Semiconductor," Appl. Phys. Letters, 7, p. 167, September 1965.

When the applied field is above threshold, then it can be shown that a high field region (domain) with two low field regions are created within the sample. These domains then travel the length of the sample, L, in a transit time, τ.

$$\tau = \frac{L}{V_D}$$

Where V_D is the saturation velocity. The domains are created at the negative electrode, travel across the sample to the anode where they disappear simultaneously with the formation of the next domain. The fundamental frequency of the modulated current which results is given by

$$f = \frac{1}{\tau} = \frac{V_D}{L}$$

Since the frequency is dependent upon transit time, it is essential to have a planar surface at the negative electrode. Curved surfaces can lead to erratic domain formation in space and thus erratic output frequency.

LSA (LIMITED SPACE CHARGE ACCUMULATION) POWER SOURCES

LSA solid state devices avoid some of the limitations of IMPATT and Gunn oscillators to present promise of much higher rf power.

LSA power sources do not operate in a transit time limited mode as do the IMPATT and Gunn oscillators. Thus, a power-frequency-impedance restriction does not dictate the performance of the devices and allows the use of a bulk sample of the material many times larger than the transit length for the frequency of interest. Also, since the space charge is immediately quenched after traveling only a small portion of the total length of the active region of the device, the field remains in the negative resistivity range throughout most of the sample. This means that a greater volume of the sample contributes to microwave power generation than in the other solid state devices and a comparatively large piece of active material may be used to obtain the high power levels predicted.

Because LSA devices are not transit time controlled, the frequency of oscillation is determined by the tuning of the microwave circuit. The nature of the LSA operation and the state of the present devices is such that a fast rise-time bias pulse must be applied to power the generation of the microwaves and yet not destroy the device. LSA modes occur when the applied potential is several times the threshold for the formation of space-charge domains (approximately 4 or 5 times this threshold for best efficiency). If such domains are allowed to form and are not quenched after traveling a small portion of the device length, the heat generated by the large internal currents destroys the present devices. A radio-frequency voltage large enough to swing the field in the material below the threshold, must therefore be applied to the device as early as possible; at least within one transit time for a domain (1/2 to 1 nanoseconds for 350 to 700 micron thick devices now being studied). The large radio frequency voltage is started by ringing the microwave tuning cavity with a fast rise-time pulse. The start or turn-on time of the microwave output is therefore determined largely by the characteristics of the microwave resonator. The applied pulses presently have rise-times of less than 1 nanosecond.

The maximum theoretical power output from an LSA device is determined largely by the active bulk volume. The thermal conductivity of the present LSA material, GaAs, is 0.81 W/cm$\cdot$ C^{o} for good material, which is about 1/2 that of silicon. However the heat in an LSA device is not generated in a small volume junction which can be located less than 1 micron from a good heat sink, such as in the case of the IMPATT diodes. GaAs LSA devices therefore have the problem of adequately removing heat from the bulk of the device and present devices have been limited to short pulse length operation. By physically forming the devices to provide better heat transfer to a heat sink, longer pulse lengths and, consequently, greater average power can be obtained.

It has been predicted that LSA devices will deliver several hundred kilowatts peak power within several years. A main limitation is one of materials technology. In order to create and quench the space-charge near the cathode of the device, the dielectric relaxation times of the carriers for fields, below and above the threshold, must be adjusted for the desired frequency of operation. The relaxation times are a function of the doping of the material and a limitation on the $^{n}/f$ ratio arises. (Here, n is the doping/cm^3, and f is the desired frequency.) It can be shown that $2 \times 10^4 < (^{n}/f) < 2 \times 10^5$, in order for LSA modes to occur, meaning that the doping for an X-band device must be in the neighborhood of 10^{14} cm^{-3}. With the present state of the art of GaAs technology it is difficult to obtain large pieces of material with these doping levels and the carrier mobility required for LSA devices. When they become available, it will be possible to make devices in a physical shape with the thermal characteristics required for production of higher peak powers and much longer pulse lengths.

Preliminary noise investigations on LSA devices have shown that FM and AM noise figures are better by 10 to 20 db than those available from IMPATT devices.

STATE OF THE ART FOR LSA, IMPATT, AND GUNN MICROWAVE SOURCES

LSA, IMPATT, and Gunn oscillators have all demonstrated considerable power generation capability, especially for pulsed operation.

Current state of the art for solid-state devices is shown in the Table.

IMPATT Oscillators

Ultimate performance of IMPATT oscillators remains in doubt; many of the current results are being obtained from off-the-shelf varactor diodes which are not optimized for IMPATT operation.

An IMPATT oscillator circuit built at Hughes in microwave circuitry exhibited the characteristics shown in Figure A.

An analysis of the anticipated noise performance when used in amplifiers predicts noise figures of 37 to 40 db. Accordingly, it is anticipated that IMPATT oscillators will be relatively noisy. Brand,[1] et al., have observed a relatively high noise level in gallium arsenide oscillators. They note a significant increase in the noise figure of a single-ended mixer using the IMPATT oscillator as a local oscillator when compared with results using a klystron. However, in a balanced mixer configuration, they are able to duplicate the performance obtained with the klystron. Also by injection locking IMPATT oscillators considerable reduction in noise can be achieved as is shown in Figure B.

In summary, IMPATT oscillator characteristics are as follows:

1. Relatively high power-frequency characteristic
2. Frequency tuned by external circuit
3. Electronically tuned by bias current
4. Relatively high noise content in output

LSA Oscillators

The performance evaluation of the LSA solid state sources includes their promise for very high power but the large difficulty in material and cooling.

Gunn Oscillators

The state-of-the-art for power generation by Gunn oscillators is shown in the Table. Again it is difficult to anticipate ultimate performance from these relatively new devices. However, speculative estimates of pulsed powers range from 10 kw at L-band to 100 watts at X-band.

---

[1] Brand, F. A., et al., "Performance Characteristics of CW Silicon and GaAs Avalanche Diode Oscillators," G-MTT Symposium, Palo Alto, California, May 16-19, 1966.

Published Performance of Solid State Microwave Devices

LSA Pulse	LSA CW	GUNN Pulse	GUNN CW	IMPATT Pulse	IMPATT CW
615 W. peak 2. 3% efficiency 100 ns. 60 cps 7. 7 GHz (Cornell)	20 mw 44-88 GHz 2% efficiency (BTL)	143 W. peak 19% efficiency 2. 2 GHz 55-200 ns 60 cps (RCA)	110 mw 11 GHz 3% efficiency (BTL)	16 W. peak 0. 1% duty 4. 5% efficiency (Hughes)	1. 2 w. (9. 6% effective) 10. 7 GHz (Hughes)
3 W. peak 10 s 60 cps 50 GHz (Cornell)		1 GHz 20% efficiency (Varian)	43 mw 9-11 GHz 1. 8% efficiency (RCA)	2 W. peak X-band 1. 0% efficiency (Hughes microstrip)	544 mw 3% efficiency 10. 2 GHz (Hughes microstrip)
85 W. peak 100 s 60 cps (Cayuga diode, Hughes)				28 W. peak 3% efficiency 8 GHz 1 s 1 KHz (M. A.)	1. 1 W. 7. 7% efficiency 12 GHz (BTL)
50 W. peak 6% efficiency 100 ns 60 cps 8 GHz (Varian)				435 W. peak* 22% efficiency 425 MHz 10% duty (RCA)	
200-100 mw peak 9% efficiency 50 GHz (BTL)				180 W. peak* 60% efficiency 775 MHz 10% (RCA)	

*Characterized as an "Anomolous IMPATT," Theory and predicted performance are not well understood. It is not known whether or not this type of diode can be scaled or will perform at X-band.

STATE OF THE ART FOR LSA, IMPATT, AND GUNN MICROWAVE SOURCES

Evaluation

Currently, the consensus of opinion seems to favor the IMPATT oscillator as the most useful on the basis that its power frequency characteristic is higher, its frequency can be adjusted by external circuitry and bias current, and the width of a depletion zone can be made extremely small with relative ease as compared to the thickness of bulk samples.

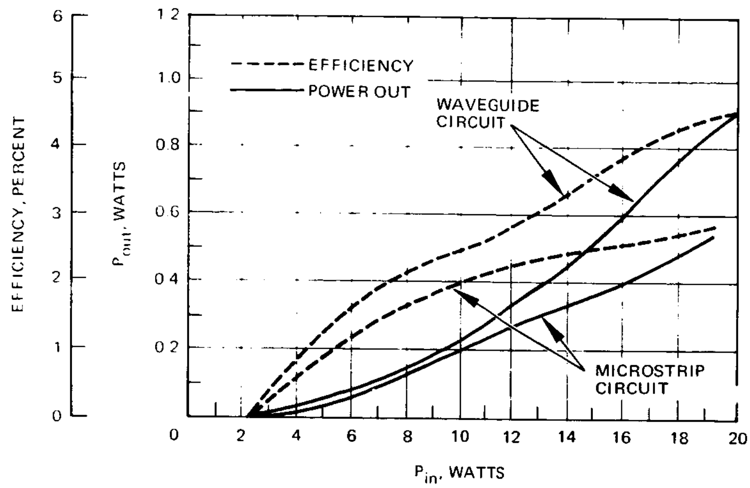

Figure A. CW Power Output and Efficiency Versus Power Input

For comparison the performance is shown for diodes from the same batch used in a waveguide circuit and a microstrip circuit operated at X-band.

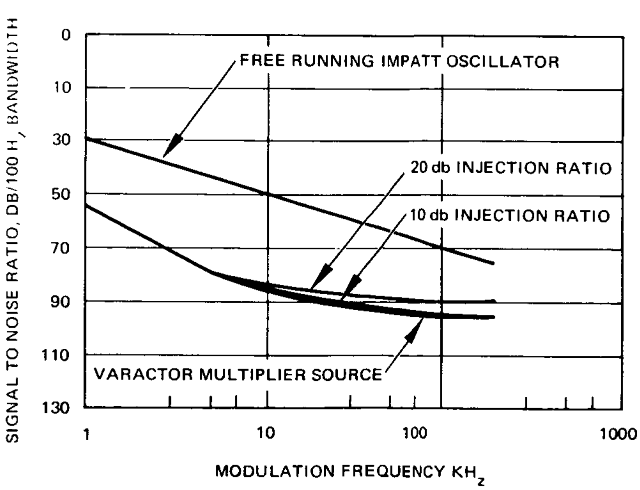

Figure B. FM Noise Characteristics of Injection Locked Microstrip IMPATT Power Source

RADIO FREQUENCY BURDEN RELATIONSHIPS

Cost and weight burden values are given for 2. 3 GHz carrier frequency

---

A main purpose of this contract (NAS 5-9637) is to compare the performance of several communications systems operating at different wavelengths. In order to do this an extensive modeling was undertaken which expressed parameters in the communication link equation in terms of cost or weight. (See Appendix A of this Volume.)

From the material given in this Part; Part 1, Transmitting Power Sources; and from other investigations, constants have been chosen which relate the transmitted power, P_T, to the weight of the transmitter, W_{P_T}, and to the cost of the transmitter, C_{P_T}.

The values used in these relationships are the best that could be determined at the date of this final report and are certainly subject to change. This is especially true in the cost relationships which represent estimates of fabrication costs only and do not include development costs.

Figure A gives the expected weight of a 2. 3 GHz transmitter and Figure B gives the expected cost, both given as a function of transmitted power, P_T.

The efficiency of a 2. 3 GHz source is taken as 25 percent.

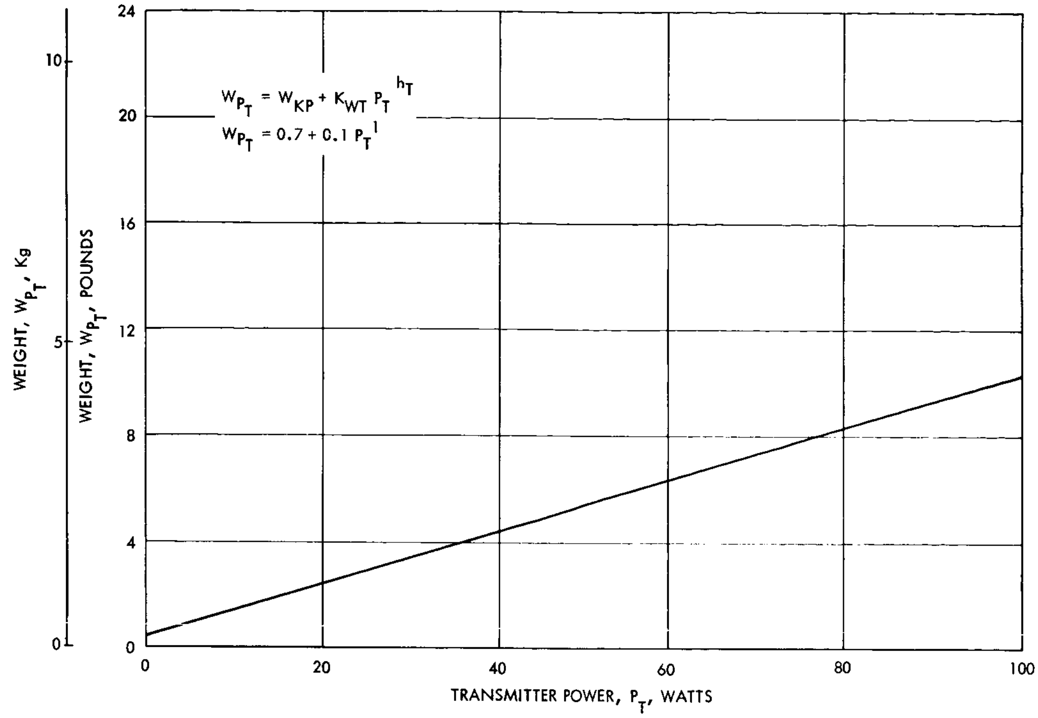

Figure A. Weight of S-Band Transmitting Power Source

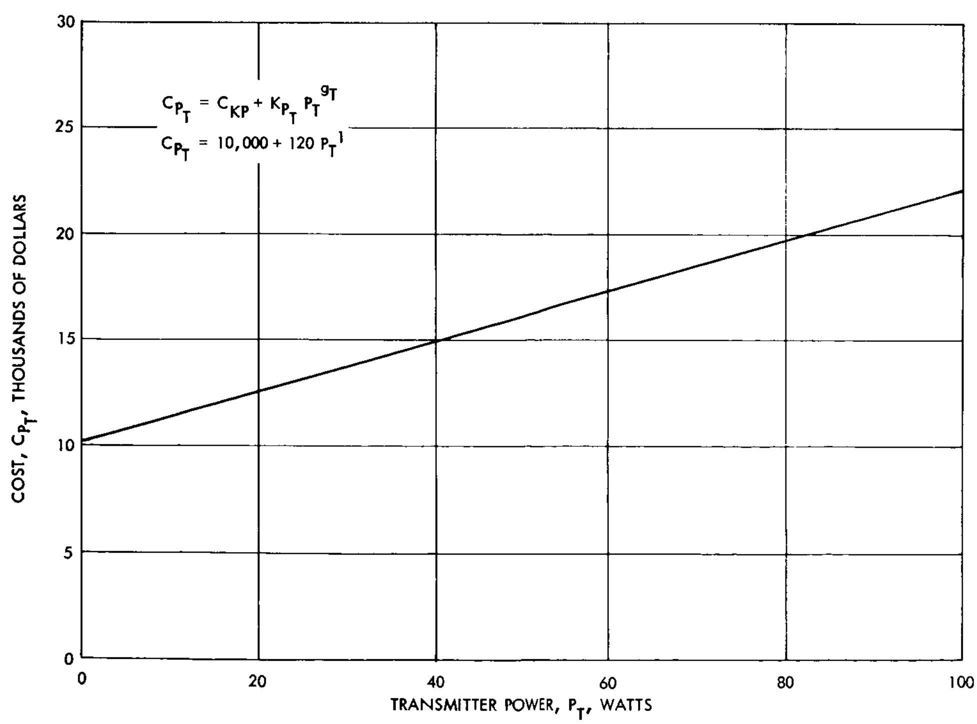

Figure B. Cost of S-Band Transmitting Power Source

TRANSMITTING POWER SOURCES

Optical Frequency Source Characteristics

	Page
Introduction	46
Laser Operating Fundamentals	48
The Argon Laser, Excitation Processs	50
Laser Amplifier Gain	54
Laser Power Output and Efficiency	58
CO_2 Laser Excitation Process	64
CO_2 Laser Frequency Spectrum	70
CO_2 Laser Scaling Laws	72

OPTICAL FREQUENCY SOURCE CHARACTERISTICS

INTRODUCTION

The laser sections describing Theory, scaling laws, mode coupling, AFC, and state of the art are introduced.

Optical frequency sources, in the form of gaseous and solid state lasers, are discussed in the following three sections. The purpose of this discussion is to provide the designer with an understanding of laser sources, some of the problems that must be solved for application to communications, means for solving these problems and finally the state of the art for several laser implementations. A brief summary of each of the major areas of interest is given below.

Fundamentals

Indicates the basic construction and operation of lasers.

Theory

The theory of laser operation is known with varying degrees of completeness. Some phenomena can be described quite well while others require further study and experimentation.

Scaling Laws

These have resulted from the theory and provide general guidelines which relate laser physical parameters with output power.

Mode Coupling

Lasers tend to operate in a number of oscillation modes simultaneously. Since some communication applications require a single oscillation, means for obtaining such performance is discussed.

AFC

Frequency stabilization is important in lasers operating in a communication system using heterodyne or homodyne detection. The stabilization of the laser frequency is extremely high compared to normal microwave requirements. Methods of stabilizing and effects of environment or stability are given.

State-of-the-Art

The state-of-the-laser-art is given in terms of power art, stability obtained and emperical relationships derived for the methodology which relate laser weight and cost to power out.

LASER OPERATING FUNDAMENTALS

Basic laser configurations and components are illustrated.

The basic requirements for a laser are twofold: A suitable material and a source of energy. The materials that have been used include solids, liquids and gases. Forms of energy that have been used include dc energy, r.f. energy, heat energy, and light energy.

A laser material is excited by the externally applied energy on a molecular or atomic level. When the excited atoms return to a lower energy level a discrete amount of energy is emitted. This energy is in the form electromagnetic energy of a fixed wavelength.

Many means have been developed to increase the amount of energy from the laser. A prominently used method is to put mirrors at each end of the laser material. The mirrors reflect the laser light through the laser material several times. In this way there is built up in the laser cavity of a relative high energy at the laser wavelength. One of the two mirrors is partially reflecting to allow the output energy to be coupled out of the laser. Figure B illustrates a typical configuration.

The cavity formed by the two mirrors has a ratio of stored energy to output energy or Q. Generally if the Q is too low no laser action results. It is possible then to change the Q to stop and start the laser action. Two common ways of varying the Q are to insert an electroptic switch (Kerr cell) in the laser cavity or to rotate one of the mirrors. This is often called "Q-switching". And can be used to generate very narrow pulses which start at a known time. Figure C illustrates this.

Laser modulation may be achieved either within or without the laser cavity as is indicated in Figures D and E. Internal modulation has the advantage of the laser energy passing through the modulator more than once and thus multiplying its effectiveness but has the disadvantage of having a larger amount of energy passing through the modulator (the circulating energy is Q times the output energy) and thus heating problems must be solved.

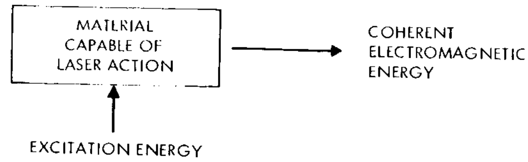

Figure A. Basic Requirements for Laser Action

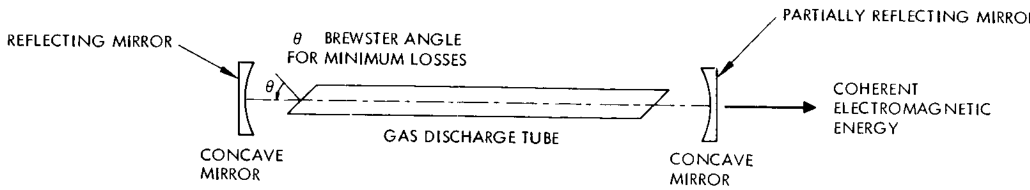

Figure B. External Confocal Mirror Laser Employing Brewster - Angle Windows

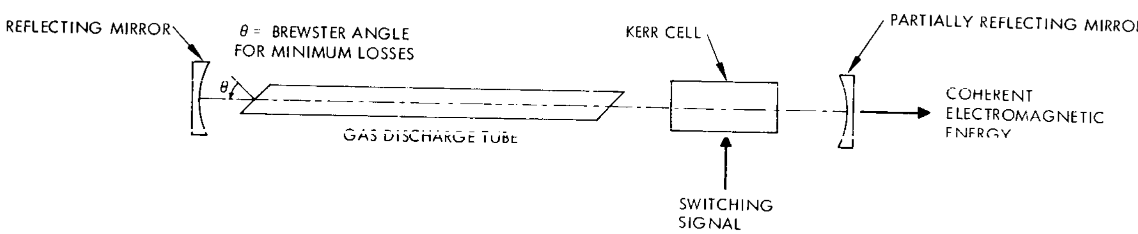

Figure C. Laser Employing Kerr cell for "Q-Switching"

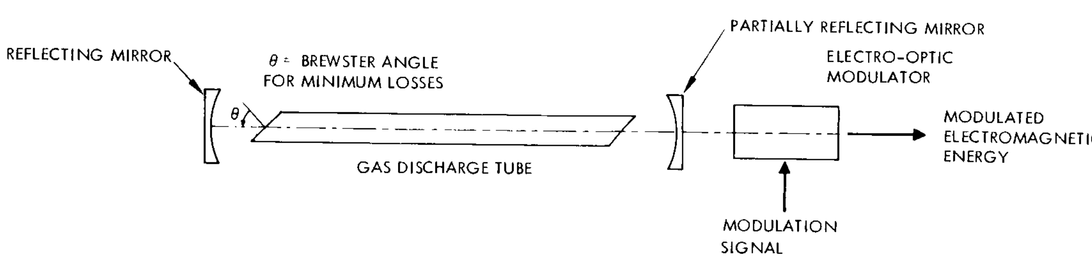

Figure D. External Laser Modulation

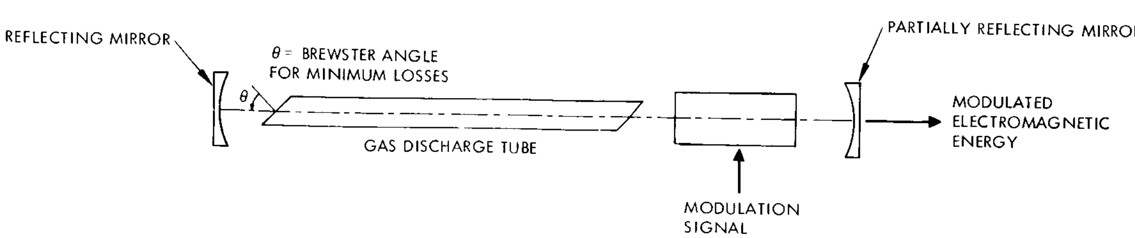

Figure E. Internal Laser Modulation

THE ARGON LASER, EXCITATION PROCESS

Ion lasers theory may be described in terms of excitation processes.

The model which seems to fit best the observed behavior of the argon ion laser is a three-level system originally proposed by Gordon, Labuda, and Miller. In this model, the upper laser level is populated by two successive electron collisions; the first produces an unexcited ion from a neutral atom, and the second excites the ion to the upper laser level. This two step process is consistent with the observed I^2 dependence of spontaneous emission from the singly ionized laser upper levels and the I^4 dependence of power output. The depopulation of the lower laser level then occurs by vacuum ultraviolet radiation to the ion ground state; this suggests a lifetime for the lower level roughly $(\lambda_{vac}\ UF/\lambda_{laser})^3$ shorter than the upper level.

The population processes are shown schematically in Figure A. It is not known directly whether the atom makes a "round trip" to the neutral ground state for each laser photon emitted. (This is an important factor in the laser's efficiency, since the electron energy that goes into the creation of the ion is essentially wasted.) However, the observed I^2 and I^4 dependences seem to indicate that it does. There is also some evidence that ionic metastable levels may play a role in the second electron collision, so that the picture of the three level system shown may be oversimplified.

The ultraviolet radiation which depopulates the lower level can be increasingly trapped as the ion density builds up. The "dead" region which develops at higher currents is a region of high attenuation rather than gain and is caused by radiation trapping. The gain is quite sensitive to the trapping coefficient* which, in turn, depends on the gas temperature. As the current pulse persists, the gas temperature rises and the trapping decreases, producing an inversion and oscillation for the remainder of the pulse, even if it extends to continuous operation. For lower currents or shorter pulse lengths this effect is not observed and the laser pulse follows the current pulse exactly.

Bennett, et al., have proposed that direct electron excitation from the neutral atom ground state to the upper laser level is the dominant populating mechanism. The preponderance of laser lines with p upper states follows from the selection rules of the "sudden perturbation" process referred to by Bennett. The short radiative lifetimes of the s and d lower levels then guarantee an inversion. From the evidence available at the present time, it seems likely that this population mechanism is dominant only in pulsed discharges with high E/p and short pulse

*Briefly, when trapping is included in the rate equations, the current-independent part of the expression for the population inversion appears as the small difference of two large terms, one of which contains the gas temperature. Changes in the gas temperature can then swing the population difference from attenuation to amplification.

duration; these are not conditions conducive to high efficiency or high average power. If very short pulse lasers (nanoseconds) are desired, then this mode of excitation may prove interesting.

In general, we may say that the excitation and de-excitation mechanisms are reasonably well identified for cw argon ion lasers. However, quantitative measurements of the relative importance of the various processes and construction of a numerically accurate mathematical model will require further detailed experimental study.

A 5 watt Argon laser is shown partially disassembled in Figure B, with the laser cavity removed from the solenoid. Figure C shows a simular laser mounted in a fixture with end mirrors.

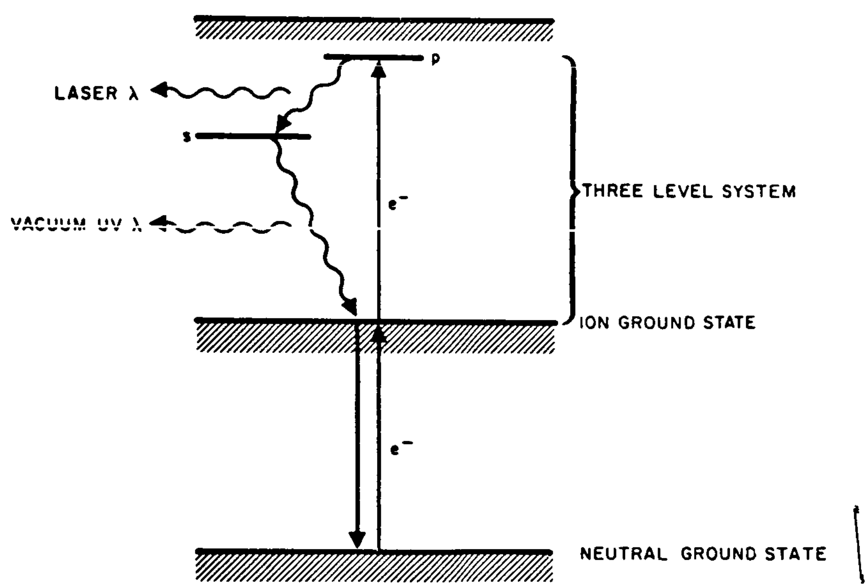

Figure A. Schematic Energy Level Diagram and Processes for Singly Ionized Atoms

THE ARGON LASER, EXCITATION PROCESS

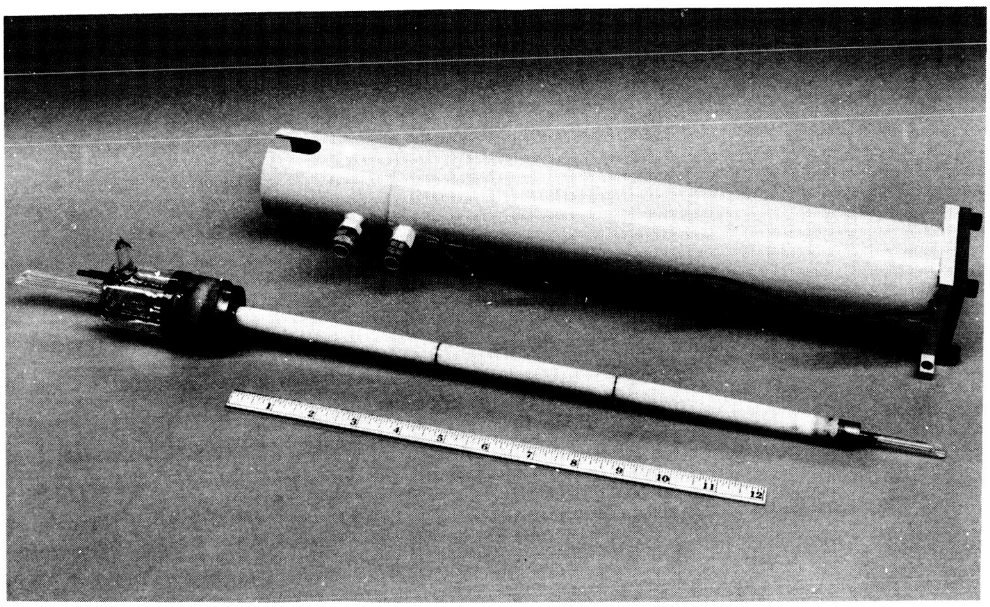

Figure B. Five Watt Argon Laser With its Solenoid

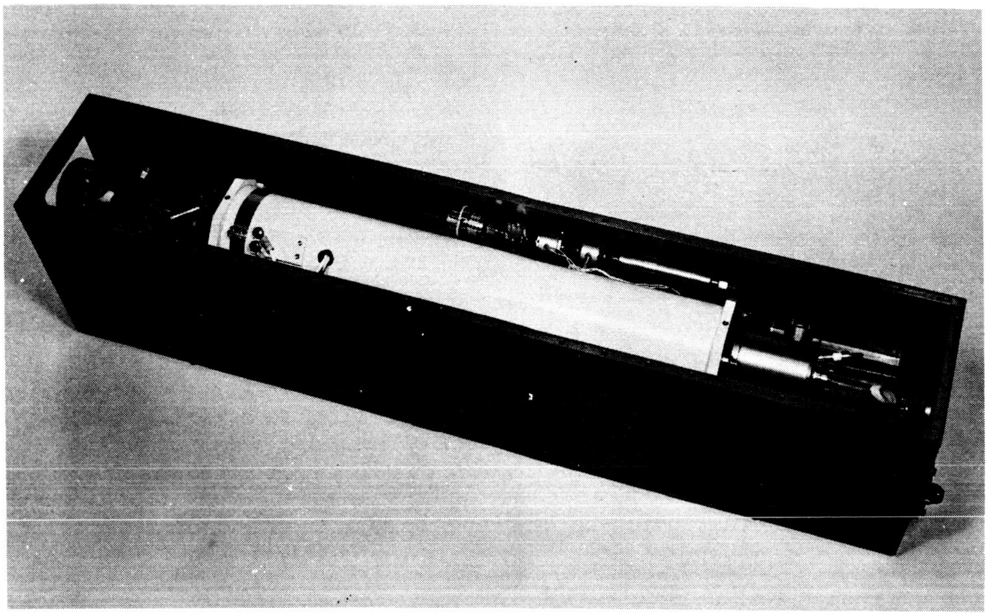

Figure C. Five-Watt Argon Laser Mounted Between Mirrors

LASER AMPLIFIER GAIN

The gain of a laser amplifier is given and it is to the Doppler broadened laser line is discussed.

The gain of a laser amplifier may be expressed as

$$G(S) = 1 + \frac{g_o L}{(S/S_{3dB})^n} \tag{1}$$

where G(S) is the actual gain in a single pass of a signal of intensity $S(w/m^2)$ through a laser of small signal gain coefficient g_o (m^{-1}) and length L. The power level S_{3dB} is the signal power density at which the small signal gain has been reduced by 3 dB (in the case n = 1). The exponent n equals 1 for homogeneous interaction (that is, interaction in which the signal may, with equal probability, interact with any atom in the laser), and is equal to 1/2 for inhomogeneous interaction (that is, the interaction may take place between the wave and only a small fraction of the excited atoms).

Equation (1) is valid of $S \gg S_{3dB}$ and if G(S) is not too large (i. e., if the approximation

$$\exp\left[G(S)\right] \approx 1 + G(S) \tag{2}$$

is valid). Note this does not require that $g_o L$ be close to unity.

Low power gas lasers usually fall into the category of inhomogeneous interactions; since the Doppler line width is so much greater than the natural line width, radiation at a single frequency can interact only with a small fraction of the atoms, e. g., those whose Doppler-shifted frequency falls within one natural line width of the incident radiation. We say this radiation "burns a hole" in the Doppler line when it depletes the excited atoms available to it without affecting the remainder.

Figure A contrasts the cases of (a) a hole burned by inhomogeneous interaction and (b) the depletion of the entire line by true homogeneous interaction. This description in terms of inhomogeneous interaction remains valid for the gas laser even when many frequencies are present (multimode operation), provided the holes do not "overlap" sufficiently (Figure B). With sufficient overlapping, the gain line is effectively "burned off" (Figure C) and the laser behaves as if the interaction were homogeneous. Essentially, every atom can interact with some radiation in the closely spaced multimode case.* Even if the modes are not closely spaced, the line will burned off and behave as if the interaction were

---

*Note that this is a physically different effect from the case of a homogeneously broadened line that typically occurs in solid state lasers (ruby, for example). In the case of a homogeneously broadened line, every atom can interact with a single frequency signal. The net effect on the gain saturation is the same, however.

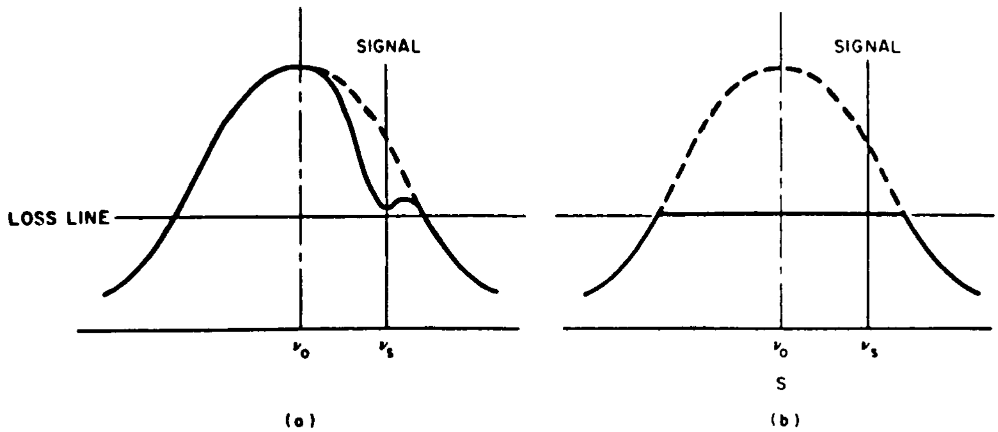

Figure A. Comparison of (a) Inhomogeneous Interaction (Hole Burning) and (b) Homogeneous Interaction With a Single Frequency

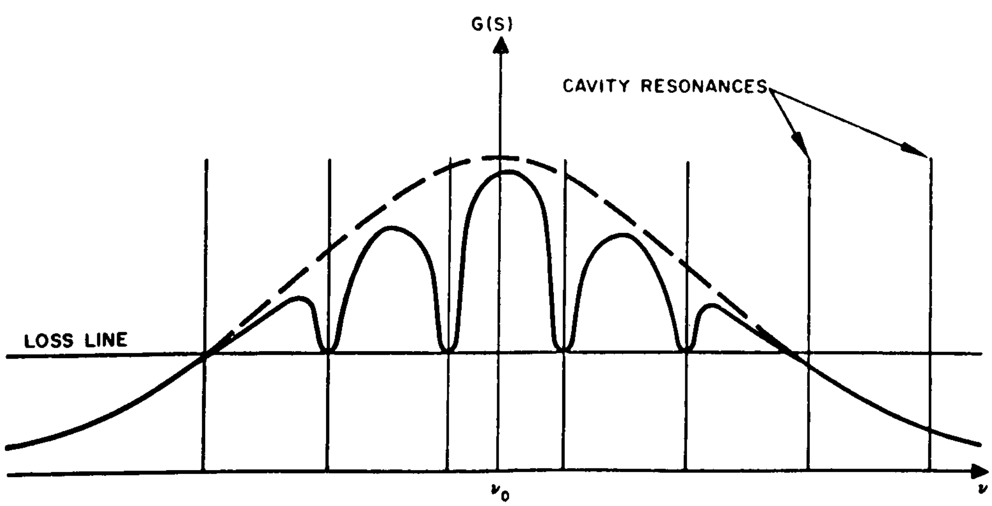

Figure B. Nonoverlapping Holes Burned in the Gain Line by a Multimode Laser

LASER AMPLIFIER GAIN

homogeneous, provided the signal intensity becomes sufficiently high. This is a result of the Lorentzian shape of the hole: it has broad "wings" which do not fall off rapidly from the hole center (not nearly so fast as the Gaussian, for example). Thus a gas laser capable of high power operation under multimode conditions will exhibit inhomogeneous interaction at low signal levels and homogeneous interaction at high signal levels.

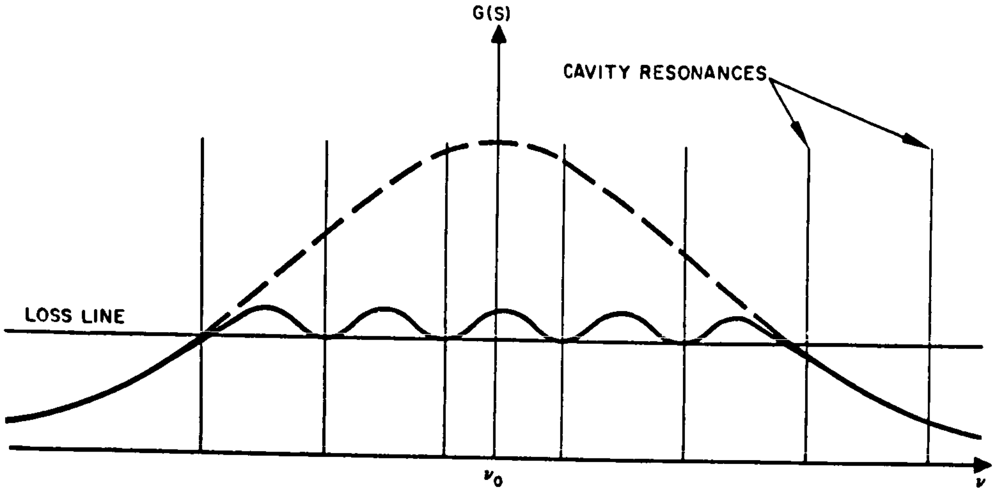

Figure C. Gain Line "Burned Off" by a Multimode Laser

LASER POWER OUTPUT AND EFFICIENCY

Qualitative expressions are derived for laser output power and laser efficiency.

Power

The condition for steady state oscillation is

$$R\ G(S) = 1$$

where

R is the fraction of the total laser power that is reflected back into the laser cavity

G(S) is the amplifier gain in a single pass of a signal with intensity S.

From the previous topic,

$$S = S_{3dB} \left(\frac{Rg_oL}{1 - R}\right)^{1/n} \tag{1}$$

Assuming further that $Rg_oL/(1 - R)$ is $\gg 1$ (which will be true for the important ion laser lines), equation (1) simplifies to

$$S \sim \begin{cases} g_oL & \text{homogeneous interaction} \\ g_o^2L^2 & \text{inhomogeneus interaction} \end{cases} \tag{2}$$

where S is the power circulating in the cavity. The output power will be S(1 - R - losses). R and the losses are assumed to be constant.

To relate equation (2) to the discharge conditions, it is necessary to know the dependence of gain on the current. Spontaneous emission measurements show that the number density in both upper and lower levels N_2 and $N_1 (m^{-3})$ vary as J^2 (J is the current density in amperes per square meter)

$$N_2 - N_1 \sim J^2 \tag{3}$$

The "constant" of proportionality actually contains some implicit current dependence (viz., the effect of gas heating on the Doppler line width and the effects of radiation trapping on N_1 caused by the current dependence of the ion density N_o). However, if this variation may be neglected for the moment, equation (3) gives the major variation of inversion with current. The gain coefficient of a laser discharge is approximately proportional to the inversion

$$g_o \sim N_2 - N_1 \tag{4}$$

except very near threshold, where it varies more as the 3/2 power

$$g_o \sim (N_2 - N_1)^{3/2} \tag{5}$$

(Actually, this is very approximate; the actual dependence is not expressable as a simple exponent.) For a discharge tube of diameter D, the power output (watts) and current (amperes) is given by

$$P = \frac{\pi D^2 S}{4} \tag{6}$$

$$I = \frac{\pi D^2 J}{4} \tag{7}$$

The above equations assume uniformity of S and J in the radial direction. This is probably a good assumption for J but not for S; however, to first order only the numerical coefficient (the cavity mode filling factor) will change and $P \sim D^2 S$ for a given cavity. Combining (2) through (7) yields:

$$P \sim \begin{cases} D^2 g_o L \sim D^2 (N_2 - N_1) L \sim D^2 J^2 L \sim \dfrac{I^2 L}{D^2} & \text{saturated} \\[2ex] D^2 g_o^2 L^2 \sim \begin{cases} D^2 (N_2 - N_1)^2 L^2 \sim D^2 J^4 L^2 \sim \dfrac{I^4 L^2}{D^6} & \text{moderate levels} \\[2ex] D^2 (N_2 - N_1)^3 L^2 \sim D^2 J^6 L^2 \sim \dfrac{I^6 L^2}{D^{10}} & \text{near threshold} \end{cases} \end{cases} \tag{8}$$

LASER POWER OUTPUT AND EFFICIENCY

The existence of $I^6 \rightarrow I^4 \rightarrow I^2$ behavior has been well verified in this laboratory; however, the exact limits of each regime are not well known as a function of the other parameters of the laser discharge (that is, those parameters which make up the constant of proportionality). The Figure indicates, in a highly schematic way, the expected variation of power output with current as the discharge length L and the cavity length ℓ are varied. The assumptions made are, of course, that $c/2\ell > \Delta\nu_N$ and $\ell > L$.

When a magnetic field is used to confine the plasma, the scaling is slightly different. Since the rate at which ions leave the discharge by diffusion to the walls is reduced by the magnetic field, the rate at which plasma is generated must also decrease in order to maintain an equilibrium state. The plasma generation rate is proportional to the electron density and the average electron energy, and the new equilibrium is maintained by a decrease in the average electron energy. The longitudinal electric field is roughly proportional to the electron energy, and it is the decrease in the longitudinal electric field (and the corresponding decrease in tube voltage) which accounts for the improvement in the efficiency of the discharge.

However, since the excitation of ions to the upper laser level is by electron-ion impact, the excitation rate is proportional to the plasma density squared and the average electron energy. The laser performance should be enhanced in a magnetic field because of the increased plasma density and efficiency of the discharge, this improvement should eventually be balanced or reversed by the decrease in the average energy of the plasma electrons.

Magneto-optical effects can further complicate the dependence of laser performance on the magnetic field.

It is quite clear that one of the major first steps toward improving the power output and efficiency of the ion laser is to make a thorough and careful set of measurements of gain, gain saturation, power output, and efficiency with the physical parameters I, L, ℓ, D, B, and pressure varied over as wide a range as is practicable. Such measurements will confirm, explore the limits of validity of the theory discussed here and provide a set of design criteria for future laser development.

Efficiency

The variation of efficiency with the major parameters may also be estimated. The power input to the discharge is approximately

$$P_{in} = IEL + IV_{cath}$$

where E is the average longitudinal electric field in the positive column and is a function of the diameter and the magnetic field. V_{cath} is the cathode fall, a function only of the cathode type and material. (For hot cathodes, such as those used in our cw tubes, V_{cath}=20 to 40 V; for cold cathodes, V_{cath} may be several thousand volts.) The exact dependence

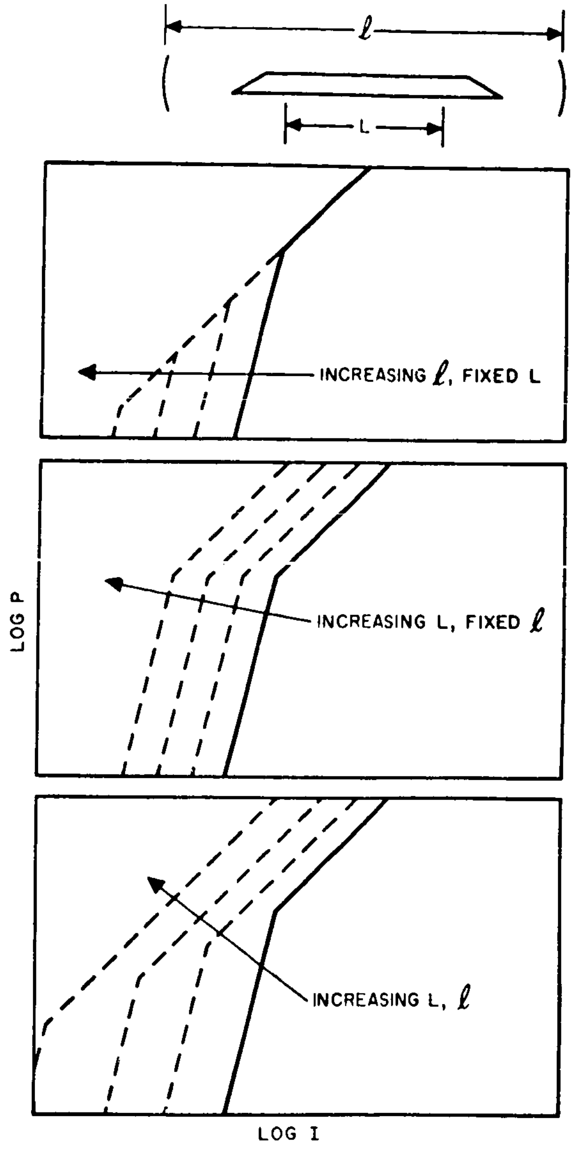

Schematic Representation of the Change in Power With Different Discharge and Cavity Lengths

LASER POWER OUTPUT AND EFFICIENCY

of E on diameter and magnetic field is not known. For the helium-neon laser the scaling relation pD = constant results in the relation ED = constant. Observations to date indicate that in the Ar II laser (and in the neutral xenon 3.5μ laser) the variation of E is faster than 1/D. The efficiencies corresponding to the three regions of operation may then be written

$$\eta \sim \begin{cases} \dfrac{I}{ED^2 + \dfrac{V_{cath}\, D^2}{L}} & \text{saturated} \\[2ex] \dfrac{I^3 L}{ED^6 + \dfrac{V_{cath}\, D^6}{L}} & \text{moderate level} \\[2ex] \dfrac{I^5 L}{ED^{10} + \dfrac{V_{cath}\, D^{10}}{L}} & \text{near threshold} \end{cases}$$

The saturated region will give the region of highest efficiency. For tubes long enough that V_{cath}/L is $\ll$ E, the saturated efficiency is independent of length, V_{cath} is typically 20 to 40 V, and E ranges from 0.5 to 20 V/cm, depending on the diameter and the magnetic field. With these numbers, it is apparent that the cathode fall will significantly degrade the efficiency in short tubes (20 cm or so).

CO_2 LASER EXCITATION PROCESS

The effects of various gas additives upon CO_2 laser performance is described.

This topic contains a discussion of the excitation processes for several types of CO_2 lasers. The types are distinguished by the gas additives to the basic CO_2 gas.

CO_2

Laser action in CO_2 has been observed on both the P- and R-branches of the 00^01 - 10^00 and 00^01 - 02^00 vibrational bands and on the P-branch of the 01^11 to 03^10 vibrational band. The following discussion will be primarily concerned with the high power P-branch rotational transitions of the 00^01 - 10^00 vibrational band which occur in a narrow wavelength interval near 10.6μ. The Figure illustrates the pertinent energy levels for CO_2 and CO_2-N_2 lasers. For simplicity the rotational levels are not shown for each vibrational state. The vibrational levels at the left of the CO_2 energy level diagram are those of the symmetric stretching mode (ν_1), at the right are those of the asymmetric stretching mode (ν_3), and in the center are those of the doubly degenerate bending mode (ν_2).

Excitation of the upper laser level in the CO_2 laser may occur via recombination and/or cascade from higher levels, or by electron impact, either directly or via a compound. Experiments indicate that the dominant mechanism may vary as conditions of the discharge are changed.

Decay of vibrationally excited CO_2 molecules is by spontaneous emission and/or collisional de-excitation. The calculated spontaneous radiative transition probabilities between the lower vibrational levels in CO_2 are listed in the Table. [1]

It is evident that for transitions other than 00^0n_3 - $00^0(n_3-1)$, spontaneous radiation is negligible. The lifetime of the 00^01 level, in the presence of radiation trapping, is $\sim 2 \times 10^{-2}$ seconds.

The amount of power produced by CO_2 lasers requires that the lifetime of the lower laser levels be 10^{-3} seconds. Consequently, de-excitation by CO_2-CO_2 collisions involving the conversion of vibrational energy to translational energy is the dominant relaxation mechanism. The levels of each vibrational mode reach internal thermal equilibrium via vibration-vibration exchange, then cross-relax to the fastest relaxing mode. In CO_2 the most probable vibration-translation relaxation mechanism involves vibrational quanta of the lowest frequency mode ν_2, i.e.,

$$CO_2(01^10) + M \rightarrow CO_2(00^00) + M + KE \qquad (1)$$

---

[1] Statz, H., Tang, C. L., and Koster, G. F., "Probabilities for Radiative Transitions in the CO_2 Laser System," presented at 1966 International Quantum Electronics Conference, Phoenix, Arizona, April 1966.

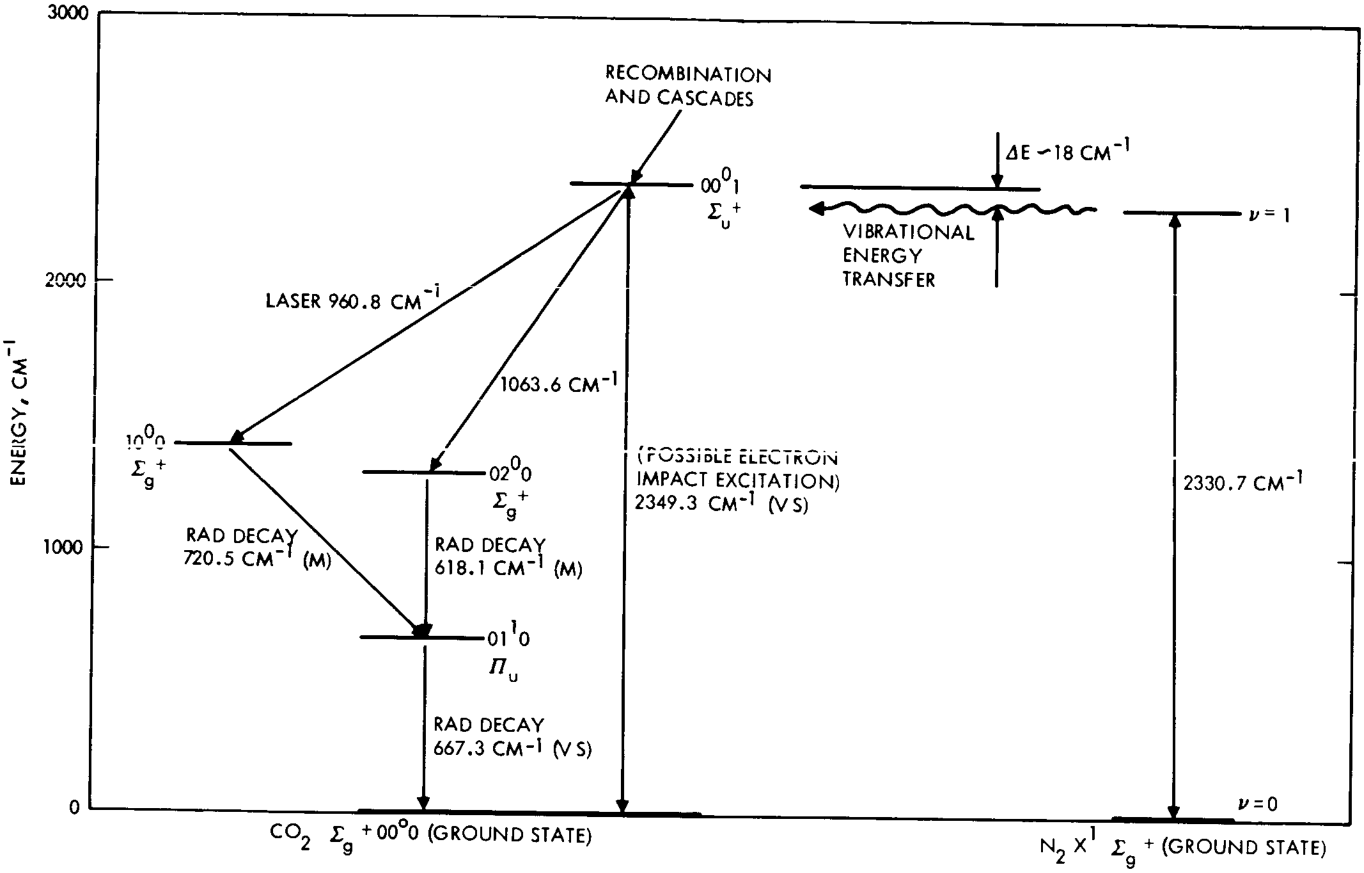

Energy Level Diagram Showing Pertinent Levels in CO_2 and N_2

CO_2 LASER EXCITATION PROCESS

Spontaneous Radiative Transition Probabilities in CO_2

Transition	Dominant Branch	Spont. Trans. Prob.
$00^01 - 10^00$	P	0.34 sec^{-1}
$00^01 - 02^00$	P	0.20 sec^{-1}
$10^00 - 01^10$	Q	0.53 sec^{-1}
$02^00 - 01^10$	Q	0.48 sec^{-1}
$01^10 - 00^00$	Q	1.07 sec^{-1}
$00^01 - 00^00$	P	2×10^2 sec^{-1}

where M is CO_2 or another species. The corresponding relaxation rates to the ground rate for molecules in the lowest vibrational levels of the ν_1 and ν_3 modes, 10^00 the lower laser level, and 00^01 the upper laser level, respectively, are several orders of magnitude slower. The lower laser level (10^00) relaxes to 01^10 by

$$CO_2\,(10^00) + M \rightarrow CO_2\,(01^10) + M + KE \tag{2}$$

or, since the 10^00 and 02^00 levels are in Fermi resonance, by

$$CO_2\,(10^00) + CO_2\,(00^00) \rightarrow CO_2\,(02^00) + CO_2\,(00^00) \tag{3}$$

or

$$CO_2\,(10^00) + CO_2\,(00^00) \rightarrow 2\,CO_2\,(01^10) \tag{4}$$

In each case, the final relaxation process is governed by (1). Calculations indicate that the rates for processes (1) and (2) are of the same order of magnitude, although the latter is somewhat slower, while the rate for $02^00 - 01^10$ vibration-translation relaxation is faster. Thus, the de-excitation of the lower laser level 10^00 is by vibration-vibration exchange with the bending mode which then relaxes via vibration-translation exchange to the ground state. The rate of this latter process controls the relaxation of the lower laser level.

CO_2 - N_2

The increase in output power from the CO_2-N_2 laser over that from the pure CO_2 discharge may be attributed to population of the upper laser level in CO_2 by transfer of vibrational energy from N_2 molecules in the $\nu = 1$ vibrational level of their electronic ground state. The selective excitation of the CO_2 molecule from its ground state to the 00^01 state takes place during a two-body collision involving a CO_2 ground-state molecule and a vibrationally excited N_2 molecule. From the Figure it is evident that the $\nu = 1$ vibrational level of N_2 at 2330.7 cm^{-1} is in very close coincidence with the 00^01 vibrational level in CO_2 at 2349.16 cm^{-1} ($\Delta E = 18.46\ cm^{-1} < kT_{rotational} \sim kT_{translational} \sim 210\ cm^{-1}$.) In addition, since N_2 has a zero permanent dipole moment, vibrational relaxation times for excited N_2 molecules are long and are determined by collisions with other molecules and walls. The addition of CO_2 allows excited N_2 molecules to relax via vibration-vibration exchange with 00^0n_3 levels of CO_2. The process with the largest cross section is

$$N_2\ (\nu = 1) + CO_2\ (00^00) \rightarrow N_2\ (\nu = 0) + CO_2\ (00^01) - 18\ cm^{-1} \qquad (5)$$

For N_2 molecules in higher energy vibrational states

$$N_2\ (\nu = \nu') + CO_2\ (00^00) \rightarrow N_2\ (\nu = \nu' - 1) + CO_2\ (00^01) + \Delta E \qquad (6)$$

Because of the large energy difference ($\sim 950\ cm^{-1}$) between the lower laser level 10^00 in CO_2 and the $\nu = 1$ vibrational level in N_2, the cross-section for excitation of ground state CO_2 molecules to the lower laser level through collisions with N_2 ($\nu = 1$) is much smaller than that for the reaction described in equation (5). In addition, the excitation of CO_2 (00^00) molecules to the 10^00 energy level involves a reaction in which both transitions; i.e., $N_2\ (\nu = 1) \rightarrow N_2 (\nu = 0)$ and $CO_2\ (00^00) \rightarrow CO_2 (10^00)$, are optically forbidden. It has been shown[2] that, for reactions involving collisions of the second kind, the cross-section for a reaction involving two optically forbidden transitions is smaller than that involving one forbidden transition for the same energy level discrepancy.

CO_2-N_2-He

A significant increase in power over that produced by CO_2 and CO_2-N_2 lasers is achieved by the addition of relatively large amounts of He to either discharge. At this time the role of the He has not been clearly defined although it has been determined experimentally that the He affects

[2] Bates, D. R., "Collision Processes not Involving Chemical Reactions," Discussions Faraday Soc., 33, p. 7, 1962.

CO_2 LASER EXCITATION PROCESS

the excitation of the upper laser level as well as the relaxation of the lower laser level. The former effect may result from the creation of plasma conditions (e. g., electron temperature) which favor excitation of the 00^01 level in CO_2. In addition there is the possibility of a three-body collision involving the transfer of energy from metastable He(2^3S_1) atoms to N_2 molecules, viz

$$\text{He}\ (2^3S_1) + 2\ N_2 \rightarrow \text{He} + 4N + \Delta E \qquad (7)$$

where $\Delta E < 0.1$ eV. The atomic nitrogen, thus produced, recombines to form vibrationally excited nitrogen in high vibrational levels which excite CO_2 molecules to the 00^01 vibrational level by the processes described in Equations (5) and (6).

The addition of He has little effect on the decay of the upper laser level 00^01. However, the rate for vibration-translation relaxation of CO_2 via the bending mode is dependent on the reduced mass of the colliding particles and is thus greater for CO_2-He collisions than for those involving two CO_2 molecules. The former collision process is one to two orders of magnitude more efficiency for relaxation.[3] Thus, it appears that improved laser performance due to the addition of He may be due in part to an increased relaxation rate of the terminal laser level.

An entirely different role may be played by the He in that it is able to reduce the gas temperature because of its high thermal conductivity. A low gas temperature leads to a reduction in thermal excitation of the lower laser level, which may be appreciable since the energy is only 0.17 eV, as well as an increase in the gain coefficient for the laser transitions.

Other Gas Additives

The addition of other gases (air, CO, H_2, water vapor, etc.) influences the output from the CO_2 laser in varying degrees; however, none is as effective as He. In the case of H_2 and water vapor it is felt that the primary effect is to enhance the relaxation rate of the terminal laser level by collisions. Air is thought to combine the roles of N_2 and water vapor. CO, which has a long relaxation time, may selectively excite CO_2 by vibration-vibration exchange with asymmetric stretching mode ν_3.

Effect of Gas Temperature

The lower level of 10^00 of the laser transition lies sufficiently close to the ground state ($\sim$0.17eV) that a significant fraction of the CO_2 molecules may be thermally excited to that state if the gas temperature becomes too high. This effect may be quite appreciable in large diameter tubes.

[3] Patel, C.K.N., Tien, P.K., and McFee, J.H., "Cw High-Power CO_2-N_2-He Laser," Appl. Phys. Letters, 7, p. 290, 1965

Under the assumption that laser action will cease when 10 percent of the ground state molecules are thermally excited to the lower laser level, the cut-off temperature is 662°C. With a power input of 0.1 W/cm^3 and in the absence of any cooling, this temperature can be reached and laser action cease in times of the order of 0.1 second. Under steady-state conditions in which cooling is provided at the discharge tube walls, thermal excitation of the lower laser level will present oscillation along the laser axis for diameters greater than approximately 5 inches.

With the assumptions that the laser transition is predominantly Doppler-broadened and that the rotational level populations are described by a Boltzmann distribution at a temperature $T_{rotational} \simeq T_{translational}$, it can be shown that the gain coefficient of the laser transitions is inversely proportional to the molecular temperature, i.e.,

$$g_o \propto (T_{translational})^{-3/2} \tag{8}$$

The validity of the latter assumption is supported by the fact that rotational thermalization times are of the order of microseconds while in CO_2 the vibrational and radiative lifetimes are of the order of milliseconds and seconds, respectively. In addition, increased laser gain and output power have been observed experimentally by cooling the walls of the discharge tube.

CO_2 LASER FREQUENCY SPECTRUM

The transitional frequencies for a CO_2 laser are tabulated.

Vibrational-Rotational Transitions

The transitions of the P and R branches of the 00^01 - 10^00 vibrational band of CO_2 on which cw laser oscillation has been observed are listed in the Table. All the lines do not oscillate simultaneously but are obtained by placing a dispersive element, such as a prism or grating, in the optical cavity. In the absence of such a wavelength selective resonator, several of the strongest P-branch transitions will oscillate at the same time.

Single Wavelength Operation

The gain of the CO_2 laser is sufficiently high that several rotational transitions may oscillate simultaneously. For single wave-length operation, wavelength selective cavities utilizing prisms or gratings will be required. Because of the rapid rotational thermalization ($\tau \sim 10^{-6}$ sec), molecules in the other rotational levels of the 00^01 level may cross-relax into the upper laser level of the rotational vibrational transition which is selected by the resonator configuration. Similarly, molecules in the lower laser level may cross-relax into other rotational levels of the 10^00 level. Consequently, the output power obtained under single wavelength operation may be close to the total power produced when several transitions oscillate simultaneously.

Single Mode Operation

The narrow Doppler width of the CO_2 laser transition (50-75 MHz) allows operation in a single axial mode with resonators 2 and 3 meters long. Single transverse mode operation in low power lasers ($\leq$10W) may be achieved by proper resonator design. However in very high power CO_2 lasers, transverse mode control may be complicated by the presence of self focusing and the production of a filamentary structure in the laser output.

CO_2 Continuous Wave Laser Oscillation Wavelengths in the 00^01 to 10^00 Band of CO_2

Transition	Measured Frequency (cm^{-1})	Transition	Measured Frequency (cm^{-1})
P_2	959.43	R_2	963.33
P_4	957.76	R_4	964.74
P_6	956.16	R_6	966.18
P_8	954.52	R_8	967.73
P_{10}	952.88	R_{10}	969.09
P_{12}	951.16	R_{12}	970.50
P_{14}	949.44	R_{14}	971.91
P_{16}	947.73	R_{16}	973.24
P_{18}^*	945.94	R_{18}^*	974.61
P_{20}^*	944.15	R_{20}^*	975.90
P_{22}^*	942.37	R_{22}^*	977.18
P_{24}^*	940.51	R_{24}^*	978.47
P_{26}	938.66	R_{26}	979.67
P_{28}	936.77	R_{28}	980.87
P_{30}	934.88	R_{30}	982.08
P_{32}	932.92	R_{32}	983.19
P_{34}	930.97	R_{34}	984.35
P_{36}	928.94	R_{36}	985.42
P_{38}	926.96	R_{38}	986.49
P_{40}	924.90	R_{40}	987.56
P_{42}	922.85	R_{42}	988.63
P_{44}	920.77	R_{44}	989.61
P_{46}	918.65	R_{46}	990.54
P_{48}	916.51	R_{48}	991.47
P_{50}	914.41	R_{50}	992.46
P_{52}	912.16	R_{52}	993.34
P_{54}	909.92	R_{54}	994.18
P_{56}	907.73		

* Strongest transitions in the group

CO_2 LASER SCALING LAWS

Scaling laws for power as a function of the laser tube diameter are given. Some early CO_2 laser developments are also documented.

Variation of Output Power

The variation of output power per unit volume and per unit length as a function of discharge tube diameter is shown in Figure A. The data points which are shown represent actual reported performance of laser oscillators as achieved by Hughes, Raytheon, Perkin-Elmer, Bell Telephone Laboratories, and C. G. E. in France. The shaded areas represent an estimate of the uncertainty implied with the dark curve through the center representing a best estimate for use in establishing design criteria. Because of the scatter of data points in the 6 to 9 cm range, extrapolation of the power per unit length parameter is difficult. The power per unit volume estimates are more consistent and may indicate the existence of some asymptotic value.

Variation of Input Power

In Figure B, the axial electric field along the discharge tube for optimum laser performance is plotted as a function of tube diameter. As expected, it decreases rapidly with diameter until the loss of ions to the walls become negligible. It is apparent that the field is approaching an asymptote of approximately 30 volts/cm. In Figure C, the optimum discharge current is plotted as a function of tube diameter. Although difficult to prove conclusively from the data it is expected that this current is increasing with a dependence very close to $(\text{diameter})^2$. These conditions lead to an asymptotic value for input power of approximately 0.1 watt per cm^3 as the diameter is increased beyond 10 cm. Since high efficiency operation (i.e., approximately 18 percent) has been claimed for diameter of 6 centimeters it is reasonable to assume that an output power of 10 to 20 milliwatts per cm^3 is a possibility. This is consistent with the graphic extrapolation shown in Figure A.

Modes of Operation

CW

As illustrated in Figures B and C, the CO_2-N_2-He laser is a relatively low current, high voltage discharge. These features, plus the fact that heated oxide coated cathodes are extremely susceptible to poisoning by this type of discharge, suggest the use of cold cathode discharges. Both dc and ac excitation can be used. Although the latter method produces slightly higher power, it has several disadvantages. The light output is amplitude modulated at twice the ac excitation frequency, and, because the discharge is self-striking, the current, and hence the output, exhibits random fluctuations.

By using rf excitation, the electrodes can be removed from the discharge altogether. With small diameter discharge tubes (<2.5 cm), rf excited lasers have exhibited essentially the same output power, efficiency and pressure dependence as comparable dc excited tubes. However, the latter have two distinct advantages: (1) no rf interference in auxiliary

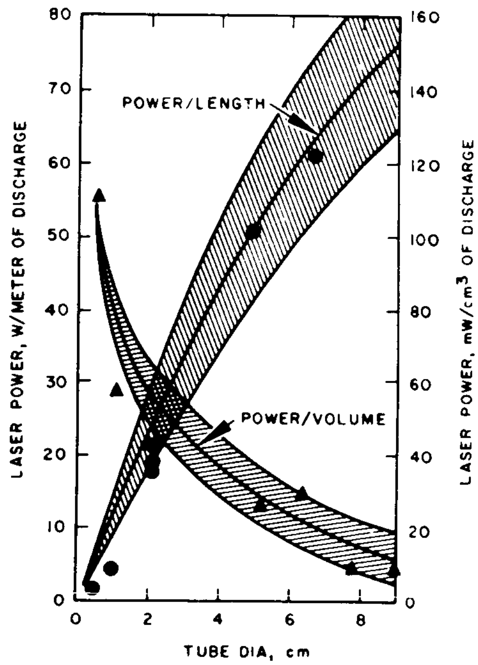

Figure A. Variation of CO_2 Laser Power per Unit Volume of Discharge and Laser Power per Unit Length of Discharge With Discharge Diameter

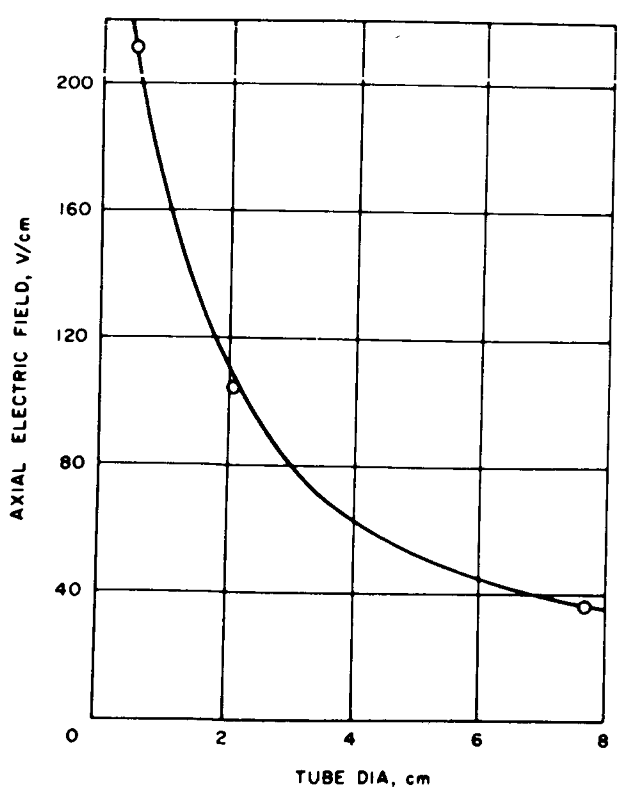

Figure B. Variation of Axial Electric Field With Discharge Tube Diameter, CO_2 Laser

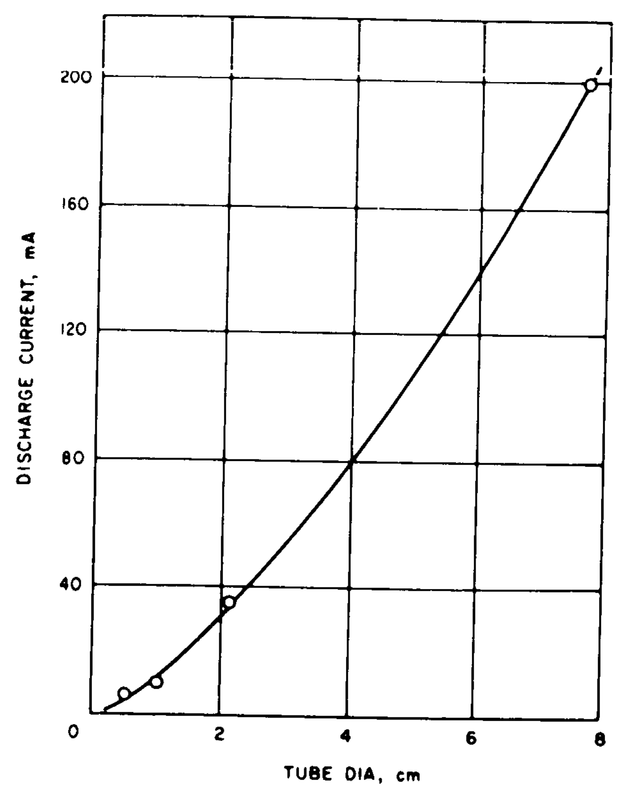

Figure C. Variation of Optimum Discharge Current With Discharge Tube Diameter, CO_2 Laser

CO_2 LASER SCALING LAWS

equipment, and (2) higher power dc supplies are easier to build and operate. No data are presently available regarding rf excitation of large diameter (≥5 cm) lasers.

Pulsed

High peak power can be obtained by exciting the CO_2-N_2-He laser with dc pulses (e.g., peak power of 825 w from a laser producing 17 w cw, current pulse 100 µsec, light pulse 150 µsec[1]). No delay is observed between the current pulse and the light output.

Q-Switched

Because of the long lifetime ($\sim 2 \times 10^{-2}$ sec) and small spontaneous emission transition probability (~ 0.34 sec^{-1}) of the upper laser level 00^01, the CO_2-N_2-He laser may be Q-switched.[2] Lasers whose cw output is a few watts will produce giant pulses of the order of 10 kw with a pulse length of approximately 100 nsec when operated in the Q-switched mode. The maximum switching speed is determined by the rate at which the upper laser level is excited and is in the neighborhood of several KHz.

State-of-the-Art in CO_2 Lasers

Since the first report of laser action in CO_2 in April 1964, CO_2 laser technology has developed at a much faster rate than that of any other laser device. In approximately two years, the output power has been increased from milliwatts to hundreds of watts, the latter obtained at efficiencies of 10 to 20 percent. The Table lists the characteristics of some early CO_2-N_2-He lasers.

[1] Frapard, C., "Vibrational Excitation of CO_2 by Electronic Impact in Pure CO_2 Laser," presented at 1966 International Quantum Electronics Conference, Phoenix, Arizona, April 1966.

[2] Kovacs, M.A., Flynn, G.W., and Javan, A., "Q-Switching of Molecular Laser Transitions," Appl. Phys. Letters, 8, p. 62, 1966.

State-of-the-Art CO_2 Lasers (May 1966)

P_{out} (w)	Length (m)	Diam (cm)	Eff. (%)	Comments	Organization
500	10	5	15.5	Multimode output Flowing gas system	Raytheon
10	0.5	1	10	Single TEM mode output^{oo} Sealed-off tube	HRL
150	2.4	6	18	Multimode output Flowing gas system	CGE (France)
130	4	7.5	13	Multimode output Flowing gas system	BTL

TRANSMITTING POWER SOURCES

Laser Mode Coupling and Frequency Stabilization

	Page
Laser Mode Coupling	78
Laser Frequency Stabilization Considerations	84
Laser Stabilization by Mechanical and Thermal Methods	88
Laser Frequency Stabilization Using Feedback Systems	90
Optical AFC Systems Using Passive Cavity Discriminants	92
Results of AFC for Lasers	98

LASER MODE COUPLING

Lasers typically operate simultaneous and more than one frequency or mode. Means are suggested which reduce the number of modes by using AM, PM, and FM techniques.

Introduction

The atomic populations of most gas lasers are sufficiently inhomogeneously broadened to allow the simultaneous oscillation of a large number of axial modes. Each of these modes is driven by spontaneous emission from atoms in different regions of the atomic fluorescence line; to a first approximation, these modes are uncoupled and oscillate independently. Under normal conditions, and especially for closely spaced modes (long optical cavities), the amplitudes and phases of the individual modes will fluctuate in a random manner. The output of a multimode laser is therefore amplitude modulated and has a frequency coherence much less than that of any single axial mode.

By introducing an optical modulator within the laser cavity, the previously uncoupled modes may be coupled together so that their relative amplitudes and phases are constant in time. In gas lasers, suitable modulators vary either the optical path length of the cavity (phase modulation), or the cavity losses (loss modulation). The frequency spectrum and the time domain output of a mode-coupled laser vary with the type, frequency, and amplitude of the modulation.

The effect of mode-coupling within the laser cavity is to change the form of the laser signal. The laser output may be considered as an optical carrier. By mode coupling, the carrier can be converted to a more useful form, such as an unmodulated pulse train or a single frequency. These internal modulation techniques should not be confused with schemes which use a modulator within the cavity to impose information on a direct or scattered beam.

A general discussion of the characteristics of loss and phase modulated, mode-coupled lasers is given in the paragraphs below.

Internal Loss Modulation of Multimode Lasers

The theory of internal loss modulation has been presented by several authors,[1, 2, 3] and successful mode-locked operation has been reported for He-Ne at 6328 Å[3, 4] and for A II at 4880 Å.[3] To introduce a time-varying loss, a suitable modulator is placed within the optical cavity as near as possible to an end mirror. The coupling effect is independent of the manner in which the losses arise.

[1] Yariv, A., J. Appl. Phys., 36, pp. 388-391, February 1965.

[2] DiDomenico, M. Jr., J. Appl. Phys., 35, pp. 2870-2876, October 1964.

[3] Crowell, M.H., IEEE J. of Quantum Electronics, QE-1, pp. 12-20, April 1965.

[4] Hargrove, L.E., Fork, R.L., and Pollack, M.A., Appl. Phys. Letts., 5, pp. 4-5, 1 July 1964.

When the frequency of the time-varying loss, ν_m, is equal to or very close to the mode spacing $c/2L$, coupling of the modes results from the nonlinear polarization of the medium. The relative amplitudes of the modes becomes approximately Gaussian, centered about the line center, and all modes oscillate with equal phase. For a mode-coupled laser with a spontaneous emission linewidth $\Delta\nu$ and n axial modes oscillating in phase (normally $n \sim \Delta\nu/(c/2L)$ the laser output (as predicted by simple Fourier analysis) is a pulse train of ν_m pps with the following characteristics:

1. The pulse width is roughly $(n\,\nu_m)^{-1} \sim (\Delta\nu)^{-1}$.
2. The average power is approximately equal to the free-running laser power.
3. The peak pulse power is n times the average power.

The effect of the internal loss modulation on a multimode laser is then to convert the output to a pulse modulated signal. Experimental results[3] obtained for two types of lasers with $\nu_m = c/2L \sim 100$ MHz are:

Laser	λ	$\Delta\nu$	Pulse Length	Peak Power/ Average Power
He-Ne	6328 Å	1.5 GHz	0.5 nsec	17
A II	4800 Å	4.5 GHz	0.25 nsec	20-30

Such a high-intensity pulse modulated source may have applications in PCM systems where an external optical shutter is provided to modulate the pulse height.

Internal Phase Modulation of Multimode Lasers

A mode coupling of a gas laser may also be accomplished by placing a phase modulator (KDP crystals have been used to date) inside the laser cavity. When an rf field is applied to the electro-optic crystal, its index of refraction is changed, causing a change in the length of the optical path of the cavity. This approach is equivalent to vibrating one end of the cavity mirrors at the modulation frequency, and gives rise to the generation of fm sidebands for each oscillating mode.

Two different types of mode-coupling can result depending on the frequency of the modulation. When the crystal is driven at a frequency which very nearly, but not exactly, corresponds to the frequency separation of the free running modes, the laser operates in the fm region. If the driving frequency is tuned to exactly the frequency separation of the modes, then "phase locked" operation occurs which has different characteristics from the fm region. These two modes of operation will be

LASER MODE COUPLING

discussed separately below. A detailed discussion of the limits of operation of the two regions as predicted by theory[5, 6] and observed in experiments[7] is contained in the literature.

Mode Coupling in the FM Region

Since the modulation frequency is roughly the frequency separation of the free running modes, the fm sidebands of each mode very nearly coincide with the frequencies of other axial modes. While each mode and its sidebands are originally a distinct fm oscillation, a parametric energy exchange takes place which allows the previously independent modes is coupled to other modes through the overlapping sidebands. There is then a competition between the fm oscillations for the gain of the active material, and under appropriate conditions it is possible for one fm oscillation to quench or extinguish other oscillations. The result is that the total output can be made up of only one fm carrier and its sidebands. The output signal then appears as a single frequency which is swept back and forth about line center at the modulation frequency. The fm signal E(t) can be represented as

$$E(t) = E_o \cos (\omega_c t + \Gamma \cos(\omega_m t))$$

where ω_c is the carrier frequency (the laser frequency) Γ is the modulation index, or ratio of the peak phase deviation to the modulation frequency, and ω_m is the modulation frequency (approx. the axial mode spacing). The relative amplitudes of the output laser modes have Bessel function relationships to each other; the central mode will have an amplitude given by $J_o(\Gamma)$, the first sidebands $J_1(\Gamma)$, and so on.

The modulation index can be written as

$$\Gamma = \frac{1}{\pi} \frac{\Delta\Omega}{\Delta\nu} \delta \qquad (1)$$

where $\Delta\Omega$ is the frequency separation of the modes, $\Delta\nu$ is the difference in frequency between $\Delta\Omega$ and the modulation frequency ν_m, and δ is the single pass phase retardation of the phase modulator, in radians. Typical values for a He-Ne laser with $\Delta\Omega$ equal to 150 MHz are $\Delta\nu$ = 150 kHz, δ = 0.01 and Γ = 3.19.

[5] Harris, S.E., and McDuff, O.P., Appl. Phys. Letts., 5, pp. 205-206, November 15, 1964.

[6] Harris, E.E., and McDuff, O.P., IEEE J. of Quantum Electronics, QE-1, pp. 245-262, September 1965.

[7] Amman, E.O., McMurtry, B.J., and Oshman, M.K., IEEE J. of Quantum Electronics, QE-1, pp. 263-272, September 1965.

The above equation makes it clear why fm operation is not obtained when the modulation frequency exactly equals the mode spacing. In this case, $\Delta\nu$ would be zero and Γ would be infinite. At that point the output no longer resembles an fm signal, and a new phase-locked coupled mode solution occurs.

The fm region of operation offers promise as a means to stabilize the amplitude of a cw laser. In addition, by employing the "supermode" technique or selective output coupling as discussed below, the fm laser may yield single frequency operation.

Mode Coupling in the Phase-Locked Region. When the modulation frequency is equal to the separation between axial modes ($\Delta\nu' = \Delta\Omega$), the modulation index describing fm operation becomes infinite. Under these conditions, all the modes oscillate in phase and the amplitudes of the modes have a Gaussian distribution about the center frequency. The output in this case is the same as is observed for loss modulation; that is, a train of narrow pulses with a repetition rate corresponding to the frequency separation of the modes.

Single Frequency Operation of Mode-Coupled Lasers

The "Supermode" Laser

The so called "supermode" laser[8] approach uses the controlled spectral output of the fm laser to produce a single frequency. To accomplish this, the output of the fm laser is passed through a second phase modulator located outside of the cavity which is driven at the same frequency as the internal modulator. If Γ' is the modulation index of the external modulator and ϕ is the difference in phase between the two modulators, then the output of the external modulator will be

$$E(t) = E_o \cos\left[\omega_c t + \Gamma \cos\omega_m t + \Gamma' \cos(\omega_m t + \phi)\right]$$

when Γ' is made equal to Γ and $\phi = 180^o$, then $E = E_o \cos\omega_c t$. This is a monochromatic signal at a frequency near the center of the original free-running spectrum. Briefly then, the supermode laser produces a single-frequency output by first controlling the free-running modes in a specific manner through the f-m laser technique, and then converting this controlled signal to a single frequency.

The major limitation of this approach is the difficulty in building a practical external modulator for which Γ' can be equal to Γ. Typical values of Γ for an fm laser lie in the range of from 1 to 7. Because of the multiple pass characteristic of the laser cavity (as reflected in the term $\Delta\Omega/\Delta\nu'$ in Equation (1), Γ may be obtained using values of δ less than

[8] Massey, G.A., Oshman, M.K., and Targ, R., Appl. Phys. Letts., 6, pp 10-11, 1 January 1965.

LASER MODE COUPLING

0.3. For an external modulator, $\Gamma' = \delta'/2\pi$ so that the required values of δ' are in the range of 5 to 40 radians. It is not practical at this time to construct modulators having such large phase retardations. Future development of multipass modulators using new material such as KTN or $LiNbO_3$ may make it practical to use the supermode technique to obtain a single output frequency.

Frequency Selective Output Coupling to the Mode-Coupled Laser

The important property of a mode-coupled laser utilized in this approach to obtaining single frequency operation is that all the modes are coupled together in amplitude and phase. If the gain or loss of any one of the coupled modes is changed, the relative amplitudes of the modes will still be very nearly maintained and the oscillation level will adjust such that the net average power absorbed or dissipated by all modes remains zero. The method of single frequency operation discussed here is based on the fact that there is an optimum output coupling (mirror transmission) which allows the maximum power to be taken from the mode-coupled laser- and that whether this coupling is provided as a sum of equal increments to all modes, or instead is provided entirely to one mode, is not of significance. Theory[9] has shown that if it is desired to extract the entire output as a single frequency from the 9th mode from line center, the ratio of necessary coupling to that mode, as compared to the coupling which should optimally be seen by all modes, is $1/J_q^2(\Gamma)$.

The method which has been used thus far,[9, 10, 11] to obtain the selective output coupling to a single mode of a phase modulated laser is to replace one end mirror of the laser with a Fabry-Perot etalon having a free spectral range greater than the line-width of the transition. Fine tuning of the etalon allows the narrow transmission curve of the etalon to be tuned so as to couple to just one mode. Ideally it should be possible to extract the total power which was originally available from all the modes to just one mode.

Single frequency operation of a multimode laser using internal modulation to achieve mode coupling and an output etalon to select a single frequency has been demonstrated for He-Ne[10] and AII lasers.[11] A He-Ne laser, which as a free-running oscillator produced 68mW, yielded 53mW at a single frequency using these techniques. For argon, 45mW of single frequency power has been obtained from a 100mW free-running laser. This approach is still being refined, and higher powers can be expected, especially from argon ion lasers.

---

[9] Harris, S.E., and McMurtry, B.J., Appl. Phys. Letts., 7, pp. 265-267, 15 November 1965.

[10] Targ, R., and McMurtry, B.J., paper presented at 1966 International Quantum Electronics Conference, Phoenix, Arizona, April 12-15, 1966.

[11] Osterink, L., Byers, R., and Harris, S.E., paper presented at 1966 International Quantum Electronics Conference, Phoenix, Arizona, April 12-15, 1966.

LASER FREQUENCY STABILIZATION CONSIDERATIONS

The stabilization of lasers is difficult due to the small fractional bandwidths available. Fractional bandwidth is expressed in terms of the dimensions of the laser.

Introduction

For all but the most simple communications systems, the laboratory laser does not possess the frequency stability, amplitude stability, or spectral purity equivalent to conventional microwave sources. The following discussion assumes that the amplitude is stable and the spectrum is pure, and is directed to the problems of obtaining improved frequency stability.

To first order, the exact oscillation frequency of a laser is determined by the mechanical properties of the optical cavity rather than the parameters of the atomic line. Thus, a brief review of optical cavity properties and materials will be given. Following this topic will be other topics containing stabilization methods, and the most recent results.

System Stability Requirements

Consider the simplest microwave heterodyne receiver with an operating frequency of 10 GHz and an i-f bandwidth of 1 MHz, the required local oscillator (and transmitter oscillator) stability must be better than 10^6 in 10^{10} or 1 part in 10^4 to keep the received signal within the receiver passband. For most practical communications systems the actual stability required might be two orders of magnitude greater than this, or 1 part in 10^6. For the present, however, consider the crudest system which requires the signal remain within the passband. The same bandwidth used in an optical heterodyne receiver, with operating frequency of 500 THz (TerraHertz = 10^{12} Hz), corresponding to a visible wavelength of 6000 Å, requires an oscillator stability of 10^6 in 5×10^{14} or 2 parts in 10^9. By translating the same information bandwidth from the microwave to the optical region, the stability requirements have changed from that of everyday hardware to that of a primary frequency standard. The Figure shows the fractional stability required as a function of the desired absolute stability (equal to the information bandwidth in the example considered here) for the most commonly used gas laser transitions. For a practical heterodyne system, the required stability would be an order of magnitude tighter. The curves end at the points marked "Doppler widths" since at least this stability is required to keep a given cavity mode within the gain line half-power points and to keep the laser oscillating.* Also shown for comparison with conventional sources are curves for 1-mm and 1-cm wavelengths.

---

*Typical laboratory lasers have stability much worse than this; however, because of the multimode nature of the cavities, the dropping in and out of oscillation of a given mode is not ordinarily seen. For the optical heterodyne consideration must be given only to a single mode (i. e., single frequency) oscillators, so that the stabilization must be at least good enough to keep this mode within the gain line width.

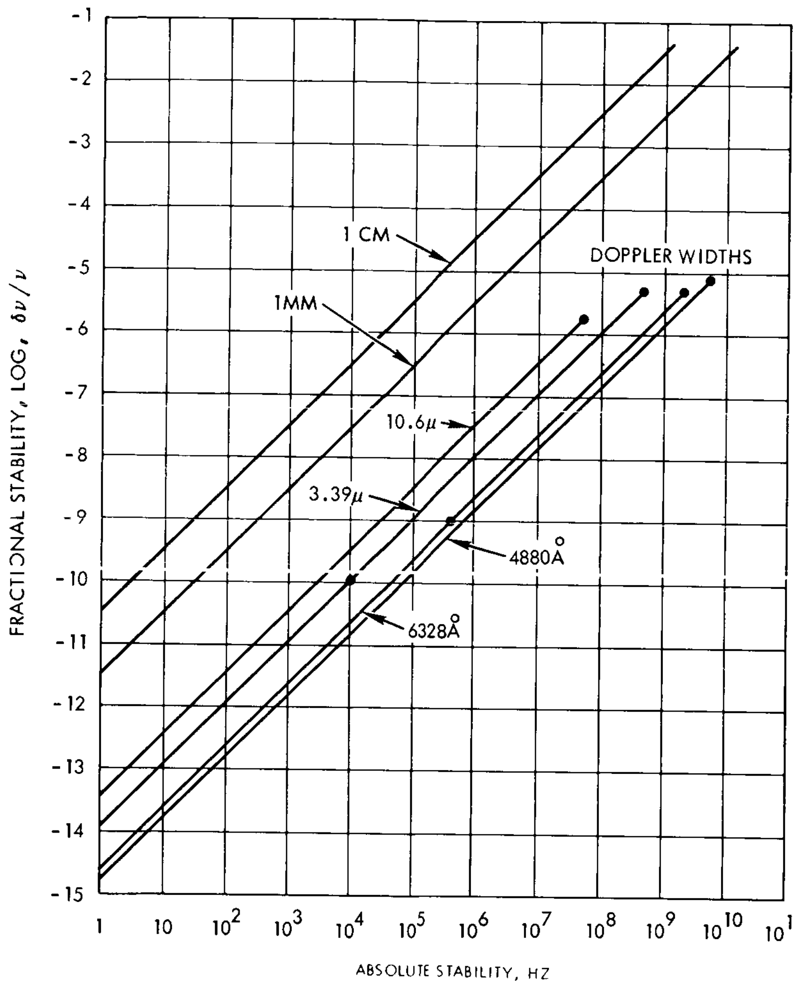

Fractional Stability Required as a Function of
Desired Absolute Stability

LASER FREQUENCY STABILIZATION CONSIDERATIONS

The best results obtained to date[1] are shown as dots on the various curves. No stabilization has been reported for those wavelengths with no dot shown.

Properties of the Optical Cavity

The resonant frequency, ν, of an optical cavity formed by mirrors of radii b_1 and b_2, spaced a distance, L, apart is[2]

$$\nu = \frac{c}{2L}\left[q + \frac{1}{\pi}(1+m+n)\cos^{-1}\left\{\sqrt{\left(1-\frac{L}{b_1}\right)\left(1-\frac{L}{b_2}\right)}\right\}\right] \qquad (1)$$

where c is the velocity of light and m, n, q are three integers that describe the particular optical mode (field distribution); q is the number of half wavelengths between mirrors and m and n are number of zeros (or phase reversals) the electric field contains in the transverse direction. Typically q is of the order of 10^6, while m, n are small (0, 1, 2, . . .). Modes are usually designated TEM_{mnq}; the most useful, i. e., the ones providing the closest to a uniform illumination and thus possessing the lowest diffraction spread for a given diameter, are the TEM_{00q}. In all that follows it is assumed that only these modes are present, selected by intracavity apertures, cavity dimensions, etc. In addition, it is assumed that by proper choice of L compared to the gain line width, only one particular value of q will oscillate at a time.

For TEM_{00q} modes equation (1) reduces to

$$\nu = \frac{c}{2L}\left[q + \frac{1}{\pi}\cos^{-1}\left\{\sqrt{\left(1-\frac{L}{b_1}\right)\left(1-\frac{L}{b_2}\right)}\right\}\right] \qquad (2)$$

Since $q \gg 1$, this formula, for first order effects, reduces further to

$$\nu \approx \frac{cq}{2L} \qquad (3)$$

[1] White, A. D., "Frequency Stabilization of Gas Lasers," IEEE J. of Quantum Electronics, QE-1, pp. 349-357, November 1965.

[2] Boyd, G. D., and Kogelnik, H., "Generalized Confocal Resonator Theory," Bell Sys. Tech. J., 41, pp. 1347-1370, July 1962.

Then, to first order, the cavity frequency depends only on the spacing L. The variation in frequency $\delta\nu$ caused by a change in cavity length δL is

$$\delta\nu = -\frac{cq}{2L^2}\,\delta L = -\frac{\nu}{L}\,\delta L \tag{4}$$

or,

$$\frac{\delta\nu}{\nu} = -\frac{\delta L}{L} \tag{5}$$

Second order corrections arise because of the occurrance of L in the second term in equation (2), but equation (5) will be accurate enough for most purposes.

If, in addition to changes in the physical length, δL, there is a change in the effective length due to a change, δn, in the index of refraction of the intracavity medium, then

$$\frac{\delta\nu}{\nu} = -\left(\frac{\delta L}{L} + \frac{\delta n}{n}\right) \tag{6}$$

Equation (6) is most applicable to solid-state lasers where the mirrors are coated directly on a dielectric rod of index n. For gas lasers in which the active medium has index ℓ, but the atmosphere fills the space from the end windows to the mirrors, a fraction $L-\ell/L$, where ℓ is the length of the discharge tube, then

$$\frac{\delta\nu}{\nu} = -\left(\frac{\delta L}{L} + \frac{L-\ell}{L}\;\frac{\delta n}{n}\right) \tag{7}$$

LASER STABILIZATION BY MECHANICAL AND THERMAL METHODS

Lasers may be stabilized by using materials which are mechanically "stiff" and have low coefficients of expansion with temperature.

The most direct method of laser stabilization is to control the environment of the optical cavity sufficiently well so that the resonant frequency variation falls within the prescribed limits. This requires accurate control of the cavity temperature (often in the presence of a strong heat source, for example, the laser discharge tube), control of or isolation from mechanical stresses and vibrations, and isolation from air currents (or other fluctuations in the intracavity medium).

The change in frequency with change in cavity length caused by thermal temperature variation is given by equation (1) and considering the definition of thermal expansion coefficient, μ.

$$\frac{\delta \nu}{\nu} = - \frac{\delta L}{L} = -\mu \delta T \qquad (1)$$

The Figure shows the fractional stability resulting from a given temperature fluctuation, δT, for several common materials suitable for cavity fabrication. This figure may be combined with the figure of the previous topic to see the resulting absolute frequency change for the different laser wavelengths. To achieve a long term stability of 1 part in 10^9 using the lowest expansion coefficient material, fused quartz, a temperature control of 10^{-3} degrees Centigrade is required. By choosing a proper geometry and composite material for the package laser cavity, one may temperature-compensate to achieve perhaps an order of magnitude improvement over simple cavity expansion. Also, there are now some experimental glasses and ceramics that are internally compensated in their composition to achieve lower expansion coefficients.

The change in frequency produced by a change in air pressure depends on the fraction $L-\ell/L$ of the optical path that is exposed. A value of 0.1 for this fraction is typical for Brewster-angle gas lasers. The fractional frequency change produced by a change in air pressure, δp, is then

$$\frac{\delta \nu}{\nu} = - \frac{L-\ell}{L} \frac{\delta n}{n}$$

$$= - \frac{L-\ell}{L} (0.00029) \frac{\delta p}{760}$$

$$\cong - \frac{L-\ell}{L} \times 3.8 \times 10^{-7} \delta p$$

or,

$$\cong 4 \times 10^{-8} \delta p$$

for $L-\ell/L = 0.1$, and δp in Torr*. The long-term variation in pressure due to weather changes may be of the order of 20 to 30 Torr or more. Thus, $\delta\nu/\nu > 10^{-6}$, determined by atmospheric variations. Launching a gas laser into space (δp = 760 Torr) would produce a $\delta\nu/\nu$ of approximately 3×10^{-5}, which is greater than the maximum variation allowed to maintain oscillation within the doppler linewidth for all the gas lasers listed in the Figure of the previous topic. Of course, internal mirror lasers do not suffer from pressure effects, except through possible mechanical stresses set up by changes in pressure.

Perhaps the most difficult source of laser instability to describe is that resulting from room microphonics and mechanical vibration. Needless to say, every precaution must be taken to isolate the laser form sources of vibration. (This may be easier to do in a space vehicle than it is on the earth's surface.) Even when electronic stabilization is used with the laser, the microphonics determine the loop gain required and the trade-off between capture-range and sensitivity of the frequency discriminator to be used.

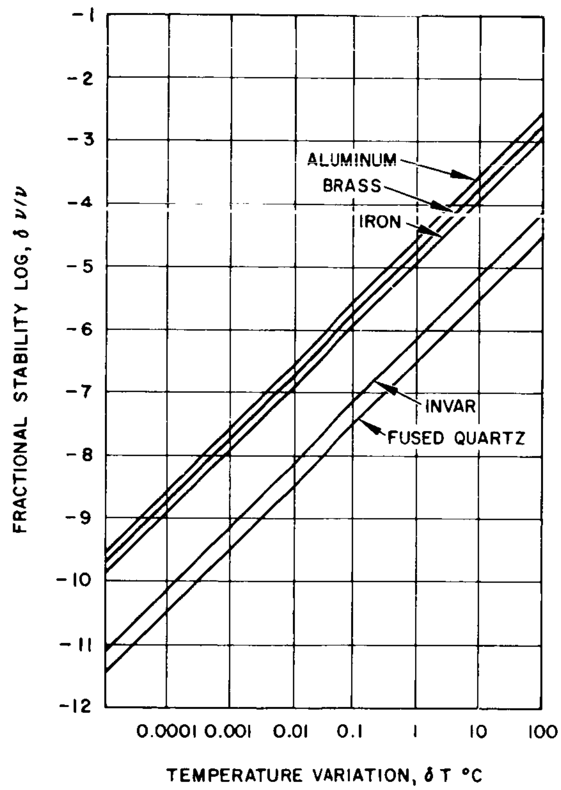

Fractional Stability Resulting From a Given Temperature Fluctuation, δT, for Several Common Materials Suitable for Cavity Fabrication

---

*1 Torr ≡ 1 mm of Mercury

LASER FREQUENCY STABILIZATION USING FEEDBACK SYSTEMS

The types of discriminants which could be used in an optical AFC are listed and a typical block diagram discussed.

It is possible to generate a discriminant or discriminator characteristic as shown schematically in Figure A in several ways for use in a feedback frequency control system. These include: passive cavity discriminants such as the Fabry-Perot discriminator and the two-beam interference discriminator, atomic line discriminants such as the laser gain curve or Zeeman effect discriminant and other discriminants such as a "frequency pushing" discriminant. Of these, the Fabry-Perot and the two-beam interference discriminators will be given in the next topic to show typical implementation. (For implementation of the other methods, the reader is referred to the Third Quarterly Report of this contract published June 1966.) Before these examples are given, general characteristics of optical frequency control systems will be discussed.

A discriminant must (1) measure the amount of frequency deviation from some desired center frequency (it is desirable but not necessary that the output amplitude be a linear function of the frequency deviation), and (2) indicate the sense of the deviation, usually by a positive or negative output. The discriminator output should also be independent of the signal amplitude. If it is not, the independence may be achieved as it is usually done in the radio-frequency case by limiting; unfortunately, optical frequency limiters are rare, occurring only for those transitions which possess a high, saturable gain characteristic, such as the Xe I 3.508μ transition. Otherwise, the signal source must be stabilized to obtain amplitude independence for those amplitude-dependent discriminants.

Having obtained a suitable optical discriminator, the output is then fed to a frequency-controlling element in the laser--for example, to an electromechanical element controlling the mirror spacing, or to an electro-optic element controlling the effective index of a portion of the cavity. This servo loop may become quite sophisticated in its detail. Integrators to obtain zero-error characteristics may be included; multiple loops derived from different discriminants may be used to stabilize for different "terms" i.e., short-ter, long-term*), or different loops may be added to correct for mirror tilt in addition to mirror spacing, a second order effect. A typical system block diagram is shown in Figure B.

It is useful to recall a few general facts about frequency discriminator systems. If a discriminant is derived from a resonance phenomena, then it is quite generally true that the discriminator curve will resemble the derivative of the amplitude function of the resonance. If the width of the resonance is $\Delta\nu$ then the width between the peaks of the discriminator curve will be about $\Delta\nu$; if the resonance is asymmetrical, the discriminant will be asymmetrical, etc. The finer details depend on the exact method

---

*Short term means the low audio range to perhaps 1 kHz; long term means hours to years. Optical cavity discriminants are suitable for short term stability, while atomic discriminants are better suited for long term stability.

of obtaining one from the other. It is also true that the steeper the slope of the discriminant (or the higher the gain of the feedback loop) the tighter the frequency lock will be. On the other hand, the capture range is proportional to the discriminant width.

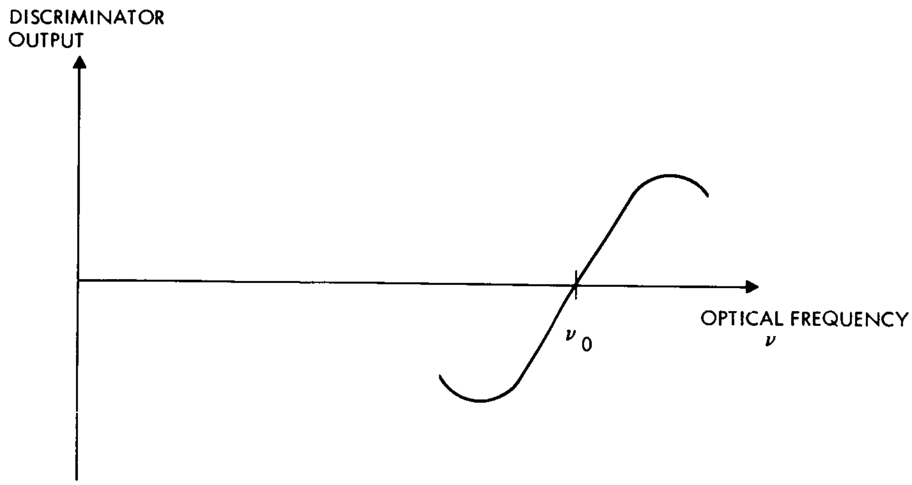

Figure A. An Optical Discriminant for Use in Feedback Frequency Control System, Schematic

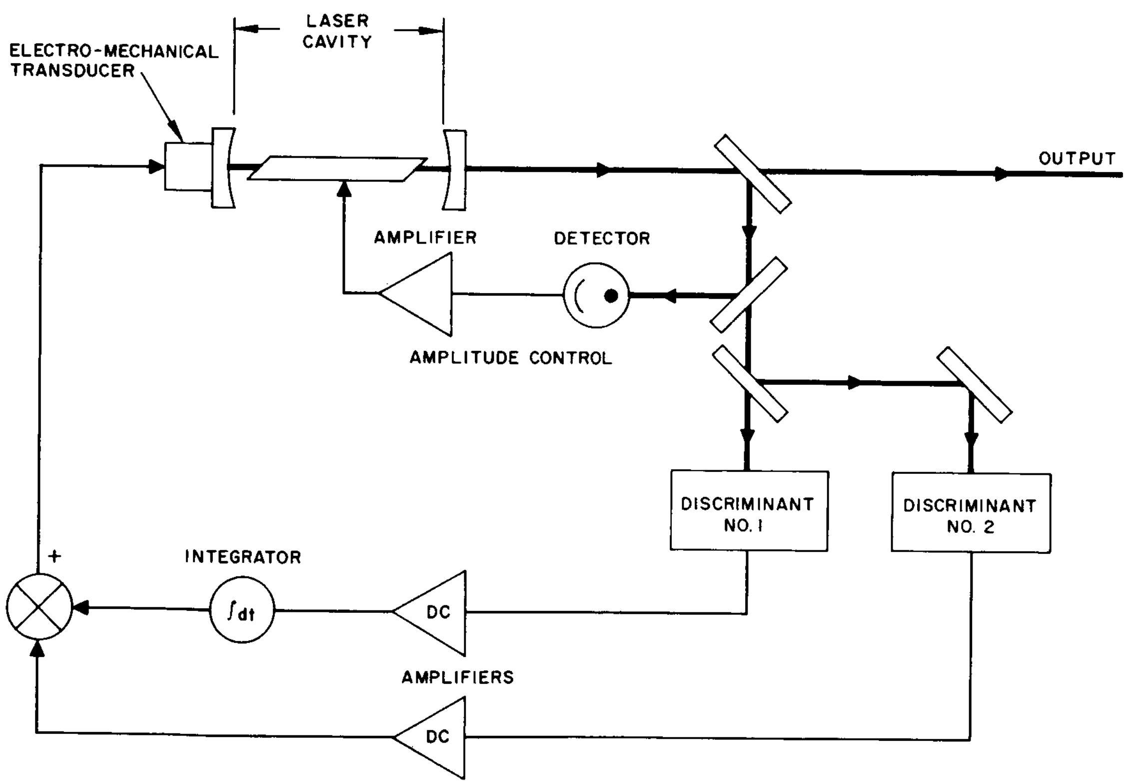

Figure B. Typical Feedback Laser Frequency Control System

OPTICAL AFC SYSTEMS USING PASSIVE CAVITY DISCRIMINANTS

Typical implementation of two passive cavity discriminators are shown for frequency controlling a laser.

It is possible to generate an optical discriminant by using interference in optical cavities. Such discriminants are probably best used for short-term stabilization, since the small cavities used can be made quite rugged and free from microphonics. However, there is no guarantee of long-term stability because of temperature drift, mechanical drift due to strains, etc.

Interference can may be classified as two-beam or multiple beam. The Michelson and Mach-Zehnder configurations are perhaps the best known examples of two-beam instruments, while the Fabry-Perot is the best known multiple beam device.

a. Fabry-Perot Interferometer Discriminator

The transmission characteristic of a typical Fabry-Perot (F-P) interferometer is shown in Figure A. Typical numerical values are given in parentheses. The bandwidth $\Delta\nu$ may be only a few MHz, much less than the Doppler width of a typical visible or near-IR laser transition. The simplest method of obtaining a discriminant from this resonator is shown schematically in Figure B. The laser output is passed through the F-P to an amplitude detector; a bias level is subtracted from the detector output and fed in the proper phase through a dc amplifier to the mirror transducer. The resulting discriminant is shown in Figure C. The output amplitude of the laser itself must be stabilized by an independent loop, since fluctuations in laser amplitude would be sensed the same as fluctuations in frequency, as shown in Figure C.

A better method is shown in Figure D. Here a small modulation ("dither"), typically at an audio rate is applied to the mirror transducer. The modulated beam is passed through the F-P. A sample is envelope-detected and the modulated output of the detector is compared with the modulating source in a phase-sensitive detector. The filtered (dc) output is then amplified and fed to the mirror transducer. That the output of the phase detector produces the desired discriminant is easily seen from Figure E. The amplitude of the modulation on the light increases as the slope of the transmission curve increases. The maximum modulation occurs at the inflection points ν_1 and ν_2. The modulation amplitude is zero at ν_0. (Only the second harmonic of the modulation frequency occurs at ν_0, and it is a maximum here, zero at the inflection points--it may also be used as an error signal). The phase of the modulation on the light with respect to the modulating signal also changes as the frequency passes through ν_0.

By adding a bias voltage to the dc amplifier output, the frequency may be stabilized at ν_3 rather than ν_0.

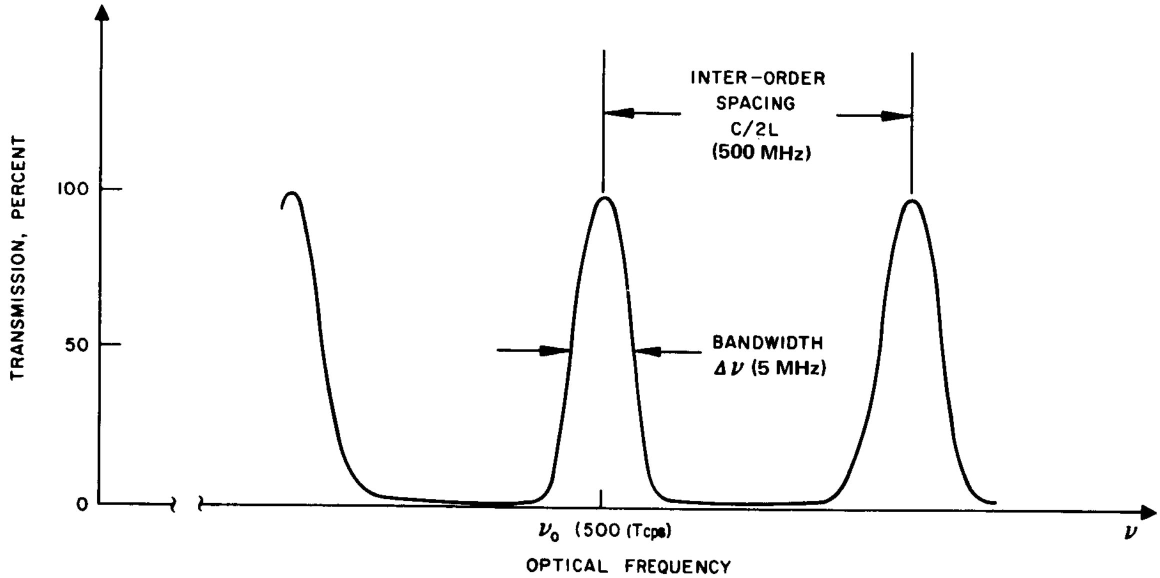

Figure A. Typical Fabry-Perot Transmission Characteristic
Numerical values typical of gas lasers are given in parentheses.

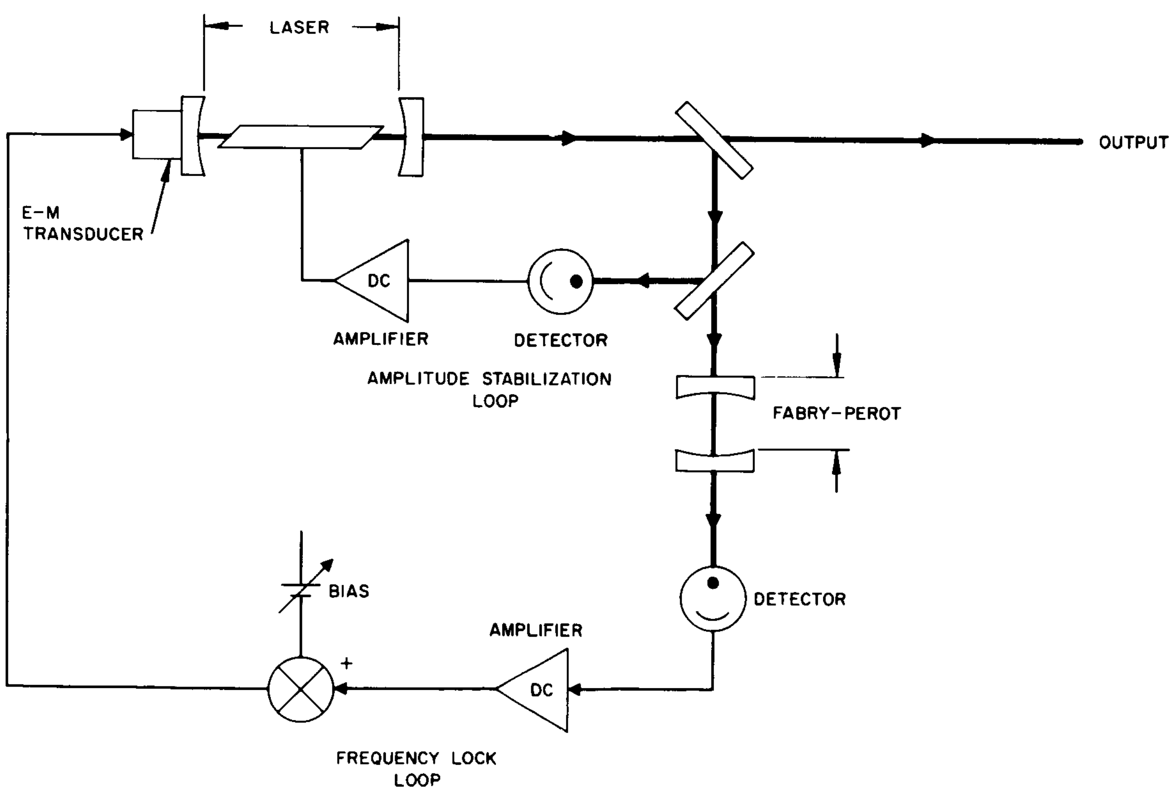

Figure B. Simple Stabilized Laser Using a Fabry-Perot Cavity as a Reference

OPTICAL AFC SYSTEMS USING PASSIVE CAVITY DISCRIMINANTS

One of the disadvantages of the system shown in Figure D is that the laser output is frequency- and amplitude-modulated at the "dither" frequency. To eliminate this, the F-P mirrors may be dithered instead of the laser mirrors; the dc error signal is fed back to the laser as in the first system. The operation is otherwise the same.

b. Two-beam Interferometer Discriminator

Consider the simple arrangement shown in Figure F, this system may be thought of as an unequal-arm Mach-Zehnder interferometer. It is easily shown[1] that the output of photodetectors 1 and 2 is

$$\dot{Z}_1 \sim \sin^2 \left[\frac{\pi \nu}{C}(L_a - L_b)\right]$$

$$\dot{Z}_2 \sim \cos^2 \left[\frac{\pi \nu}{C}(L_a - L_b)\right]$$

The photo currents may be subtracted to form the discriminant shown in Figure G. The lengths L_a and L_b are adjusted so that the zero occurs at the desired optical frequency. The width of the discriminant between peaks is

$$\Delta \nu = \frac{C}{2(L_a - L_b)}$$

and can be made smaller (more sensitive) by increasing the inequality in the arm lengths. Of course, the mechanical stability becomes worse the larger L_a - L_b is made, so that there will be an optimum design for a given set of construction techniques and environment.

Instead of using two arms of physically different lengths, it is possible to use a birefringent crystal to obtain the necessary two paths of different optical length. A discriminator based on this idea has been proposed by Harris.[2]

[1] Kaminow, I. P., "Balanced Optical Discriminator," Appl. Optics, 3, pp. 507-510, April 1964.

[2] Harris, S. E., "Demodulation of Phase-Modulated Light Using Biretringent Crystals," Proc. IEEE, 52, pp. 823-831, July 1964.

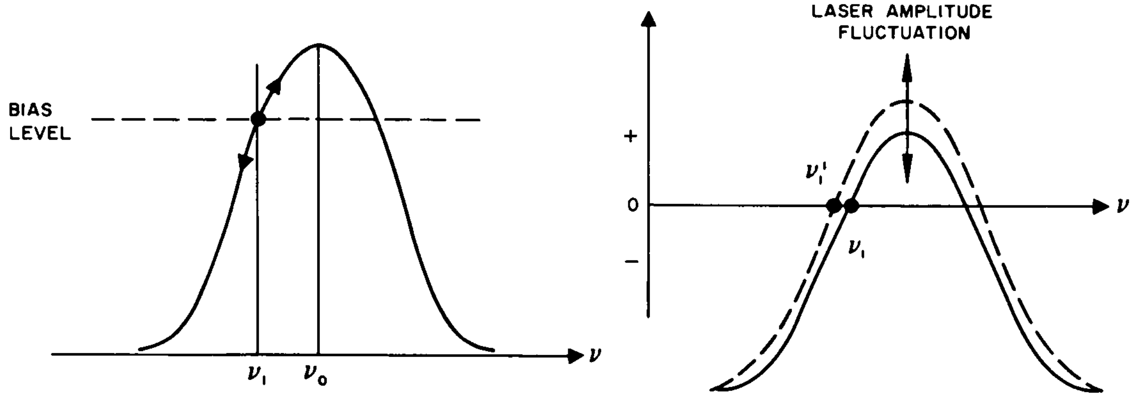

(a) TRANSMISSION CURVE (EXPANDED SCALE)

(b) RESULTING DISCRIMINATOR OUTPUT. AMPLITUDE FLUCTUATIONS IN THE LASER RESULT IN FLUCTUATIONS IN FREQUENCY, ν_1 TO ν_1'.

Figure C. Discriminant Characteristics

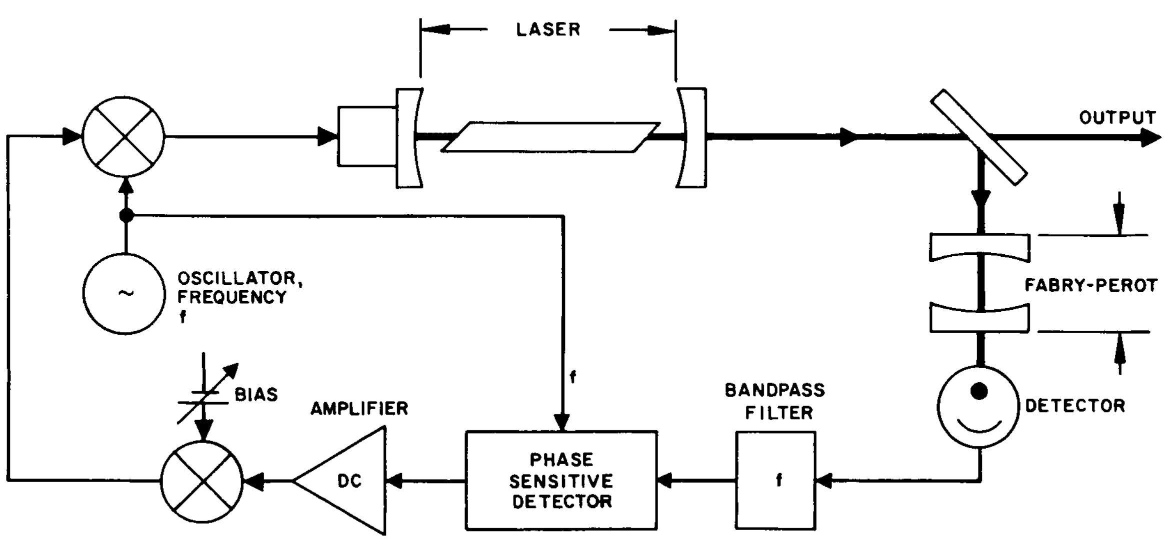

Figure D. Dither Method of Locking a Laser to a Fabry-Perot Cavity Resonance

OPTICAL AFC SYSTEMS USING PASSIVE CAVITY DISCRIMINANTS

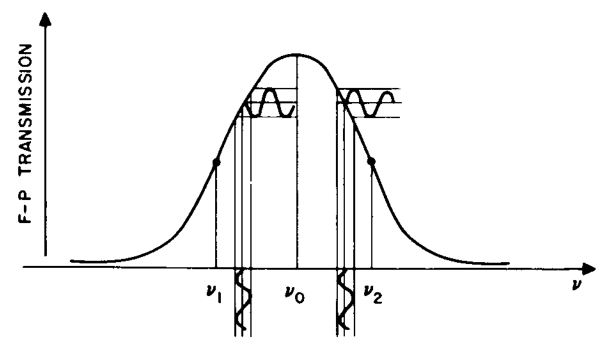

(a) TRANSMISSION OF AN F-P RESONANCE. FREQUENCY MODULATION ABOUT A POSITION OFF LINE CENTER PRODUCES AMPLITUDE MODULATION OF THE TRANSMITTED SIGNAL. RELATIVE PHASE SHIFTS 180° GOING THROUGH LINE CENTER. MAXIMUM MODULATION OCCURS AT INFLECTION POINTS ν_1, ν_2.

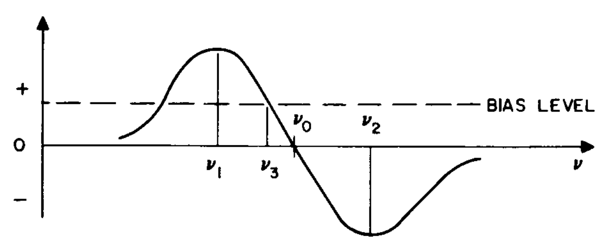

(b) DISCRIMINANT PRODUCED BY THIS SYSTEM. OSCILLATION IS LOCKED AT ν_0 WITH NO BIAS, AT ν_3 FOR BIAS SHOWN.

Figure E. Discriminant Characteristics

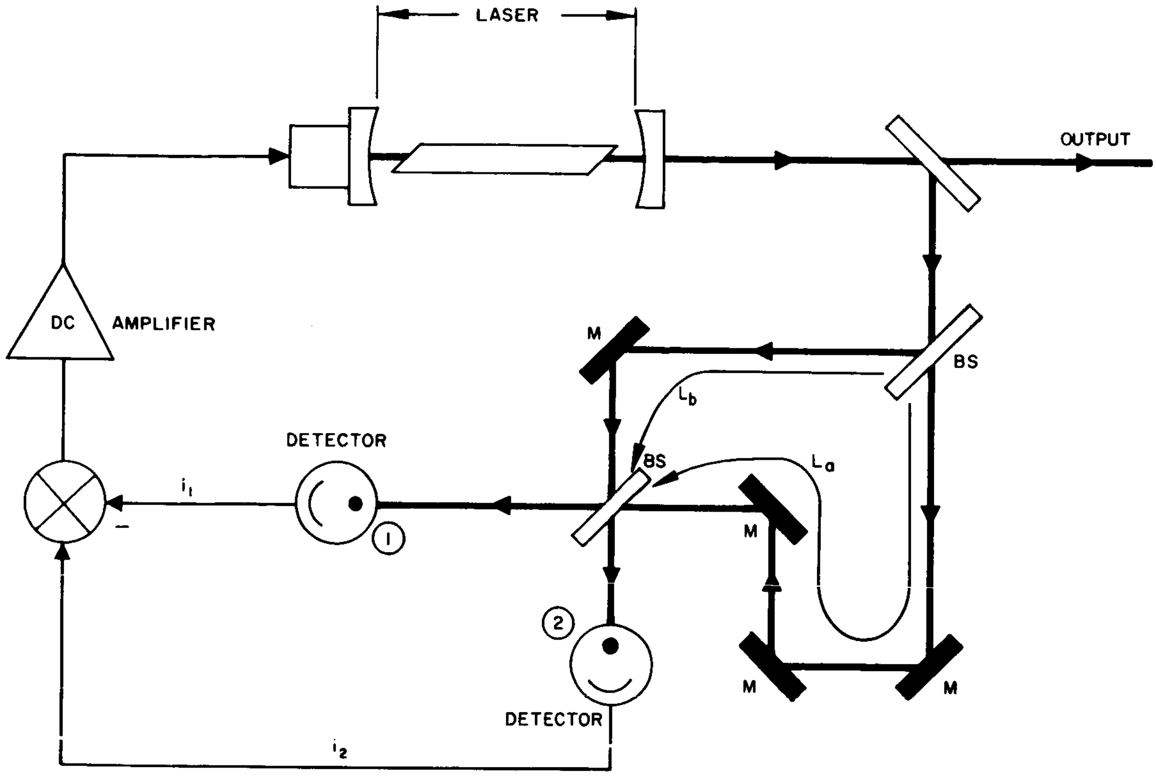

Figure F. Two-beam Interferometer Balanced Discriminator Frequency Stabilizing System (After Kaminow[1])

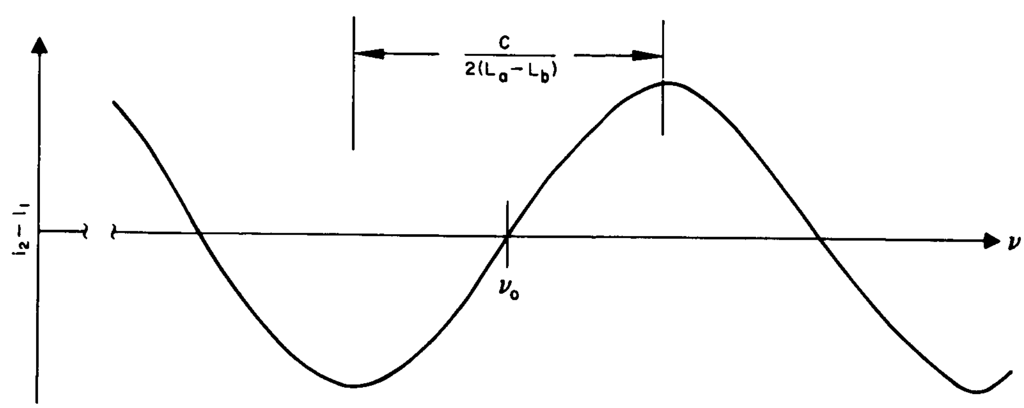

Figure G. Optical Discriminant Obtained From a Two-beam Interferometer With Path Length Difference of $L_a - L_b$

RESULTS OF AFC FOR LASERS

AFC stabilization developmens have achieved stabilization of lasers as good as one part in 10^{10} for a duration of 8 hours.

For a good review and summary of results obtained to date, the reader is referred to the excellent review article by White.[1] The best fractional stability for any laser system quoted is one part in 10^{10} for a duration of 8 hours, obtained by Bennett, et al.,[2] using the hole-repulsion effect with a 3.39μ He-Ne laser. For certain favorable periods of 1-minute duration or so, one part in 10^{12} was obtained. The best stability obtained to date for a free-running laser in a controlled mechanical and thermal environment is two parts in 10^8 obtained by Collinson[3] with an r-f excited 6328 Å He-Ne laser in a fused quartz cavity. Using a Brewster's angle window laser and a dither scheme, Rowley and Wilson[4] have achieved one part in 10^8 at 6328 Å. Shimoda and Javan[5] have used a somewhat more elaborate dither system with a 1.15μ internal mirror He-Ne laser to achieve two parts in 10^9 for many days. White[6] has used a combination of the Zeeman effect system for long-term stability and a passive cavity loop for short-term stability to achieve one part in 10^9 at 6328 Å.

No results of frequency stabilization experiments on the ionized argon transition (e.g., Ar II 4880 Å or AR II 5145 Å) have been reported. This is no doubt due to the difficulty in obtaining single-frequency operation with such a large Doppler linewidth (~5 GHz). Intracavity methods of obtaining single-frequency operation show promise of self-stabilization and may well be applied to the argon ion laser.

---

[1] White, A. D., "Frequency Stabilization of Gas Lasers," IEEE J. of Quantum Electronics, QE-1, pp. 349-357, November 1965.

[2] Bennett, W. R., Jr., Jacobs, S. F., Latourett, J. T., and Rabinowitz, P., "Dispersion Characteristics and Frequency Stabilization of a Gas Laser," Appl. Phys. Letts., 5, pp. 56-58, August 1964.

[3] Collinson, J. A., "A Stable, Single-Frequency r-f Excited Gas Laser at 6328 Å," Bell Sys. Tech. J., 44, pp. 1511-1519, September 1965.

[4] Rowley, W. R. C., and Wilson, D. C., "Wavelength Stabilization of an Optical Maser," Nature, p. 745, November 1963.

[5] Shimoda, K., and Javan, A., "Stabilization of the He-Ne Maser on the Atomic Line Center," (pt. 1), J. Appl. Phys., 36, March 1965.

[6] White, A. D., "A Two-Channel Laser Frequency Control System," IEEE J. of Quantum Electronics, QE-1, pp. 322-333, October 1965.

TRANSMITTING POWER SOURCES

Laser Oscillators and Amplifiers

	Page
CW Laser Performance	100
Pulsed Laser Oscillators	104
Laser Amplifiers	108
Gas Laser Selection for Space Communications	110
Laser Burden Values	114

CW LASER PERFORMANCE

CW laser sources have been demonstrated from a number of laser types producing powers as high as 8000 watts.

This section provides an initial survey of lasers for space communications and tracking. This survey list is far from complete but does exhibit those lasers which have promising performance with respect to relevant communications system parameters.

Laser oscillators have been classified according to their mode of operation as: cw, pulsed-high energy, pulsed-high power, pulsed-high repetition rate. CW operation for gas lasers is discussed in this topic. Other classifications are discussed in subsequent topics.

The following operating characteristics are also of interest: average power, pulse energy,peak pulse power, pulse repetition frequency. Other aspects of laser oscillators information needed include: wavelength, frequency stability, beam divergency/lateral coherence, noise, efficiency, temperature, size, and weight.

The cw laser oscillator will be discussed first. The output signal is a highly monochromatic beam of light with nearly constant output power.

The active materials which are used in cw laser oscillators include gases, solids, and semiconductors. While laser action has been demonstrated in materials other than those listed in the Table, only the most commonly used or most promising materials are included here.

The wavelengths available for operation comprise a set of discrete spectral lines associated with the various active materials. Generally more than one line is excited in a given laser; however, techniques exist for suppressing oscillation on all but the desired lines. Laser frequency tuning may also be accomplished, but only over a very limited range (usually less than one part in 10^4).

The output powers of existing cw laser oscillators vary from a few milliwatts for single mode operation to hundreds of watts for multifrequency operation in gas lasers. Recently 40 watts cw has been realized in a Nd:YAG laser pumped by an experimental 20 kw argon lamp. The most important factor limiting the output power is the very low energy conversion efficiency of most cw lasers. It usually ranges from 0.01 to 1.0 percent; however, a few exceptions are the CO_2 molecular laser (15 percent) and the GaAs injection laser (approximately 25 percent at cryogenic temperatures). Scattering losses in the laser material and in the cavity mirrors must be overcome in order to obtain high power output in practical devices. In addition, cryogenic temperatures are needed in present injection lasers for efficient operation.

The spectral bandwidth of the laser output, which is an indication of the frequency stability, may range from a few Hertz to several tens of giga-Hertz. Thermal fluctuations and mechanical vibrations are chiefly responsible for line broadening in single mode operation. For multimode operation, the spectral width of the output is closely related to the fluorescence linewidth of the atomic transition. Gas lasers exhibit the most

CW Laser Oscillators

Active Material	Wavelength, μ	Output Power	Dimensions of Active Material	Comments	References
1. He-Ne	0.6118 0.6328 1.084 1.152	5 mW 50 mW 5 mW 20 mW	6 mm x 1.8 m	Single mode, commercially available	1
2. He-Ne	0.6328	900 mW	10 mm x 5.5 m	Research devices	2
3. He-Ne	0.6328	100 mW	5 mm x 1.2 m		
4. Xe	3.5 9.0	0.1 mW 0.5 mW	2.6 mm x 50 cm	Research device	3
5. Ar^+	0.4579 (0.05) 0.4765 (0.1) 0.4880 (0.25) 0.4965 (0.1) 0.5107 (0.1) 0.5145 (0.4)	10 W	6 mm x 60 cm	Research devices, 0.1 - 0.2% efficiency	4
6. Ar^+	(as in 5)	16 W	4 mm x 2.6 m		5
7. Ar^+	0.4880	1 W	3 mm x 45 cm	Airborne development device	6
8. CO_2	10.57 (0.75) 10.59 (0.25)	16 W	25 mm x 2.0 m	4.0% efficiency, single mode for each line,	7
	10.59	135 W		15% efficiency	8
	10.59	2000		Hughes Research Labs	9
	10.59	8000		Raytheon	9
9. Cr^{+3}	0.6943	70 mW	2 mm x 2.54 cm	Water cooled	10
10. $Nd^{+3}(CaWO_4)$	1.06	1 W	3 mm x 3.5 cm	Methyl alcohol cooling (approximately 300°K)	11
11. Nd^{+++}(YAG)	1.06	1.5 W	2.5 mm x 3.0 cm		12
12. Nd^{+++}(YAG)	1.06	0.5 W	---	Water cooled, commercially available, portable	13
13. $Dy^{+2}(CaF_2)$	2.36	0.75 W	4.8 mm x 2.54 cm	Liquid neon (27°K) bath	14
14. GaAs	0.84	12 W	0.5 mm x 0.4 cm (diode dimensions)	Liquid He (4°K) bath, 23% efficiency	13
15. Ruby	0.6943	2.4 W	2 mm diam. x 7.5 mm rod	Water cooled, 0.11 percent efficiency	15

CW LASER PERFORMANCE

monochromatic output since their fluorescence linewidths are typically one to two orders of magnitude less than for solids or semiconductors.

The spectral characteristics of laser oscillators depend primarily upon the material used. As mentioned previously, gas lasers display a narrower fluorescence linewidth than solid or semiconductor lasers. The linewidths of these latter oscillators vary from between 0.001Å for ruby at cryogenic temperatures to several hundred Å for Nd:glass. It should be pointed out that the linewidth of ruby oscillators depends heavily on the operating temperature.

The beam divergence for axial mode operation is given in the diffraction limit by λ/D, where λ is the operating wavelength and D is the diameter of the beam at the output aperture. For most laser oscillators, the output beam diameter is of the order of a few millimeters, so beam divergences of the order of 0.1 milliradian can be obtained for visible light. (The semiconductor laser oscillator is somewhat unique since the active region has dimensions of the order of a few microns. The resulting beam divergence, even in the diffraction limit, is of the order of a few degrees.) For maximum output power, however, nonaxial modes are excited in the oscillator and the beam divergence increases to as much as 10 milliradians.

The beam divergence of the output from a laser oscillator can be made smaller by passing the beam through an optical system. The price one must pay for smaller beam divergence is a larger beam diameter and a small loss in signal strength due to reflection and absorption in the lens system.

Laser oscillators can have three types of noise: (1) spontaneous emission noise, (2) gain fluctuations, and (3) mode-interference noise. Except for operation near threshold, spontaneous emission noise can be neglected. Gain fluctuations due to pump power modulation can generally be reduced to an insignificant level by careful design of the pump source and associated power supplies. Mode-interference noise is not so easily eliminated. It does not occur in lasers operating is a single mode; however, if two or more modes are excited, then beat frequencies between the various modes will be produced. These may range from several kiloHertz to hundreds of megaHertz. Schemes for phase locking the various modes by means of an intracavity modulator are currently under development and promise to make it possible to obtain high power output with little or no mode-interference noise.

Laser operation is frequently compromised by thermal problems. One of these is associated with the low energy conversion efficiency which leads to excessive heating of the laser components. Another problem is the reduction of optical quality of the laser material due to thermally-induced distortion, or stress birefringence. The effect of a non-linear temperature distribution across the laser rod, such as that which arises during the pump cycle, is to cause depolarization of the laser output. This depolarization is not constant but displays a radial dependence. As a result, the output from the laser has a seemingly random polarization and, if one requires a polarized signal, the beam must be repolarized, introducing a loss in signal energy.

REFERENCES

1. Spectra-Physics Model 125 Gas Laser, Spectra-Physics, Inc., Mountain View, California.

2. Perry, D. L., "Mirror Coating Procedures for High Power Gas Lasers," 1964 NEREM (November) paper, p. 3.5.

3. Hughes Research Laboratories Final Report, JPL Contract No. 950803, April 1965.

4. Gordon, E.I., priviate communication.

5. Paananen, R., "Progress in High Power Ionized Argon Lasers," Proceedings of the Second Conference on Laser Technology, Chicago, Ill., 6-8 April 1965.

6. Hughes Research Laboratories Model 50 Argon Laser, W.B. Bridges, private communication.

7. Patel, C.K.N., Bell Laboratories Record, July/August 1965.

8. Tien, P.K., Bell Laboratories, private communication.

9. Forster, D.C., Hughes Research Laboratories, private communication.

10. Evtuhov, V. Appl. Phys. Lett. 6, 75, 1965.

11. Aldag, H.R., Appl. Optics 4, 559, 1965.

12. Geusic, J.E., Appl. Phys. Lett. 6, 175, 1965.

13. KORAD Model KY-1; Korad Corp., Santa Monica, California.

14. RCA Interim Engineering Report, No. 2, "Solid State Laser Explorations, May 1965.

15. Evtuhov, V., and Neeland, J.K., "Power Output and Efficiency of Continuous Ruby Lasers," J. of Appl. Phys. 38, No. 10, September 1967, pp. 4051-4056.

PULSED LASER OSCILLATORS

Typical pulse energies duration prf are given for high energy pulsed lasers, high peak power pulsed lasers and high prf pulsed lasers.

Pulsed Laser Oscillators - High Energy

High energy pulsed laser oscillators produce a short burst of intense monochromatic radiation in a narrow output beam. These lasers operate in a quasi-cw conversion mode - converting incoherent flashtube illumination into laser radiation. Pulse length is limited only by thermal considerations. The pulse may be smooth, as in the case of the super-fluorescent radiator, or it may consist of a series of closely spaced, random or regular spikes. Pulse repetition frequencies are very low (about one per minute for energies measured in tens of joules) due to the time required for cooling of the laser components.

Data for some high energy laser oscillators are given in Table A. Indicative of the energy available, an off the shelf pulsed ruby oscillator with a guaranteed energy of 140 joules is available. These materials are used because of their relatively high ruggedness and conversion efficiency when used to convert flashtube pumping radiation to laser emission. Large size rods of good optical quality are available to match large pumping flashtubes.

Pulse durations of a few milliseconds are usual. Peak powers may be several hundreds of kilowatts.

The energy conversion efficiency is about 1.0 percent for ruby and as high as 6.0 percent for glass. Spectral linewidths vary. For multimode glass it could be as high as 100Å - much less for ruby.

The beam divergence of high energy laser oscillators is typically of the order of 100 milliradians.

Pulsed Laser Oscillators - High Peak Power

High peak powers are obtained by using the "Q-switched" mode of operation. This is an energy storage mode rather than a conversion mode. The energy is stored in the laser rod and released impulsively. The output is a smooth, very short pulse of monochromatic radiation which is contained in a very small solid angle.

The operating characteristics of a few of these devices are summarized in Table B.

Peak powers as high as 700 megawatts from a single ruby oscillator have been achieved. The pulse duration is usually of the order of a few nanoseconds with pulse energies of a few joules being typical.

Table A. Typical High Energy Laser Oscillators

Material	Wave-length (μ)	Pulse Energy (J)	Pulse Duration	Rod Size	Comments	Refer-ences
1. Ruby	0.6943	50	0.5 msec	12 mm x 15 cm	Commercially Available; 7 mr beam divergence	1
2. Ruby	0.6943	140	0.5 msec	12 mm x 15 cm		2

Table B. High Peak Power Laser Oscillators

Material	Wavelength (microns)	Peak Power (megawatts)	Pulse Energy (Joules)	Rod Size	Comments	Refer-ence
1. Ruby	0.6943	50	1.0	---	Commercially avail-able, beam divergence = 7 mr	3
2. Ruby	0.6943	80	2.8	10 mm x 7.6 cm	beam divergence = 0.2 mr	4
3. Ruby	0.6943	500	4.0	---	Commercially avail-able; beam divergence = 7 mr	1
4. Ruby	0.6943	700	--	13 mm x 15.2 cm		5
5. Nd:glass	1.06	30	1.5	6 mm x 46 cm		6
6. Nd:glass	1.06	100	--	---	U. of Moscow	5

Table C. High Repetition Frequency Laser Oscillators

Material	Wavelength (Microns)	Peak Power	Pulse Energy	Repetition Rate	Comments	Refer-ence
He-Ne	1.118	300 w	0.25 mj	2.6 kcps	ave. power 0.6 w	7
Ar^+	several lines 0.4579-0.5145	50 w	0.05 mj	200 cps	ave. power 0.1 w	8
Nd:YAG	1.06	250 w	0.05 mj	100 cps	cw pump, output power not optimized	9
Nd:YAG	1.06	2 kw	0.2 mj	5 kcps		
$Nd:CaWO_4$	1.06	6 mw	140 mj	100 cps	ave. power 14 w	10
GaAs	0.84	2 w	2 μj	10 kcps	77°K, 7 Å, efficiency = 1%	11
GaAs	0.90	4 w	0.2 μj	1 kcps	300°K, 14 Å, efficiency = 0.04%	12

PULSED LASER OSCILLATORS

The energy conversion efficiency of this type of operation is lower than in the high energy mode - typically about 0.1 percent. Spectral line-widths can vary from 0.001Å for single mode operation in ruby to 100Å for multimode operation in Nd:glass. Correspondingly, the beam divergence for single mode operation can be as small as approximately 0.2 milliradians and for multimode operation may be as large as approximately 10 milliradians.

At the present time, these devices can operate at a pulse repetition frequency of about one pulse every second. Cooling of the laser components is the major problem to be overcome in achieving higher repetition frequencies.

Pulsed Laser Oscillators - High Pulse Repetition Frequency (PRF)

Table C contains information on a number of pulsed laser oscillators with a PRF of 100 pps or higher. Pulse repetition frequencies as high as 12 kcps have been achieved in a He-Ne laser and 5 kcps in Nd:YAG. Peak powers vary from a few watts at very high repetition rates to several megawatts with Q-switched operation at lower rep rates.

Pulse energies are quire small, usually of the order of a millijoule, with the result that the average power ranges from a few milliwatts to a maximum of about 15 watts.

When the repetition rate is comparable to build up time the efficiency of a high prf system can be severely degraded if repetition is obtained by pump modulation. Conversely if the prf is comparable to relaxation time, no loss in efficiency is obtained by using cw pumping and modulating the regeneration cavity, either by Q modulation or other intracavity modulation techniques.

REFERENCES

1. KORAD Model K-2Q; Korad Corp., Santa Monica, California.
2. KORAD Model K2; Korad Corp., Santa Monica, California.
3. KORAD Model K-1Q; Korad Corp., Santa Monica, California.
4. Peressini, E.R., Appl. Phys. Letts., 3, p. 203, 1963.
5. Sooy, W.R., private communication.
6. Snitzer, E., "Neothymium Glass Laser," Proceedings of the Third International Conference on Quantum Electronics, Paris, France, 11-15 February 1963.
7. Goldsmith, J., "Measurement of High Power Output from a He-Ne Pulse Gas Laser Employing an Exit Mirror of Optimum Reflectivity," MIL-E-CON Conference, Washington, D.C., 14-16 September, 1964.
8. Bridges, W.B., private communication.
9. Young, C.G., Appl Phys. Letts., 2, p. 151, 1963.
10. Gilmer, A., private communication.
11. KORAD Model KS-3; Korad Corp., Santa Monica, California.
12. KORAD Model KR-2; Korad Corp., Santa Monica, California.

LASER AMPLIFIERS

Laser amplifiers characteristics for CW and pulsed operation are described.

Elaborate laser transmitters may employ one or more laser amplifiers to increase the output power and energy. Another use of laser amplifiers is to amplify single mode oscillators and thus have high spectral radiance.

Laser amplifiers may be operated on a cw-pump or pulse basis. The operating characteristics of interest are

1. Small signal power gain
2. Saturation power
3. Small signal energy gain
4. Saturation energy
5. Bandwidth
6. Operating wavelength
7. Distortion
8. Noise
9. Efficiency.

CW Laser Amplifiers. The small signal power gain of a gas laser can be quite high (as much as 70 db/m for xenon). High power amplifiers have been constructed for 10.6 microns which provide output powers of several kilowatts.

The 3-db bandwidth of a laser amplifier is related to the amplifier gain, G, and to the fluorescent linewidth of the laser transition by (for large gain):

$$(\text{3-db bandwidth}) \cong (\text{fluor. linewidth})/\sqrt{\ell nG}$$

where

ℓ = length between reflectors

n = mode number

Fluorescent linewidths vary from 100 MHz to 5000 MHz for gas lasers. Thus, for a gain of 20 db, the 3-db bandwidth of the laser amplifier will be narrowed by a factor of approximately two.

The relatively narrow passband of a laser amplifier requires that the operating wavelength of the amplifier and oscillator be closely matched. The usual way to accomplish this is to use the same laser material for both oscillator and amplifier. Even in this case, however, a temperature differential may be sufficient to put the oscillator frequency outside the passband of the amplifier. The oscillator-amplifier frequency matching problem can be alleviated somewhat by the use of laser frequency tuning techniques. These allow one to change the frequency by small amounts, generally by less than one part in 10^4. Nonlinear devices may also be used to achieve frequency diversification. The distortion or spreading of the laser beam in passing through an amplifier depends on the optical homogeneity of the laser amplifier medium. For gas laser amplifiers this is not a problem. A diffraction limited input beam yields a diffraction limited output beam.

Amplifier noise is due to spontaneous emission. It increases with the gain of the amplifier according to the relation

$$P_s = h\nu\Delta f(G-1)$$

where $h\nu$ is the photo energy, Δf is the passband of the amplifier, and G is the gain. At 10 db gain, gas laser amplifiers produce noise powers ranging typically from 10^{-10} to 10^{-8} watts depending on the passband.

Pulsed Laser Amplifiers. For pulsed laser amplifiers, the input pulse power is always sufficient to cause power gain saturation. For very short pulses, only the leading edge of the input pulse sees the gain of the fully pumped amplifier. Subsequent portions of the input pulse see a smaller gain due to depopulation by the leading edge of the pulse. The result of this saturation phenomena is a "pulse-shaping" or distortion of the input pulse envelope. Small signal power gains of 30 db in a 15-cm ruby rod have been achieved. Due to the finite rise time of the input pulse generated by a laser oscillator, the peak power gain is more like 10 to 15 db for the same rod.

Since power gain varies during the pulse, it is sometimes convenient to define an energy gain as (output pulse energy)/(input pulse energy).

Small signal energy gains of 20 db in a 15-cm ruby rod have been achieved. Saturation occurs when the input pulse energy density (joules/cm^2) is sufficient to completely depopulate portions of the amplifier rod. For ruby and Nd:glass this occurs at approximately 7 j/cm^2; for Nd:YAG at 0.06 j/cm^2. Solid state materials are used for high power or high energy laser amplifiers due to their energy storage capability. Ruby and Nd:glass can store typically from 1 to 5 j per cc. Consequently, the available wavelengths are 0.6943 micron in ruby and 1.06 microns in Nd^{+++}. Pulsed solid state laser amplifiers have larger passbands than cw gas laser amplifiers; the passband for ruby is about 1 Å and for Nd:glass, it is several tens of Å.

Distortion in pulsed amplifiers in the form of increased beam divergency may exist due to transient thermal gradients in the amplifier material. However, operation of ruby amplifiers with no spreading of the input beam in passing through the amplifier has been demonstrated.

Two factors tend to limit oscillator-amplifier performance. These are damage thresholds for power density and for energy density. If the power density in a dielectric becomes too high, the resultant electric field can cause dielectric breakdown of the material. If the energy density in a pulse, whose duration is short compared to some thermal relaxation time, becomes large, energy will be absorbed by the material faster than it can be carried away and the material will melt. This seems to be the most important factor limiting the performance of high energy glass laser amplifiers. The efficiency of ruby and Nd:glass laser amplifiers approximates the values obtained in high energy quasi-cw conversion mode oscillators.

GAS LASER SELECTION FOR SPACE COMMUNICATIONS

A CO_2 transmitter for a spaceborne communication link and an Argon laser for an up link beacon appear to be the best choice for laser space communication.

The Table summarizes the characteristics of six wavelengths produced by gas lasers. Hundreds of other wavelengths are available, but these six have been selected as representative of each type (ion, molecular, and neutral gas). The reported output power, length and input power are given for the lasers selected.

Notes

1. This is a Hughes airborne quartz laser with a 46 cm bore length, ~1 meter overall package length. It requires a magnetic field of ~1000 gauss, which implies a heavy structure and possibly more power.

2. This laser was reported by Raytheon in Electronic News; it is a quartz tube. The power out is 18 watts, provided the beam in the cavity was chopped to prevent damage to the mirrors.

3. This was produced under carefully controlled conditions at Bell Labs.

4. This is a commercially available Spectra-Physics model 125. 50 mw is guaranteed, but selected tubes produce 100 mw.

5. This is the Spectra-Physics model 125. It may be possible to double the power in a tube this size, but drastic improvements are quite unlikely at this wavelength.

6. This is an Hughes Research Laboratories (HRL) Laborabory-type tube. The output may be doubled, but more power than this is doubtful in a tube this size.

7. This is a TRG Laboratory-type tube and represents approximately two years of effort in developing a high power Xe laser. It is probably close to the ultimate for a tube this size.

8. This is an HRL Laboratory-type tube using flowing CO_2-N_2, mirrors were not optimized; more output power can be expected from this same tube (~20 watts). Seven watts were obtained with the tube sealed.

9. This is the Bell Telephone Laboratories work (C. K. N. Patel, Appl. Phys. Lett., 1 July 1965). A flowing gas system was used with a mixture of CO_2, N_2, O_2, H_2O.

10. This is a BTL result with a tube 4 inches in diameter and 12 feet long. Helium was used. It is hard to estimate how much power will eventually be obtained from a tube of this size. (C. K. N. Patel).

Gas Laser Performance

Gas	λ (μ)	Manu-facturer	P out (W)	L (M)	P in (W)	η	Note
Ar II	0.5	HRL	4.0	0.46	4,000	1×10^{-3}	1
Ar II	0.5	RAY	8.0	1.6	20,000	4×10^{-4}	2
He-Ne	0.63	BTL	1.0	5	500	2×10^{-3}	3
He-Ne	0.63	S-P	0.1	1.7	~200	5×10^{-4}	4
He-Ne	1.15	S-P	0.03	1.7	~200	1.5×10^{-4}	5
He-Ne	3.39	HRL	0.01	1.7	80	1.8×10^{-4}	6
He-Xe	3.51	TRG	0.08	2.0	~200	4×10^{-4}	7
CO_2	10.6	HRL	10	2.0	150	6.7×10^{-2}	8
	10.6	BTL	12	2.0	-	3×10^{-2}	9
	10.6	BTL	130	4.0	~1,000	$\sim 1.3 \times 10^{-1}$	10
	10.6	BTL	0.1	0.5	30	3.3×10^{-3}	11

GAS LASER SELECTION FOR SPACE COMMUNICATIONS

11. This is a small, non flow tube, with external mirrors; suitable for spacecraft. This work is due to T. J. Bridges and is rather preliminary. An account of similar tubes appears in the 1 November 1965 Appl. Phys. Letters.

In comparing the various lasers listed in the Table, the suitability of the output signal for the communications task at hand must be kept in mind. All of the lasers listed can be made to operate in the lowest order spatial mode (TEM_{00}) alone with more or less difficulty. The task is easier at the shorter wavelengths where the laser output is visible and the characteristic beam size is small (proportional to the square root of the product of wavelength and a cavity parameter related to mirror radius). Mode selection at infrared wavelengths may be done with an image-converter or by listening to self-beats in a heterodyne detector. Production of a single-frequency output is still quite difficult because of the longitudinal mode structure of the long Fabry-Perot cavities used. Only the 10.6μ CO_2 and 3.5μ xenon lines are narrow enough to produce reasonable output by keeping the Fabry-Perot resonator short enough so that only one longitudinal mode oscillates. This is done to the narrow doppler-broadened line widths of these two transitions (≈50 MHz for 10.6μ CO_2 and ≈120 MHz for 3.5μ Xe). Even these two transitions will require further mode selection techniques if longer, higher power tubes are considered. Because of the broad doppler line widths of the Ar and He-Ne lasers, single-frequency operation through the use of a sufficiently short Fabry-Perot resonator entails a drastic loss in output power. Techniques involving 3 mirror resonators allow the use of longer tubes at the expense of added complexity both mechanical and electronic (servo-controlled mirror positioning), but still sacrifice output power because the entire line is not used. The most promising technique developed to date is that of intracavity mode locking[1] with a subsequent coherent recombination[2] or selective output coupling[3]. This technique has been demonstrated in the laboratory, but practical power levels at a single frequency are yet to be obtained. In any case the additional complexity will contribute to the weight, length and inefficiency of the laser, although perhaps not to a significant extent.

It appears that, at present, the best laser for optical space communications at present would be a small, efficient, light weight 10.6μ CO_2 laser in the spacecraft with coherent detection (superheterodyne) on the ground, employing a cooled Hg:Ge detector. The up-link would be best handled by a high-power multimode argon laser on the ground, employing pulse amplitude or pulse polarization modulation, and a simple ruggedized photomultiplier video receiver in the spacecraft. These conclusions are, of course, subject to revision as the state of the laser (and detector) art progresses.

---

[1] Harris, S.E., and McDuff, O.P., Appl. Phys. Letts., 5, pp. 205-206, November 15, 1964.

[2] Massey, G.A., Ashman, M.K., and Taig, R., Appl. Phys. Letts., 6, p. 10, 1965.

[3] Hanes, S.E., and McMurtry, B.J., (to be published).

LASER BURDEN VALUES

Cost and weight burden values are given for the CO_2 laser ($\lambda = 10.6\mu$) and the Argon laser ($\lambda = 0.51\mu$).

A main purpose of this contract (NAS 5-9637) is to compare the performance of several communications systems operating at different wavelengths. In order to do this an extensive modeling was undertaken which expressed parameters in the communications link equation in terms of cost or weight. (See Appendix A of this Volume.)

From the material given in this Part; Part 1, Transmitting Power Sources; and from other investigations, constants have been chosen which relate the laser transmitted power, P_T, to the cost of obtaining this power, C_{P_T}, and to the weight of a transmitter supplying this power, W_{P_T}. This has been done for a CO_2 laser ($\lambda = 10.6\mu$) and for an Argon laser ($\lambda = 0.51\mu$).

The values used in these relationships are the best that could be determined at the date of this final report and are certainly subject to change. This is especially true of the cost relationships which represent estimates of fabrication cost only and do not include development costs.

Figures A and B give the expected weight for a CO_2 laser and an Argon laser as a function of output power. Figures C and D give the cost for these two lasers as a function of output power. The efficiency of CO_2 and Argon lasers are taken as 10 percent and 0.1 percent respectively.

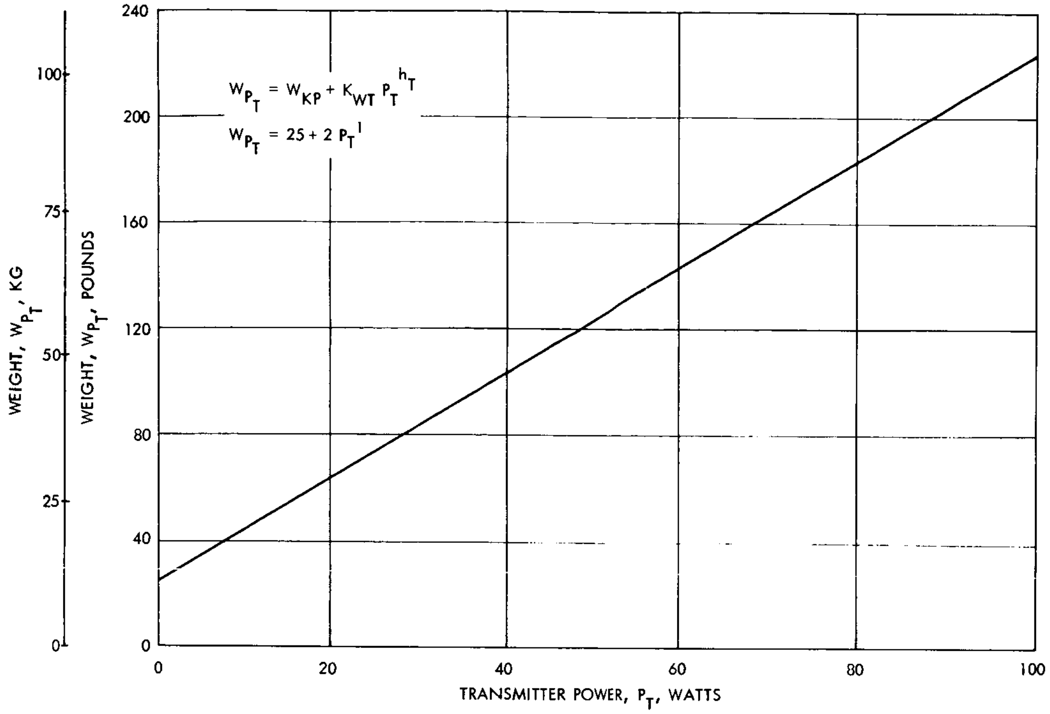

Figure A. Weight of a CO_2 Laser ($\lambda = 10.6\mu$)

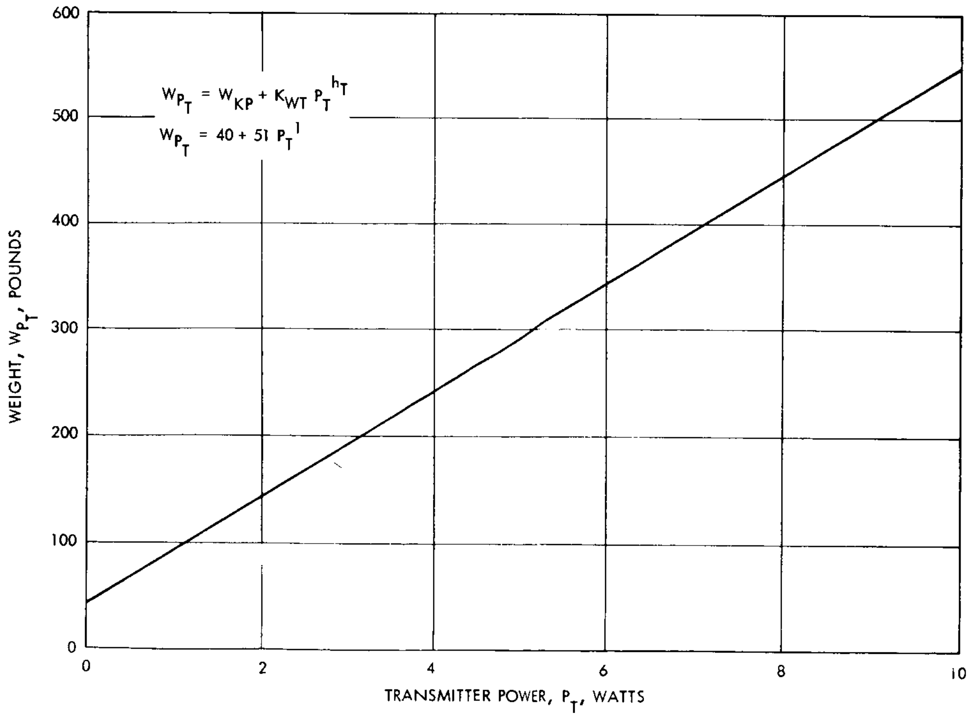

Figure B. Weight of an Argon Laser ($\lambda = 0.5\mu$)

LASER BURDEN VALUES

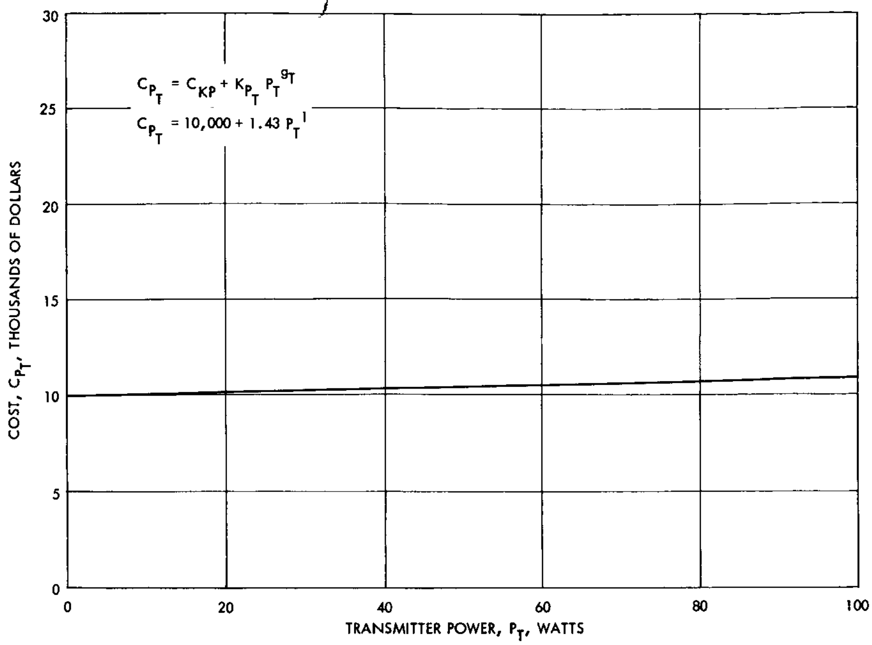

Figure C. Cost of a CO_2 Laser (λ = 10.6μ)

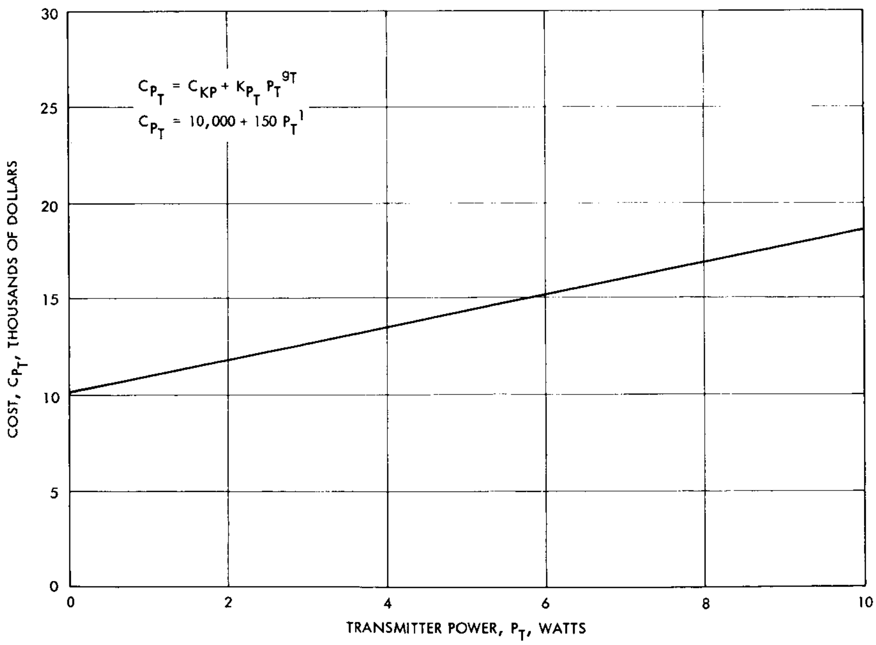

Figure D. Cost of an Argon Laser (λ = 0.5μ)